ABSTRACT

Title of Document:	INTERFACIAL SOLVATION AND EXCITED STATE PHOTOPHYSICAL PROPERTIES OF 7-AMINOCOUMARINS AT SILICA/LIQUID INTERFACES
	Debjani Roy, Ph.D, 2010
Directed By:	Professor Robert A. Walker, Department of Chemistry and Biochemistry

The properties of solutes adsorbed at interfaces can be very different compared to bulk solution limits. This thesis examines how polar, hydrophilic silica surfaces and different solvents systematically change a solute's equilibrium and dynamic solvation environment at solid/liquid interfaces. The primary tools used in these studies are steady state fluorescence spectroscopy and time correlated single photon counting (TCSPC) –a fluorescence method capable resolving fluorescence emission on the picosecond timescale. To sample adsorbed solutes, TCSPC experiments were carried out in total internal reflection (TIR) geometry. These studies used total of six different 7-aminocoumarin dyes to isolate the effects of molecular and electronic structure on solute photophysical behavior. Fluorescence lifetimes measured in the TIR geometry are compared to the lifetimes of coumarins in bulk solution using different solvents to infer interfacial polarity and excited state solute conformation and dynamics.

Steady state emission experiments measuring the behavior of the coumarins adsorbed at silica surfaces from bulk methanol solutions show that all coumarins had

a similar affinity $\Delta G_{ads} \sim$ - 25-30 kJ/mole. Despite these similar adsorption energetics solute structure had a very pronounced effect on the tendency of solutes to aggregate and form multilayers. Our finding suggests that hydrogen bonding donating properties of the silica surface plays a dominant role in determining the interfacial behavior of these solutes. The silica surface also had pronounced effects on the time dependent emission of some solutes. In particular, the strong hydrogen bond donating properties of the silica surface inhibit formation of a planar, charge transfer state through hydrogen bond donation to the solute's amine group. A consequence of this interaction is that the time dependent emission from solutes adsorbed at the surface appears to be more similar to emission from solutes in *nonpolar* solvation environments.

To test the role of solvent identity on the photophysical properties of adsorbed solutes, additional experiments were carried out with a nonpolar solvent (decane), a moderately polar solvent (*n*-decanol) and a polar aprotic solvent (acetonitrile). The results from these studies demonstrated that interfacial solvation depends sensitively on a balance of competing forces including those between the solute and substrate, the solute and solvent *and* the surface and adjacent solvent.

INTERFACIAL SOLVATION AND EXCITED STATE PHOTOPHYSICAL PROPERTIES OF 7-AMINOCOUMARINS AT SILICA/LIQUID INTERFACES

By

Debjani Roy

Dissertation submitted to the Faculty of the Graduate School of the
University of Maryland, College Park, in partial fulfillment
of the requirements for the degree of
Doctor of Philosophy
2010

Advisory Committee:
Professor Robert A Walker, Chair
Professor Michael Coplan
Professor John Weeks
Professor Janice Reutt-Robey
Professor Neil Blough

Dedication

To my beloved parents

Acknowledgements

I am most obviously indebted to my advisor Dr. Robert Walker. A special mention should go to the countless hours he committed to discuss about my research work. I learned from him how to approach scientific problems and to find solutions in most difficult situations. I want to gratefully acknowledge his continuous support and encouragement to me throughout these years; without him this work could not be completed.

I want to express a special thanks to Dr. Michael Coplan. My interactions with Dr.Coplan always motivated me to grow scientifically. I would also like to thank Dr. Doug English and Dr. Amy Grimes for their help with the instrumentation. A special thanks to Dr. Ed Castner for providing the data analysis routine in Igor.

Through my last four years, I had often held lively discussions with the past and present members of the Walker Research group which helped to hone my scientific skills. I am particularly thankful to Dr. Mike Pomfret, Dr. Suleyman Can, Dr. Wendy Heiserman, Dr. Mike Brindza, Dr.Tony Dylla, Renee Siler and Bryan Eigenbrodt for providing me the help and companionship. Surely, I am going to cherish the moments that I spend with my group members. I am also appreciative for the valuable discussions that I shared with my friend Dr. Pramit Chowdhury during my graduate career.

Finally, I thank my parents, brother and in-laws for believing in me and standing by me whenever I needed them most. Most of all, I would like to thank my Mom for the love and dedication she has shown in caring for me and my brother.

Lastly, I especially want to thank my husband Nabarun for his love, consideration and continuous support through all the good and bad times. I could never have succeeded without him.

Table of Contents

List of Tables

List of Figures

List of Abbreviations

λ	Wavelength
μ	Dipole Moment
τ	Fluorescence Lifetime
$\Delta\mu$	Change of Dipole Moment
ΔG_{ads}	Change in Free Energy in Adsorption
$\Delta\theta$	Change in Dipole Orientation
ω	Frequency
7AC	7-aminocoumarin
BBO	β -Barium Borate
CFD	Constant Fraction Discriminator
CT	Charge Transfer
d_p	Penetration Depth
h	Planck Constant
IRF	Instrument Response Function
K	Equilibrium Constant
k_r	Radiative Rate Constant
k_{nr}	Non-Radiative Rate Constant
LPF	Long Pass Filter
MCA	Multi Channel Analyzer
MCP-PMT	Microchannel Plate Photomultiplier Tube
MeOH	Methanol
Q	Quantum Yield
SPF	Short Pass Filter
TAC	Time to Amplitude Converter
TCSPC	Time Correlated Single Photon Counting
TICT	Twisted Internal Charge Transfer State
TIR	Total Internal Reflection
TIRF	Total Internal Reflection Fluorescence
TRSHG	Total Reflection Second Harmonic Generation

Chapter1: Introduction

1.1. Solvation in Bulk and at Interfaces

Interfaces are universal and delineate boundaries between any two phases of matter. As such, interfaces are necessarily anisotropic, meaning that molecules and materials at interfaces are subject to asymmetric forces that are different from what they would experience in a bulk medium. This inhomogeneity can change the electronic structure, conformation and reactivity of the molecules at or near the interface. The focus of this thesis is the change relative to bulk solution limits of photophysical properties induced in solutes by solid-liquid interfaces. This specific type of interface plays an important role in applications like solar energy harvesting[1], surface lubrication[2-6] and electrochemistry[7]. Thus, the knowledge of the effects of interfacial chemistry on the solvent-solute and solute- surface interactions will enhance our understanding of fundamental processes and help us to formulate quantitative models of solution phase surface chemistry.

Despite the prevalence and importance of solid/liquid interfaces in such a wide variety of scientific and technological applications,[8-10] the photophysical properties of adsorbed solutes due to interfacial solvation changes are not well understood. Here, solvation is defined as the noncovalent interaction between a solute and its surroundings. These interactions may be nonspecific and averaged over the entire solvent cavity, or they may be localized and directional. An example of nonspecific solvation is an environment's polarity. Hydrogen bonding stands out as an example of a specific solvation interaction. In addition to specifying the "type" of

solvation being described, one must consider whether interactions are time-averaged or time-dependent. The steady state emission spectrum of a solute represents a time averaged property. Time resolved analysis reveals dynamic information lost in time averaged processes. Steady state and time resolved fluorescence can serve as sensitive methods for probing these different aspects of a solute's solvation environment.[11-14] This thesis describes a series of steady state and time-resolved measurements of molecular fluorescence for related solutes in a variety of solvents and adsorbed to silica/liquid interfaces. The solutes themselves all have two closely related excited states with distinctly different emission properties. The goal of this work is to identify how populations in these states are affected by solvent polarity, hydrogen bonding opportunities, and the anisotropy inherent to any interface.

The general scheme of a fluorescence experiment is shown below.

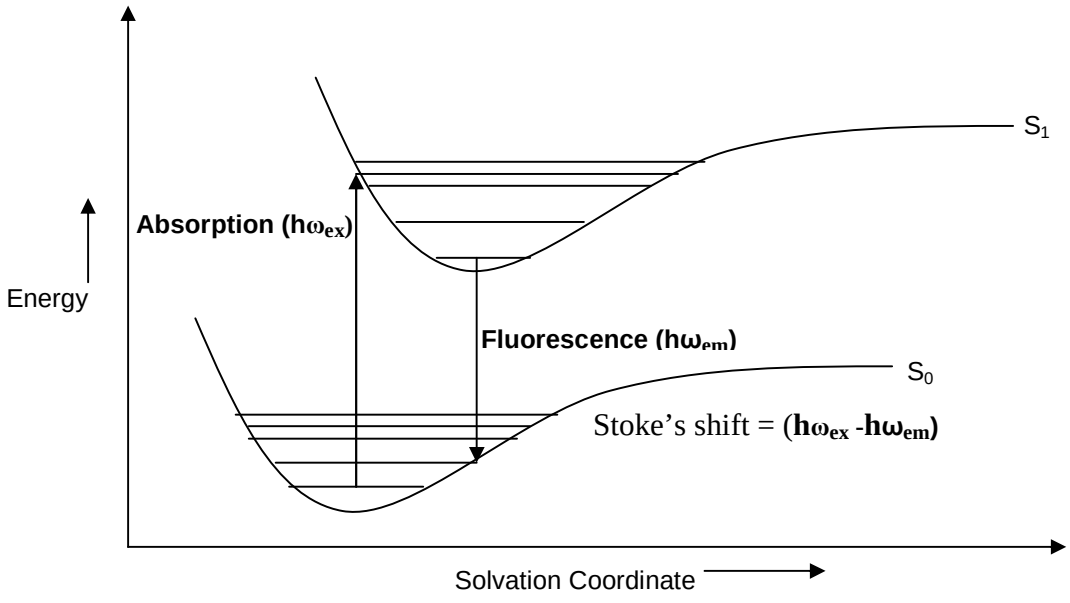

Figure 1.1. The ground (S_0) and excited (S_1) state of a solute at solvation coordinate. The absorption and emission path are shown by a solid arrow and the energy differences are depicted as $h\omega_{ex}$ and $h\omega_{em}$ respectively.

Fluorescence, by definition, is a radiative transition between electronic states having the same multiplicity. Briefly, the process begins as a solute molecule undergoes a vertical transition to a higher electronic state by absorbing a photon. Next, the excited solute molecule relaxes by a rapid dissipation of vibrational energy to the lowest vibrational level of S_1. For medium-size, fluorescent organic molecules (MW < 500) emission typically takes on the order of 10^{-9} s, and represents a vertical relaxation of the excited solute to its ground state. Figure (1.1) depicts a typical photoexcitation-relaxation process where fluorescence appears at longer wavelengths than absorption.

The spectral position of the steady state fluorescence spectrum depends on solvent properties. In general, molecules having larger dipole moments in their excited states experience a red shift in their emission spectra that grows more pronounced with increasing solvent polarity. The energy difference between the position of the absorption maxima and the emission maxima is defined as the "Stoke's shift"(Figure 1.2.). Typically, the magnitude of a fluorophore's Stoke's shift will depend upon the environment and it will increase with increasing environment polarity. The time-dependent intensity of fluorescence from any excited solute, although clearly dependent upon the radiative rate, is also dependent upon internal competing nonradiative pathways. Processes competing with fluorescence are intersystem crossing to triplet states, vibrational relaxation, and photochemical reactions.

Steady state fluorescence studies are limited in the information they can provide about many photophysical processes. Time dependent processes can be inferred from steady state data such as linewidths and band shapes, but such

correlations are indirect. One such example of a property that can not be determined from steady state data is the solvent reorganization around the excited state fluorophore, which occurs on the order of 0.5 ps to 300 ps.[15-17] Due to the temporal resolution (~ 40 ps) of our instrument, we are unable to resolve many of the fast solvent relaxation times exhibited by short chain alcohols (e.g. methanol), nonpolar solvents (e.g. decane) and small aprotic solvents (e.g acetonitrile). However, time resolved emission data presented in Chapter 6 does show evidence of slow solvent relaxation in bulk 1-decanol.

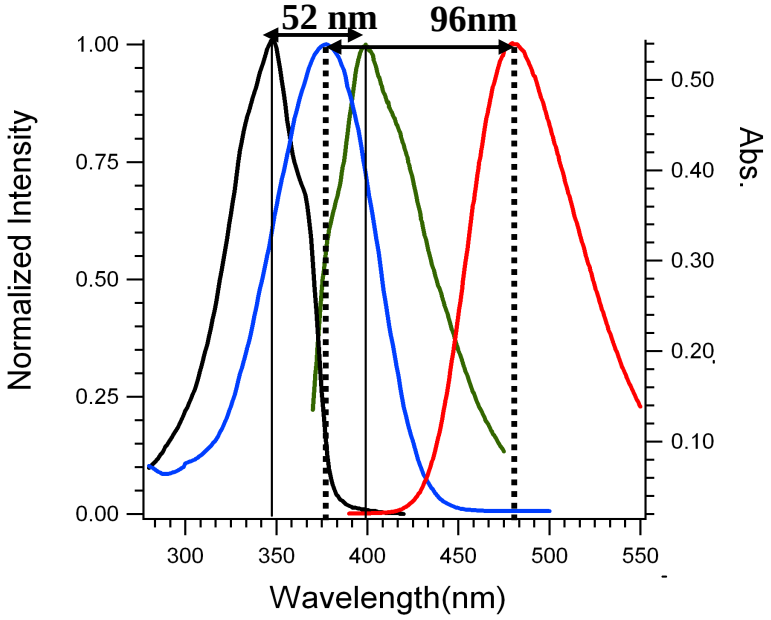

Figure 1.2. Stoke's shift of a coumarin probe in Decane and MeOH is ~ 52 nm and ~ 100 nm respectively. The black (decane) and blue (methanol) data are absorbance (Left); the green (decane) and red (methanol) data are emission (Right).

Solute photophysical properties in bulk solution have been the focus of extensive studies related to chemical and biological systems for more than forty

years. In 1964, Baldwin and coworkers first measured the fluorescence lifetime of a series of molecules, including fluorescein, acridone, perylene and others using a nanosecond flash.[18] The authors found a direct correlation between their experimental results and the theoretical predictions calculated by Strickler and Berg.[19] In 1967 Halim and coworkers studied absorption and emission spectra of sterically hindered molecules including TPB (trans-1,1,4,4-tetraphenyl-butadiene) in rigid glasses at 77^{o}K and first observed that the solute equilibrium conformation in an excited state can be markedly different from that in the ground state.[20] In 1968, Lee and coworkers used time-resolved spectroscopy and reported that temperature dependent shifts of emission in alcohol solvents are due to solvent-solute relaxation marking one of the first instances when solvation effects were identified as influencing directly the photophysical properties of a solute. [21]

These studies and others began to address many aspects of solvation in bulk solution. Based on their influence on solvent structure and dynamics, surfaces should also significantly change the properties of adsorbed solutes and do so in ways that are different from bulk solution limits.[22-24] The experiments described in this thesis examine the interplay between solute conformation, barriers to inversion motion, and photophysical properties of coumarin solutes in different environments. In particular, we address the questions related to the promotion of radiative (and nonradiative) relaxation from different excited states by different solvents and interfacial environments. Solvent polarity and hydrogen bonding properties have been shown to play key roles in determining the photochemical processes following photoexcitation of a solute. For example, the electron transfer, proton transfer, and the formation of

different charge transfer states can occur in polar solvents.[25-26] Photoexcitation results in an instantaneous redistribution of electron density in a solute. For solutes having particular combinations of electron donating and withdrawing groups, photoexcitation can lead to an electron donating group assuming a positive charge while the electron withdrawing group acquires a formal negative charge. Such charge separation leads to excited states having relatively large dipole moments and correspondingly large Stokes shifts between their absorption and emission spectra.

Solutes probed in these studies are primarily categorized based on the substituents in the amine group, namely primary, secondary and tertiary 7-aminocoumarins (7AC) as described in Figure 1.3.2. 7AC solutes are very good candidates to form charge transfer state (CT) species upon photoexcitation. The amino group can serve as an electron donor with the nitrogen then assuming a planar, sp^2 hybridization and the carbonyl acquiring the negative charge. CT formation can be facilitated/inhibited by the addition of extra electron-withdrawing/donating functional groups elsewhere on the coumarin ring. An important point to note for the 7AC used in this study is that all of the amines are free to undergo inversion about the nitrogen. Inversion, or "flip-flop" as this motion can be called, [27] represents an isomerization reaction between two equivalent conformations. Separating these two minima is a barrier that depends on the bulkiness of the amine substituents. Primary amines, for example, have an inversion barrier that is almost 40% smaller than the barrier of otherwise equivalent N, N-dimethyl tertiary analogues.[28]

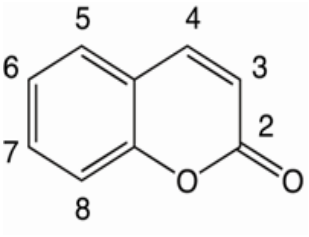

Figure 1.3.1. Structure of 1, 2 Bezopyrone

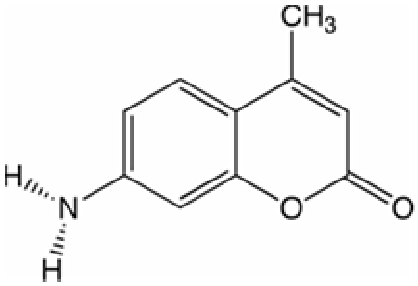

C440

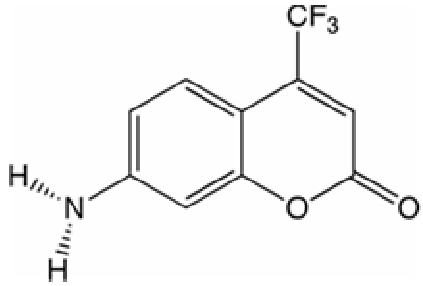

C151

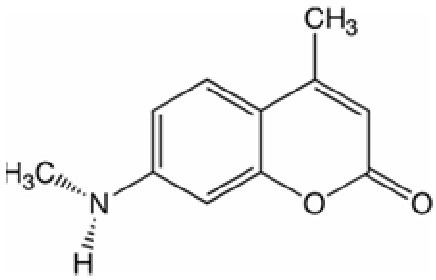

C445

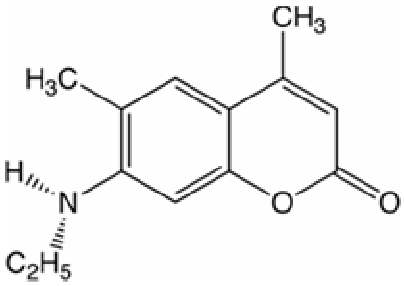

C450

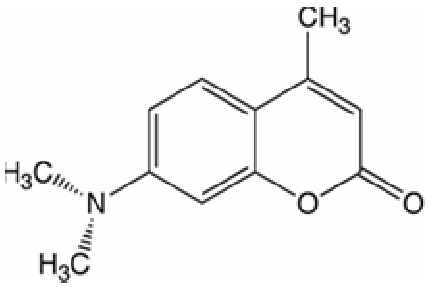

C461

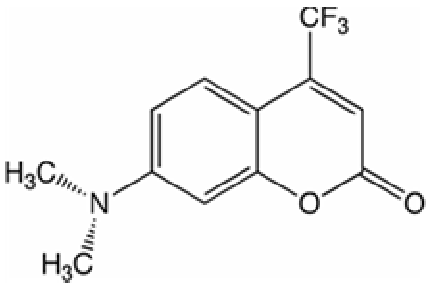

C152

Figure 1.3.2. Structures of primary amine coumarins C440 and C151; secondary amine coumarins C445 and C450 and tertiary amine coumarins C461 and C152

Our findings suggest that the barrier to inversion is a deciding factor in the nonradiative decay pathways available to photoexcited solutes as well as the tendency of solutes to form dimers or higher aggregates in solution and at surfaces. Inversion leads to faster nonradiative decay and correspondingly shorter lifetimes. Furthermore, facile inversion over a smaller barrier will allow molecules to undergo large amplitude motion with higher frequency, thus preventing individual monomers from associating with one another. Silica surfaces, with their ability to donate strong hydrogen bonds, effectively restrict this sort of aggregate formation for those solutes directly adsorbed at the surface. The work in this thesis focuses on the way interfacial solvation depends on the balance of competing forces. These forces include solute/substrate interactions, solute/solvent interactions, *and* solvent/substrate interactions.

1.2: Probing Solvation at Interfaces

Several state-of-the-art tools and techniques have been developed over the years to understand molecular properties of solutes in bulk solution. However, many of the methods designed to study bulk solvation are not easily adapted to studying solvation at surfaces. The primary challenges associated with studying interfaces are as follows:

- Surface specific measurements require sensitive methods that can probe the photophysical properties of the small number of molecules at the vicinity of a surface.
- Methods and instrumentation must be able to discriminate and detect the surface specific signal from the potentially large signal from molecules in bulk solution.

- Analytical models face numerous challenges when attempting to reproduce the asymmetric interactions found at interfaces. Modeling behavior at interfaces depends on accurate descriptions of many-body interactions in anisotropic environments. Due to the difficulty in developing robust and accurate potentials, simulations usually use simplified model potentials. Nevertheless, in past years there have been several simulation studies of surface anisotropy and interfacial solvation.[29-31] Despite of these studies and others many aspects of the interfacial solvation process, such as dynamical time scales, molecular mechanism and the conformational change associated with the interfacial species are not well known. To overcome these challenges several studies have used total internal reflection fluorescence spectroscopy (TIRF) and second harmonic generation (SHG) to characterize solvation dynamics at surfaces[32-39].

Masuhara *et al.* employed TIRF methods to study the excited state proton transfer reaction of 1-napthol at the sapphire/water interface and reported that the rate constant of the excited state proton transfer is larger at the interface than in bulk water.[32] Using the same solid (sapphire) and a polymer solution, Masuhara and co-workers created a solid/polymer interface and investigated the pyrene excimer formation process.[33] The TIRF results show a reduction of excimer fluorescence intensity and a deceleration of excimer fluorescence rise and decay time at the interface relative to the bulk media. Girault and coworkers also used TIR conditions to study the photophysical properties of Coumarin 343 at the water /dichloroethane interface and found that aggregation becomes increasingly important at interfaces compared to bulk solution limits.[34] From these benchmark studies, one can conclude

that the effects of a surface on solvation and reactivity are far-reaching and impact both equilibrium *and* time dependent aspects of solvation. Kitamura and coworkers used TIRF spectroscopy to investigate the energy transfer between two fluorescent dyes at weakly associating liquid/liquid interfaces.[35] In a separate effort, Kitamura and coworkers modeled the cell-protein interface with a water/oil interface to study DNA hybridization processes. They found that hybridization did not proceed in bulk water but only at the water/CCl_4 interface. The process was probed using TIR fluorescence spectroscopy detecting ethydium bromide (EB), a double-stranded (dsDNA) specific dye.[36]

A pioneering effort by Eisenthal and coworkers used time-resolved second-harmonic generation (TRSHG) to quantify how in-plane vs. out-of-plane solute reorientation rates differed for Coumarin 314 adsorbed to an air-water interface. They found that surface reorientational times are slower than bulk orientational diffusion times.[37] In a separate effort, Masuhara and coworkers probed Coumarin 460 in bulk 1-butanol and at a 1-butanol/sapphire interface and found that interfacial solvation times were quite disticnt from bulk limits.[38] This finding suggests the existence of an intrinsic difference between air/liquid and solid/liquid interfacial properties, that can be attributed to the H-bond forming capacity of the given solid (sapphire) substrate with the solvent. Such bonding is not possible at the air/water interface since the water molecules at the air/water interface cannot hydrogen bond with the vapor-phase. Zewail and coworkers investigated the causes of the emerged asymmetric environment by using tryptophan as a probe to study protein dynamics.[39] This study reported a slower relaxation of the tryptophan probe at the interface, compared to that

in the bulk limit and associated the cause of the asymmetric force field with the presence of local rigidity at the interface induced by the protein moiety and surface water layer.

Despite such efforts many questions about interfacial solvation at surfaces remain largely unanswered. In particular, the effects of solute-substrate and solvent-substrate interactions on interfacial solvation are not well characterized. Our efforts to systematically identify the effects of polarity, hydrogen bonding, and solvent organization on interfacial solvation use fluorescence spectroscopy to study fluorophore emission in bulk solution and at the silica/solvent interface with a TIR geometry. Our studies of solvation at surfaces use both steady state and time-resolved fluorescence measurements to understand the changes in the excited state of the solute caused by solute adsorption to polar hydrophilic silica surfaces and the role played by solvent properties such as polarity and hydrogen bonding.

Silica surfaces are terminated with silanol groups that make these substrates polar and enable them both to donate and accept hydrogen bonds. The surface can induce anisotropic ordering and will affect the properties of adsorbed solutes as well as adjacent solvent species.

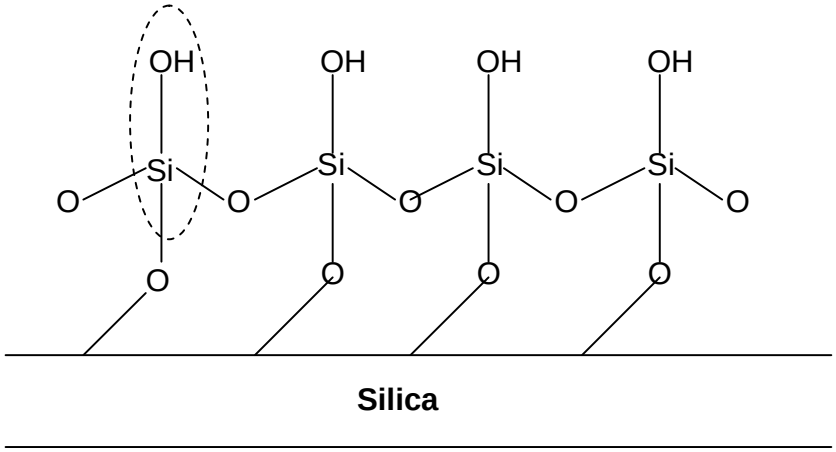

Figure 1.4. Schematic diagram of a Silica surface –Si-OH (highlighted) is the silanol group and hydroxyl (-OH) functional groups are exposed to bulk solvent.

This dissertation is focused on solutes in bulk solution and those adsorbed to the silica/liquid interface. There are many reasons for choosing silica as the solid phase. First, the silica/liquid interface is ubiquitous. In nature, silica/liquid interfaces are omnipresent in geophysical systems, and are involved in environmental initiatives such as ground water remediation and oil recovery. Silica is also the primary stationary phase in most separation technologies.[40-41] Silica is used in a wide variety of applications, its surface chemistry is reasonably well understood and a considerable amount of literature exists describing the surface's chemical and physical properties.[42-44]

1.3. Probes Studied

In order to determine how interfacial solvation differs from bulk solvation limits, solvent sensitive coumarin solutes possessing well-characterized solvatochromic behaviors were used. Coumarins are popular dyes used for various

spectroscopic investigations, namely in the study of solvatochromic properties[45,46], the determination of polarities in microenvironments[47], the investigation of photoinduced electron-transfer dynamics[48,] and measurements of solvent relaxation times[17]. The widespread usage of these solutes can be attributed to several properties associated with coumarin derivatives:

- Coumarins typically posses high chemical stability and substantial sensitivity to the local dielectric environments. [49]
- Coumarins typically have high fluorescence quantum yields, often close to unity[50] that makes these probes easily detected.
- The basic coumarin structure can be easily modified to systematically tune the interactions that individual solutes have with their surroundings. The coumarin dyes are structural derivatives of 1, 2-benzopyrone and members of the 7-aminocoumarin group. (Figure 1.3.1.) 7-aminocoumarin dyes used in the present study can be divided into three primary categories based on the structural derivatives of the amine; Coumarin-151 and Coumarin-440 are primary amine coumarins, Coumarin 445 and Coumarin C450 are secondary amine coumarins and Coumarin C152 and Coumarin C461 are tertiary amine coumarins. (Figure 1.3.2.)

Experiments described in this dissertation examine the photophysical properties of these coumarin dyes both in bulk solution and for dyes adsorbed to polar silica substrates. Studies are carried out using a polar protic solvent (methanol) as well as a nonpolar alkane (decane). Additional experiments intended to test hypotheses developed from studies using these model systems employ a longer chain

alcohol solvent (1-decanol) and a polar aprotic solvent (acetonitrile). Collectively, these solvents offer a broad range of polarities and H-bonding abilities. Surface studies employ hydrophilic silica as the solid substrate. Earlier work has shown that solvation at the silica surface is dominated by the hydrogen-bond-donating capabilities of the surface silanol groups.[51] The steady-state and time-dependent photophysical properties of these solutes at interfaces as a function of solvent identity allows us to separate the way nonspecific and specific solvation forces control the excited state properties of solutes both in isotropic and anisotropic environments.

This thesis is organized as follows. Chapter 2 describes the experimental approaches used to carry out the studies. Summarized is a theory of fluorescence spectroscopy, a brief description of the techniques used for time-resolved measurements, and a consideration of probes used for the present study. Chapter 3 discusses how the surfaces appear to decouple the equilibrium and dynamic behavior of primary amine 7AC solutes adsorbed to the silica/methanol interface. Steady state data reveal that the surface is quite polar; however time resolved data show that the boundary created by two polar phases appears distinctly nonpolar in terms of the time-dependent emission properties. We attribute this behavior to the fact that the dipoles of the silica surface (and the methanol solvent) can create a polar environment, but the surface silanol groups also can form strong hydrogen bonds with adsorbed solutes. This combination - strong hydrogen bonding from the substrate and the inability of the substrate to move - limits the conformational freedom of the adsorbed solute forcing the solute to retain a conformation more consistent with solvation in a nonpolar environment.

This phenomenon of surface constrained solute conformation is explored further in Chapter 4 where tertiary amines, namely C152 and C461, are employed in order to further our understanding of how the interfacial environment affects a solute's photophysical behavior and conformational energetics. The data shows that the silica surface induces a new time-dependent response from C152 that is consistent with a nonpolar environment. We propose that such behavior is again likely to result from the surface molecules forming a strong hydrogen bond with the lone pair of C152 amine electrons. This prevents the excited state solute from adopting a new twisted intramolecular charge transfer confirmation (TICT) for C152. The results presented in chapter 4 are used to understand how both equilibrium properties such as solvent polarity and solute molecular orientation, ***and*** dynamic properties (as inferred from fluorescence lifetime measurements) change from bulk solution to the interface.

Chapter 5 addresses the following question: how does solvent identity affect interfacial coumarin solvation? For these experiments, decane is the solvent used and the results are quite different from those measured at the silica/methanol interface. In particular, we infer that the hydrogen bonding donating properties of silica limit the aggregation of dyes adsorbed to the silica surface. Also, time resolved data show that the silica/decane interface stabilizes the polar charge transfer state of adsorbed coumarins in contrast to the silica/methanol interface that created an environment that led to emission as if coumarin were in a nonpolar environment. Overall, our results from these experiments suggest that the presence of a surface can induce significant changes in excited-state photophysical properties of solutes due to strong substrate – solute interactions, surface composition, and a solute identity**.**

Chapter 6 presents a comparative study of the 7-aminocoumarins in bulk decanol and at the silica/decanol interface. Results from these studies show that the solvent itself will solvate individual solutes differently. The different solvation behaviors of these coumarins were understood based on their local dielectric environment, hydrogen bonding properties, and solvent reorganization dynamics. Steady state data show that decanol is a moderately polar solvent. The time dependent emission behavior shows that solutes have two distinct fluorescent states due to the non-hydrogen bonded and *fully solvated* hydrogen bonded forms in the excited states. Data also show that the coumarins with large changes in dipole reorientation have much longer solvent reorganization timescales. TIR data from solutes adsorbed to silica/decanol interfaces did not show any significant change with respect to the bulk result. Coumarin remains solvated in bulk solvent as the long alkyl chains provide sufficient steric hindrance to the solute to be surface-active. Chapter 7 presents an overall summary of this thesis work and proposes directions for future work. Chapters 3, 4, and 5 are modified versions of manuscripts that have been (or are about to be) submitted for publication. There exists some redundancy in the text of these chapters, especially when discussing and interpreting results.

References

(1) Hagfeldt, A.; Gratzel, M. *Chem. Rev.* **1995**, *95*, 49-68.

(2) Corn, R. M..; Higgins, D. A. *Chem. Rev.* **1994**, *94*, 107-125.

(3) Hoppe, H.; Sariciftci, N.S. Organic solar cells: An overview. *J. Mat. Res.* **2004**, 19, 1924-1945.

(4) Kamat, P.V. *Chem. Rev.* **1993,** 93, 267-300.

(5) Gust, D.; Moore, T.; A.L. *Acc. Chem.Res.* **2001,** 34**,** 40-48.

(6) Kurashige, Y.; Nakajima, T.; Kurashige, S.; Hirao, K.; Nishikitani, Y. *J. Phys. Chem. A* **2007,** 111, 5544- 5548.

(7) Weaver, M.J. *J.Phys.Chem***. 1996,** 100, 13079-13089

(8) Du, Q.; Freysz, E.; Shen, Y.R.; *Phys.Rev.Lett*. **1994**, 72, 238-241

(9) Wirth, M. J.; Burbage, J.D. *Anal. Chem.* **1991,** 63, 1311-1317.

(10) Liu G.; Li, Y.; Jonas, J. *J. Chem. Phys.* **1991,** 95, 6892-6901.

(11) Suppan, P.J.; *Chem. Soc. Faraday Trans.1* **1987**,83,495- 509.

(12) Richert R.; Wagener, A. *J. Phys. Chem.* **1991**, 95 (24), 10115–10123.

(13) Gardecki, J.; Maroncelli, M.; *Chem Phys Lett*., **1999**, 301, 571- 578.

(14) Jarzeba,W.; Walker, G.W.; Johnson, A.E.; Barbara, P.F. *Chem Phys.* **1991**,152, 57- 68

(15) Jimenez, R.; Fleming, G. R.; Kumar, P. V.; Maroncelli, M. *Nature* **1994**, *369*, 471-473.

(16) Jarzeba, W.; Walker, G. C.; Johnson, A. E.; Kahlow, M. A.; Barbara, P. F. *J. Phys. Chem*. **1988,** *92,* 7039-7041.

(17) Horng, M. L.; Gardecki, J. A.; Papazyan, A.; Maroncelli, M. *J. Phys. Chem.* **1995,** *99*, 17311-17337.

(18) Ware, W. R. Baldwin, B. A. *J..Chem. Phys.* **1964**, *40*, 1703-7.

(19) Strickler, S. J.; Berg, R. A. *J. Chem. Phys.* **1962**, *37*, 814.

(20) Elbayoum, M. A.; Halim, F. M. A. *J. Chem. Phys.* **1968**, *48*, 2536-7.

(21) Ware, W. R.; Chow, P.; Lee, S. K. C*hem. Phys. Lett.* **1968**, *2*, 356-358.

(22) Higgins, D.A.; Abrams,M.B.; Byerly, S.K.; Corn, R. M. Langmuir **1992,** 8, 1992-2000

(23) Lagugne-Labarthet, F.; Yu, T.; Barger,W.R.; Shenoy, D.K.; Dalcanale, E.; Shen,Y.R. Chem Phys Lett**. 2003**, 381, 322-328.

(24) Perrenoud-Rinuy, J.; Brevet, P.F.; Girault, H.H; *Phys Chem Chem Phys.* **2002**,4, 4774-4781.

(25) Choudhury, S. D.; Kumbhakar, M.; Nath, S.; Pal, H. *J. Chem. Phys.* **2007,** 127, (19), 194901(1)-194901(11).

(26) Nag, A.; Bhattacharyya, K. *Chem. Phys. Lett.* **2007**, 169, 12-16.

(27) Nad, S.; Pal, H., *J. Phys. Chem. A* **2001,** 105, (7), 1097-1106.

(28) Belostoskii, A.M.; Aped. P.; Hasner, A. *J.Mol. Struct. (Theochem)* **1997,** 398-399, 427-434.

(29) Benjamin, I. *Chem Rev*. **1996**, 96, (4) , 1449-1476.

(30) Senapati, S.; Chandra, A. *Chem. Phys*. **1998,** 231, (1) 65-80.

(31) Senapati,S.; Chandra, A. *J. Chem. Phys.* **1999**,111,1223-1230.

(32) Hamai, S.; Tamai, N.; Yanagimachi, M.; Masuhara, H. *Chem. Phys. Lett.* **1994,** *229*, 389-393.

(33) Hamai, S.; Tamai, N.; Masuhara, H. *J.Phys. Chem.* **1995**, *99*, 4980-4985.

(34) Pant, D.; Girault, H. H. *Phys.Chem. Chem.Phys.* **2005**, 7, 3457-3463.

(35) Ishizaka, S.; Satoshi, H.; Kim, H.; Kitamura, N.; *Anal.Chem*. **1999**, 71, 3382-3389.

(36) Ishizaka, S.; Ueda, Y.; Kitamura, N. *Anal. Chem.* **2004** 76, 5075-5079.

(37) Zimdars, D.; Dadap, J. I.; Eisenthal, K. B.; Heinz, T. F. *J. Phys. Chem. B* **1999,** 103, (17), 3425-3433.

(38) Yanagimachi, M., Tamai, N. and Masuhara, H.*Chem. Phys. Letts* **1992**, *200*, 469-474.

(39) Zhong, D. P.; Pal, S. K.; Zhang, D. Q.; Chan, S. I.; Zewail, A. H. *Proc. Nat. Acad. Sci. USA*, **2002**, *99*, 13-18.

(40) Wang, H.; Harris, J.M. J.Phys.Chem. **1995**,99, 16999-17004.

(41) Wirth, M. J.; Swinton, D.J.; Ludes, M.D. *J.Phys. Chem. B* **2003**, 107, 6258-6268.

(42) Iler, R.K. *The chemistry of silica*; Wiley: New York, **1979.**

(43) Righetti, P.G.; GElfi, C.; Sebastiano, R.; Citterio, A. *J. Chrom.* A, **2004,** 1053**,** (1-2), 15-26.

(44) Revesz, A.G.; Hughes, H.L. *A Review : J. Non-Cryst. Solids* 2003,328, (1-3), 48- 63.

(45) Rechthaler, K.; Kohler, G. *Chem. Phys.* **1994,** 189, (1), 99-116.

(46) Jones, G.; Jackson, W. R.; Kanoktanaporn, S.; Halpern, A. M. *Opt. Comm.*, **1980**, *33*, 315-320.

(47) Sarkar, N.; Das, K.; Datta, A.; Das, S.; Bhattacharyya, K. *J. Phys. Chem.* **1996**, 100, 10523-10527.

(48) Pal, H.; Shirota, H.; Tominaga, K.; Yoshihara, K.; *J. Chem. Phys.* **1999**, *110*, 11454-11465.

(49) Chu, G.; Yangbo, F. *J. Chem. Soc. Fard. Trans* **1987**, *83*, 2533-2539.

(50) Jones, G., Jackson, W. R., Choi, C.; Bergmark, W. R. *J. Phys. Chem.* **1985**, *89*, 294-300.

(51) Brindza, M.R.; Walker, R.A. *J. Am.Chem. Soc* **2009,**131(17) 6207-6214.

Chapter 2: Fluorescence Theory And Experimental Considerations

2.1. Fluorescence Spectroscopy

Fluorescence is the emission of light from any substance undergoing an electronic transition from an excited state having the same spin multiplicity as the ground state. Most commonly, fluorescence refers to singlet-singlet transitions, i.e. the transitions between the lowest singlet excited state (S_1) and the ground state (S_0). In an excited singlet state an electron in a higher energy orbital is paired (by opposite spin) with a second electron in a lower lying, singly occupied orbital. Relaxation to the ground state is spin allowed and that relaxation leads to fluorescence. Emission processes in most aromatic molecules occur typically with a lifetime of ~ 10^{-9}s.[1]

A Jablonski diagram illustrating processes that can occur after a molecule absorbs a photon is shown in Figure 2.1. A vertical arrow represents the resonant absorption of a photon by a molecule. The timescale for the absorption is faster than 10^{-15} s. Consequently, the excited state of a molecule will initially have the same nuclear geometry as the equilibrium ground state because the nuclei of the molecule move much more slowly than the electron distribution can change. This type of excitation is known as a Frank-Condon process.[2] Following photoexcitation to the Franck-Condon allowed region of the excited state potential energy surface, molecules then relaxes to the equilibrium geometry of the excited electronic state. From the minimum of the excited state, the molecule can relax radiatively producing a photon equal in energy to the separation between the excited state minimum and the ground state corresponding to a geometry that the molecule has when it relaxes.

These considerations predict that excitation energies will always be greater than emission energies and that molecular absorbance will always be blue shifted relative to molecular emission.

For molecules having no unpaired electrons, selection rules require that electronic absorption from the singlet ground state (S_0) can only occur to higher lying singlet states (S_1,S_2 ,etc). Within each electronic state are a multitude of vibrational states that can be closely spaced. Excess vibrational energy resulting from a Franck Condon transition is redistributed on a timescale of 10^{-12} s leaving the molecule at the minimum of the excited state potential energy surface.[3] Typically, fluorescence emission occurs next, usually within 10^{-9} s, as fluorophores return to S_0 from S_1, mirroring the absorption transition. Several other relaxation pathways compete with the fluorescence emission process. The excited state energy can dissipate non-radiatively as heat, the excited fluorophore can transfer energy to another molecule in a second type of non-radiative process known as quenching or molecules can undergo intersystem crossing to the lowest excited triplet sate (T_1). Relaxation of a fluorophore from the triplet excited state (T_1) to the singlet ground state (S_0) is called phosphorescence and it occurs on the 10^{-3} s-10^{2} s timescale.[1] Transitions from a triplet excited state to a singlet state (or vice versa) are spin forbidden so the rate constant for triplet emission is several orders of magnitude slower than fluorescence.

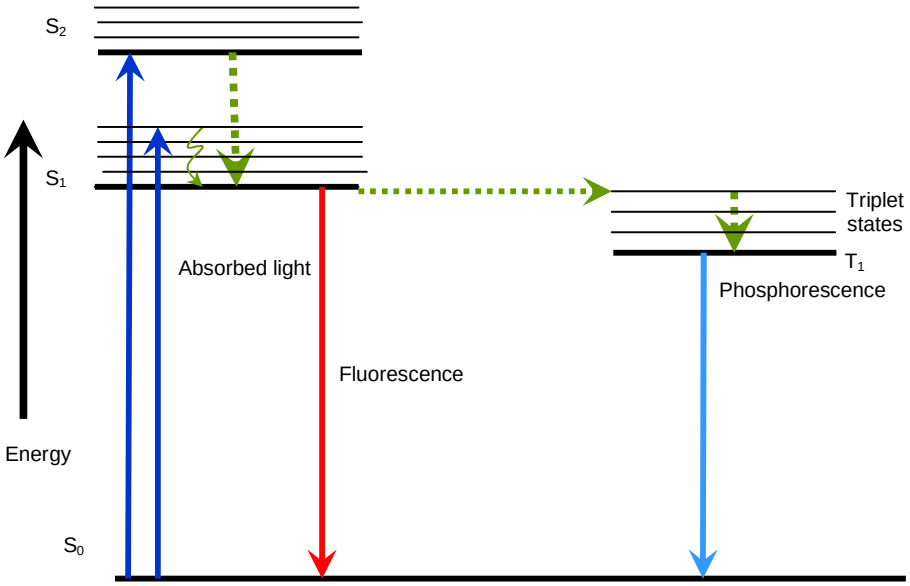

Figure 2.1: Jablonski Diagram outlining schematically the various pathways available to electronically excited molecules.

Research described in this thesis examines the fluorescence of related solutes in a variety of condensed phase environments. For the purposes of this thesis, fluorescence measurements are divided into two types: steady state measurements and time resolved mesurements.

2.1.1. Steady State Bulk Measurements

The most common form of fluorescence measurements are carried out by illuminating the sample continuously and by recording the resulting emission spectrum. Time dependent effects are averaged out in the spectrum. Steady state measurements reveal the energy separations between the electronic ground and the excited states. The difference between the maxima in absorbance and emission energies is known as a fluorophore's Stoke's shift, and this quantity depends both on

the electronic structure of the ground and excited states of the molecule as well as on the local dielectric environment.

In this dissertation all bulk, steady state absorption spectra were recorded using a Hitachi U-3010 UV/vis (resolution 0.5nm) spectrophotometer; the bulk and the surface steady state fluorescence spectra were recorded using Jobin-Yvon Horiba Fluorolog 3 FL3-11. Acquisition parameters were 1 nm/s (scan rate) with slit widths set for 5 nm resolution both for excitation and emission.

Table 2.1. Spectral data for steady state bulk measurements for the coumarins used in this thesis. Gaussian refers to a smooth profile that rises and falls monotonically. A vibronic lineshape shows distinct features corresponding to vibrationaltra nsitions within the electronic transition manifold.

Solute	Solvent	Absorption peak (nm)	Emission peak (nm)	Stoke's shift (cm^{-1})	Absorption spectral feature	Emission spectral feature
C151	Methanol	377	477	5600	Gaussian	Gaussian
C440		350	425	5000	Gaussian	Gaussian
C152		395	511	5800	Gaussian	Gaussian
C461		367	450	5000	Gaussian	Gaussian
C151	Decanol	382	460	4440	Gaussian	Gaussian
C440		355	432	5020	Gaussian	Gaussian
C152		392	492	5190	Gaussian	Gaussian
C461		365	455	5030	Gaussian	Gaussian
C151	Decane	348	400	3736	Vibronic	Vibronic
C440		332	378	3670	Vibronic	Gaussian
C152		367	425	3720	Vibronic	Vibronic
C461		348	395	3420	Vibronic	Gaussian

2.1.2. Steady State Adsorption Measurements

Adsorption studies demonstrate the importance of role of the surface on solute binding and mobility. Steady state adsorption experiments were performed using hydrophilic, fused silica slides (Quartz Scientific, Inc.). Prior to a steady state adsorption experiment, slides were cleaned with a 50:50 (by volume) solution of concentrated sulfuric acid and fuming nitric acid and then thoroughly rinsed with

deionized water. The clean quartz slides were immersed in methanol solutions having different concentrations of a given solute and allowed to equilibrate at 23 ± 1 ˚C for ≥ 12 hours. The slides were then removed slowly from solution and excess solvent was allowed to accumulate on the bottom of the slide. Fluorescence emission spectra were acquired from multiple positions on the top half of the slide using a front-surface sample holder that collected emitted light at an angle of 22^0 relative to the excitation axis. To reduce the scattered light and improve sensitivity, all experiments used crossed polarizers for the excitation and emission light. The data did not show any systematic dependence on the choice of absolute excitation and emission polarizations. Adsorption data were fit to Langmuir isotherms in order to determine free energies of adsorption ΔG_{ads}.[4]

2.1.3. Langmuir Isotherm

Fluorescence intensities from adsorbed films were plotted as a function of bulk solution concentration and the resulting data were fit to a Langmuir isotherm describing adsorption of neutral solutes. Figure 2.2 is a representation of a Langmuir isotherm for coumarin probe used in the present work.

The Langmuir isotherm model describes equilibrium between solutes in solution and solutes bound to the surface.

$$A_{solv} + S_{ads} \Leftrightarrow A_{ads} + S_{solv} \qquad \text{Eq.2.1}$$

where A denotes a solute, S is a solvent and the subscripts x_{solv} and x_{ads} represent molecules in bulk solution and adsorbed to the surface respectively. Solute adsorption

displaces a solvent from the surface. This equilibrium can be described by the constant:

$$K = \frac{[A]_{ads}[S]_{solv}}{[A]_{solv}[S]_{ads}} \qquad \text{Eq. 2.2}$$

This expression can be rearranged and $[A]_{ads}$ can be expressed in terms of $[A]_{solv}$ a modified equilibrium constant K' (where $K' = K/[S]_{solv}$).

$$[A]_{ads} = \frac{K'[A]_{solv}}{K'[A]_{solv} + 1} \qquad \text{Eq. 2.3}$$

In the limit of low bulk concentrations, $[A]_{ads} = K'[A]_{solv}$ thus slope of an isotherm is directly proportional to the adsorption equilibrium constant. ΔG can be readily calculated using the following relation.

$\Delta G_{ads} = -RT \ln K_{eq}$ Eq.2.4

This description breakdown if multilayers form at high $[A]_{solv}$.

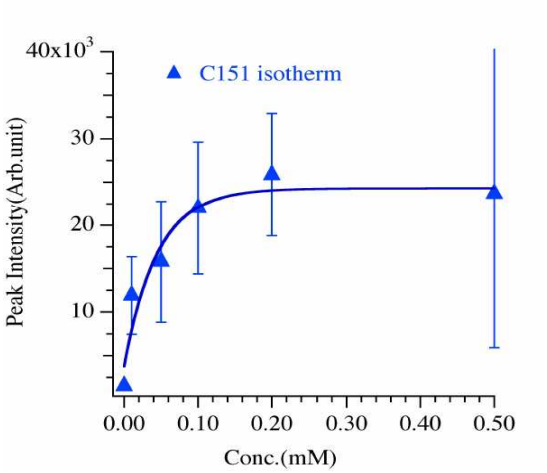

Figure 2.2. A representation of Langmuir Isotherm using a coumarin probe. Concentration refers to the bulk concentration of the particular Coumarin (C151) in methanol. The intensity refers to the peak intensity of the steady state fluorescence emission.

2.1.4. Time-Resolved Measurements

Time resolved measurements measure the rate(s) at which a molecule decays radiatively. At the start of a time resolved measurement, a pulse of light shorter than the fluorescence lifetime excites a sample. The experiment then records how much light is emitted from the sample as a function of time after excitation. For experiments performed in this work, the emitted signals are detected typically over a ~ 50 ns time interval with temporal resolution of ~ 40 ps. Data are analyzed by fitting the emission decay traces with a series of exponential functions where each function has its own unique time constant. These time constants correspond to the lifetimes associated with various processes occurring in a molecule's excited state. Time-resolved measurements carried under Total Internal Reflection Fluorescence (TIRF) spectroscopy assembly are used to study solutes near an interfacial region. In this thesis TIRF measurements were performed at the interface between hydrophilic silica and solutions prepared from various organic solvents. Given the materials and solvents used in this work, TIRF experiments sampled ~70 nm into the organic phase.[5] All data analyses was carried out using routines written in Igor Pro and provided by Dr. Castner from Rutgers University. A summary of all lifetimes measured in this work are presented in Table 2.2.

Table 2.2. Fluorescence Lifetime values in bulk solution. All measurements were made with a 420 nm Long Pass Fliter (LPF). Solute concentrations were kept as low as ~ 10 μM - 50 μM.

Solute	Solvent	A_1	τ_1(ns)	A_2	τ_2 (ns)	Result appear in:
C151	Methanol	1.00	5.26			Ch: 3
C440		1.00	4.00			Ch: 3
C152		1.00	0.90			Ch: 4
C461		1.00	3.22			Ch: 4
C151	Decanol	0.10	0.40	0.90	5.55	Ch: 6
C440		1.00	4.00	-0.20	0.28	Ch: 6
C152		0.17	0.35	0.83	4.17	Ch: 6
C461		1.00	4.00	-0.13	0.21	Ch: 6
C151	Decane	0.16	1.26	0.84	3.33	Ch: 3 and 5
C440		0.15	1.08	0.85	3.45	Ch: 3 and 5
C152		1.00	3.85			Ch: 5
C461		1.00	3.33			Ch: 5

2.2. Fluorescence Lifetime Theory

This technique measures the time elapsed between excitation of a fluorophore and emission of a photon, and thus analyzes the rates of molecular relaxation from excited states to the ground electronic state. This decay profile contains information about the fluorophore relaxation processes. If a single mechanism is responsible for radiative decay, the fluorescence intensity profile of the excited molecules is described with an exponential decay.[1]

$$\left[M^*\right]_t = \left[M^*\right]_0 e^{-t/\tau_m} \qquad \text{Eq 2.5}$$

Here [M*] and $[M^*]_0$ denote the excited state population at time t = t and time t=0 respectively. τ_M the fluorescence lifetime of the sample is related directly to the inverse rate constant for single exponential decay.

The measured fluorescence lifetime can depend on competing decay mechanisms that can be either radiative or nonradiative pathway. If all of the decay

mechanisms are radiative, then the data are fit to a sum of exponential terms with different distinct decay lifetimes. If some mechanisms lead to relaxation via nonradiative processes, then the net effect of the nonradiative processes is to quench fluorescence and the measured fluorescence lifetimes will reflect both the radiative and nonradiative rate constants:

$$\tau_m = \frac{1}{k_{rad} + k_{nonrad}} \qquad \text{Eq 2.6}$$

Here k_{rad} and k_{nonrad} are the rate constants of radiative and non-radiative pathways respectively. Different forms of quenching include excited state reactions, electron transfer, energy transfer, collisional quenching or static quenching. Collisional quenching occurs when the excited-state fluorophore is deactivated by contact with some other molecule in solution, which is called the quencher. Static quenching involves the formation of a complex between the quencher and fluorophore that does not depend on the excited state of the fluorophore.

One direct way to determine the importance of quenching is to measure the quantum yield of a fluorophore. The quantum yield of the fluorophore (Q) is the fraction of photons emitted from a sample relative to the number of absorbed photons. A fluorophore's quantum yield is related to the radiative constant and the nonradiative rate constant of the fluorophore by the following equation:

$$Q = \frac{k_{rad}}{k_{rad} + k_{nonrad}} \qquad \text{Eq 2.7}$$

From fluorescence spectroscopy, one can learn about the effects of local environment on intramolecular electronic structure. In particular, fluoresecence emission can show

quite clearly how a solute's radiative and nonradiative properties are influenced by environmental effects such as polarity, hydrogen bonding and viscosity.

Our studies of solvation at surfaces use both steady state and time-resolved fluorescence measurements to investigate the changes in solute fluorescence caused by solvent polarity and hydrogen bonding as well as the asymmetry induced by solute adsorption to hydrophilic silica surfaces. The primary focus of the next section is to present detailed description of the instrumentation used for the time resolved measurements.

2.3. Time Correlated Single Photon Counting (TCSPC)

This technique measures the time elapsed between excitation of a fluorophore and the emission of a photon, and thus analyzes the rates of molecular relaxation from excited states to the ground electronic state. Each "experiment" measures only a single emission event and data consist of a histogram that plots all of the measured photons as a function of the time at which they were emitted.[6] TCSPC traces will often contain 10^4 individual events in order to produce high quality data that can be fit according to the procedures described above.

2.3.1. Basic Operation of TCSPC

A schematic diagram of the experimental arrangement is given in Figure 2.4. The excitation pulse from the light source and the detector signal both pass through a set of discriminators providing the START and STOP signals to the Time-to-Amplitude converter (TAC). The TAC measure the time difference between the

emission pulse and the next excitation pulse and create and output pulse with amplitude proportional to the time difference. Multi-Channel Analyzer (MCA) operating in pulse height analysis mode sorts these pulses by amplitude into hiostogram of times. A description of the important components of the machines used in the present work is stated below and the related diagrams are displayed in Figure 2.3. The original TCSPC assembly was built by Dr. Amy Petrik and Professor Doug English and was then modified as a part of this research to carry out the TIRF experiments described in Chapters 3-6 of this thesis.

Light Source: The excitation source used in the present study is mode-locked titanium: sapphire laser, tunable over the range 710-920 nm, with a repetition rate of 80 MHz and typical pulse width of the laser is ~100 fs. The laser model employed is the Mai Tai, purchased from Spectra Physics. The light from the source is passed through an optoelectronic modulator, reducing its repetition rate from 80 MHz to 8 MHz. The repetition rate of the laser is decreased by the optoelectronic modulator after dividing it by an integer value. The simplest type of optoelectronic modulator consists of a Pockel cells, which is a voltage- controlled waveplate. Applying a certain voltage to the electro-optical material in the cell causes it to act as a half wave plate, changing the polarization of the incident wave. A polarizer following the Pockel cell selects for one polarization orientation, thus allowing only those pulses that have the proper polarization to pass through the exit polarizer and hence reducing the repetition rate. A driver provides the voltage to the modulator and a synchronous countdown is employed to handle the timing of the pulse train and applied voltage. This output is often frequency doubled by focusing into a β-barium borate (BBO)

crystal to generate ultraviolet-visible (UV-vis) excitation pulses between 355-460nm. Prior, to exciting the sample the light is collimated by a half –wave plate and a vertical polarizer. A filter removes any residual fundamental frequency and the light is directed towards the centre of the cuvette.

Sample Chamber (Figure 2.2): The sample chamber contains the following components set in this direction starting from the light source to the detector:

i. Sample holder; typically holds cuvette
ii. Lens to collect the emitted light
iii. Motorized Emission polarizer set at magic angle (polarization of 54.7^0 with respect to the vertical).
iv. Slit assembly
v. A filter-mount to hold the long pass filter.

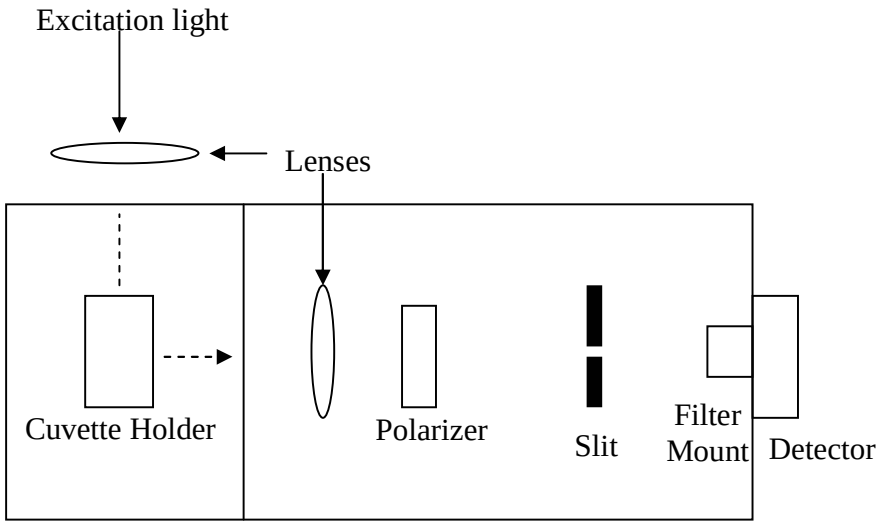

Figure 2.3. The schematic diagram of the sample chamber

Detector: A microchannel plate photomultiplier tube (MCP-PMT) is used as a detector in the present system. The emission is collected at the right angle to direction of excitation lights source. The basic principle on which the detector works is 'photoelectric effect'.[7] Typically MCP photomultipliers consist of a set of thin glass plates with many microchannels leading to a secondary emitting surface.[1] The MCP- PMT provides a better time resolution by reducing the transit time than the traditional PMT. The time that elapses between an electron ejected from a cathode and the arrival of electrons at the anode is called the transit time. The MCP-PMT used in our set-up is R30809U-50 type, which has a transit time < 25 ps.

Constant Fraction Discriminator (CFD): The discriminator improves signal to noise ratios by neglecting PMT pulses of amplitude less than a set level. In other words, input pulses greater than the threshold level will be accepted for further processing and small dark noise pulses from the PMT are ignored.[8-9] It is important to set the discriminator threshold level above than the PMT noise level but below the actual signal level. CFD acts as attenuating the input signal and then this attenuated signal is inverted and added to the delay thereafter, added to the original input pulse. The resultant waveform is a bipolar signal with a zero point crossing. The zero point crossing is the point where the pulse has risen to 20 % of its total intensity.

Time to Amplitude Converter (TAC): The output pulse from the discriminator is fed to the Time to Amplitude Converter (TAC) after passing through a nanosecond delay line as shown in the Figure 2.3. The TAC can be viewed as a stopwatch between the START and the STOP pulses. The TAC can be run in two different modes namely the (i) forward mode and (ii) reverse mode. In forward mode, the

excitation light source acts as the START signal while the pulses from the detector provide the STOP signal. However, at high repetition rate running the TAC in forward mode is a big disadvantage.[8] As TAC gets swamped by the high repetition rate of START pulses it is unable to receive a STOP pulse. This makes TAC busy, being unable to accept another START pulse. To avoid this, for the present experiments reverse mode has been used, where fluorescence signals from the detector and the triggered signals are routed towards the START input of the TAC and the STOP input respectively. Reverse mode of operation is used to minimize the number of "false starts", *i.e*. start signals that have no stop signal within the range of the TAC.

TAC measures the time interval between the start and stop pulse and converts that interval into an output pulse having a voltage proportional to the time interval. Upon receiving the START signal, the capacitor in the TAC is charged leading to the increment of the voltage linearly, until a STOP pulse is detected.

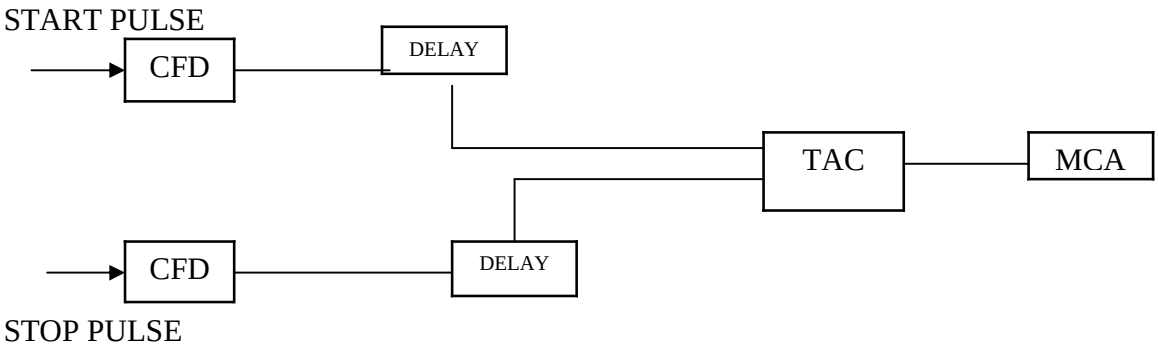

Figure 2.4. The block diagram of different components of TCSPC timing electronics

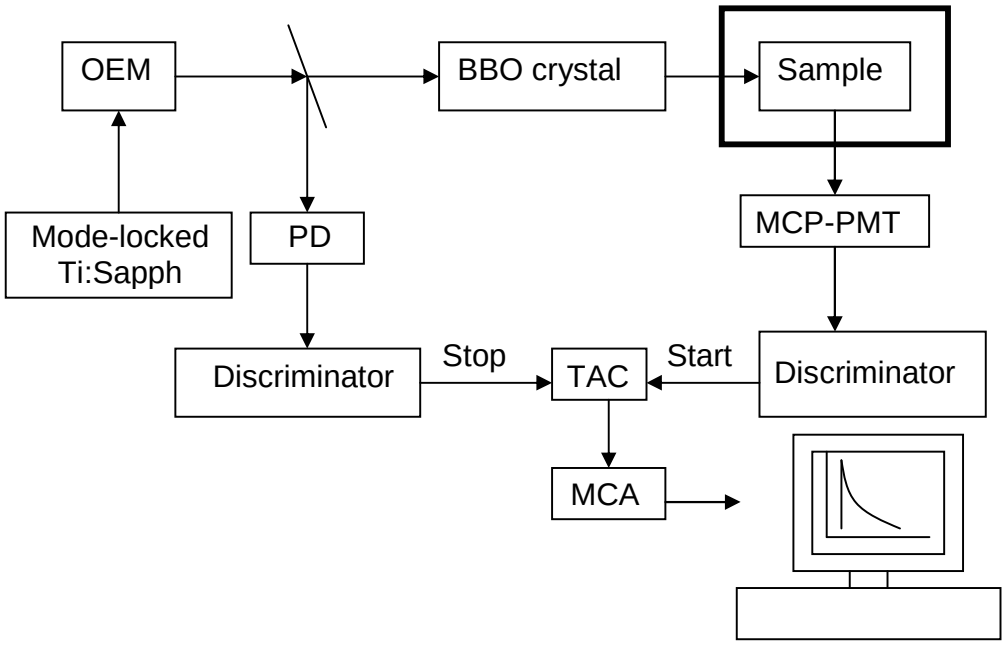

Figure 2.5. TCSPC Block diagram depicting the TCSPC arrangement used in the present project. OEM is the optoelectronic modulator. BBO is the second harmonic crystal. PD is the photodiode. TAC is the time to amplitude converter. MCA is the multi channel analyzer.

Due to the limitations of the detectors and the timing electronics the instrument response to a sample with lifetime zero is non-zero. This short response provides the temporal resolution of the instrument is known as the Instrument response function (IRF).[5] The instrument response function is measured using a nonfluorescing scattering solution made from a nondairy coffee creamer dissolved in water. A typical IRF fwhm obtained from the instrument is ~ 40 ps – 65 ps, shown in Figure 2.5. The instrument response function is convoluted with the response of the fluorescent molecule in the data collected by the instrument.

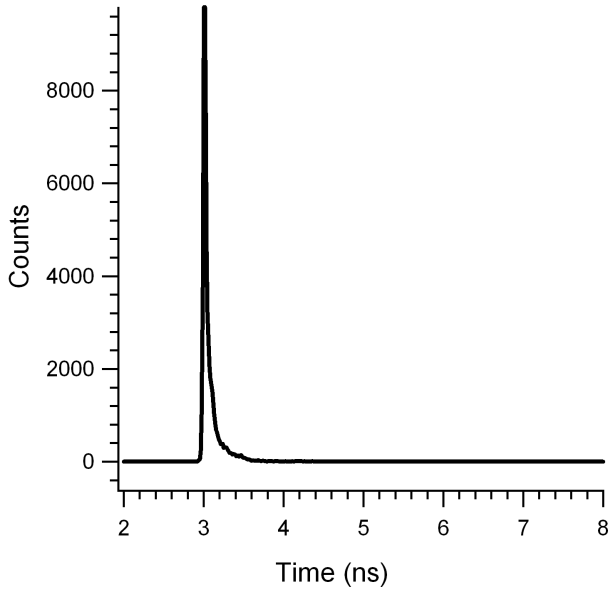

Figure 2.6. An IRF from the TCSPC spectrophotometer. Here, the excitation pulse arrives at ~3 ns and the IRF decays sharply.

2.3.2. Advantages of using TCSPC to meaure Fluorescence lifetimes.

High temporal resolution and large lifetime range: TCSPC can measure lifetimes over a large range extending from ~50 ps to ~50 μs and provides substantial flexibility in the choice of suitable systems and experimental time-windows.[10] Experimental limitations are related to the light source and detector.

Sensitivity: TCSPC measures single photons. Thus the given technique has a high level of detection sensitivity. Moreover, since only one photon is processed at a time, the sample excitation pulses are necessarily of low intensity, resulting in minimum sample degradation and the absence of nonlinear effects.

Low noise and high precession: Typically the TCSPC data are subjected to Poisson noise statistics. The uncertainty of a data set is proportional to the square root

of the the number of photon counts. TCSPC can record single photon as well as signal maxima (~10^4), thus the dynamic range of the measurement is said to be 10^4:1.[10]

The TCSPC technique has been used in a Total Internal Reflection (TIR) geometry to study energy transfer, solute rotation and relaxation dynamics at solid/liquid interfaces. [11-14]

2.4. Total Internal Reflection Fluorescence (TIRF) Spectroscopy

TIRF is a powerful optical technique that can examine the photochemical properties at liquid/liquid and solid /liquid interfaces. Surface selectivity is achieved in TIRF by detecting only the fluorescence signals excited by the evanescent wave created by the excitation field as it reflects from the interface. In a TIRF experiment, an excitation pulse reflects from the interface at an angle greater than the critical angle. The essential conditions of TIR are as follows: [15]

$$n_1 > n_2; \Theta_i > \Theta_{Critical}; \Theta_{critical} = \sin^{-1}(n_2/n_1) \qquad \text{Eq 2.8}$$

Here n_1 and n_2 are refractive index of medium 1 (light travels through this medium) and medium 2 respectively. Θ_i and $\Theta_{critical}$ are the angle of incidence and the critical angle of the two media. An evanescent wave is generated at the point of incidence when the above conditions hold. Briefly, a light beam travels from the higher to the lower refractive index material incidents on the interface at an angle greater than critical angle and excites fluorophores at the surfaces and at the interfaces. Thus, the solute molecules populating the interface are excited by the evanescent wave and fluoresce. The fluorescence intensity *I(z)* at any depth z from the interface is given by,

$$I(z) = CI_0 \exp(-z/d_p) \qquad \text{Eq 2.9}$$

The penetration depth d_p, defined as the distance from the interface is given by the following equation: [15]

$$d_p = \lambda_i /(4\pi n_1[Sin^2\Theta_i - (n_2/n_1)^2]^{1/2}) \qquad \text{Eq 2.10}$$

where λ_i, *and* θ_i are the wavelength of the incident light and the incidence angle respectively. n_1 and n_2 are the refractive indices of two media constituting the interface and $n_1 > n_2$. All experiments described in this work used around 69^0 as the common angle of incidence for TIR measurement.

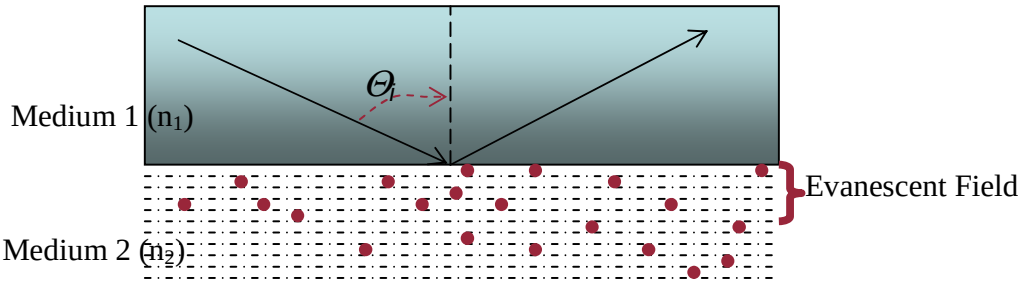

Figure 2.7: Schematic of TIRF; light wave traveled through medium 1 and reflected back to medium 1. The evanescent field is shown here, which penetrates up to ~70 nm in depth.

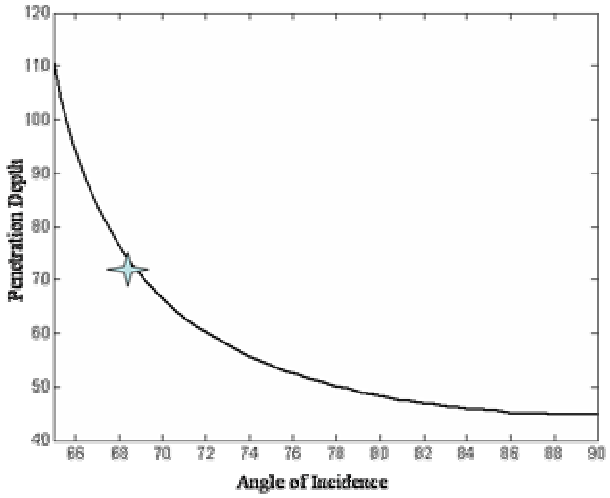

Figure 2.8. Plot of penetration depth vs. incidence angle. For the TIR condition, the excitation wavelength was 390 nm, and the angle of incidence for our experiment ~ 69 ^{0} marked by a 'star'.

2.4.1. Application of TIRF in the present work

A primary objective of this thesis is to compare the relaxation dynamics of adsorbed solutes at a silica/solvent interface to those of solutes in bulk solution. TCSPC using total internal reflection (TIR) geometry is well suited for this purpose and has already been used by a number of other researchers. [11-14] In order to carry out these experiments the sample chamber of the TCSPC instrument has been modified in order to measure the TIR fluorescence of fluorophores at the hydrophilic silica-liquid interface.

In our studies a circular sample-cell is made from Kel-F polymer, containing a concentric well and four peripheral clamping holes. The sample fills the well. A fused silica hemispherical prism (diameter: 1") is sealed to the top of the sample with an O-ring seal. The cell is vertically mounted facing the detector. The light is incident on the interface at an angle greater than critical angle and is focused onto the prism with

a biconvex lens. A cylindrical lens between the prism and the detector focuses the resultant fluorescence signal traveling through the prism into the detector. The PMT tube facing the prism detects the fluorescence. The emission polarizer is set at magic angle ~54.7^0 to eliminate the contribution of molecular reorientation of the fluorescent species. The magic angle was derived in order to avoid the unequal contribution from the in plane and out of plane polarization of light. Figure 2.8 represents the diagram of the cell used in the TIR studies. Figure 2.9 represents the TIR set-up used under the TCSPC mode.

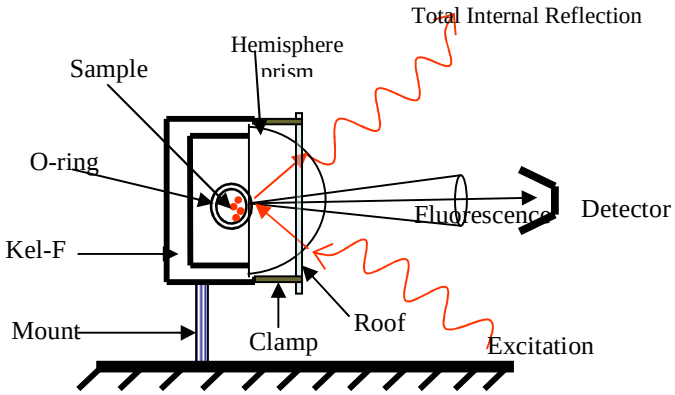

Figure 2.9. Diagram of the cell used in house

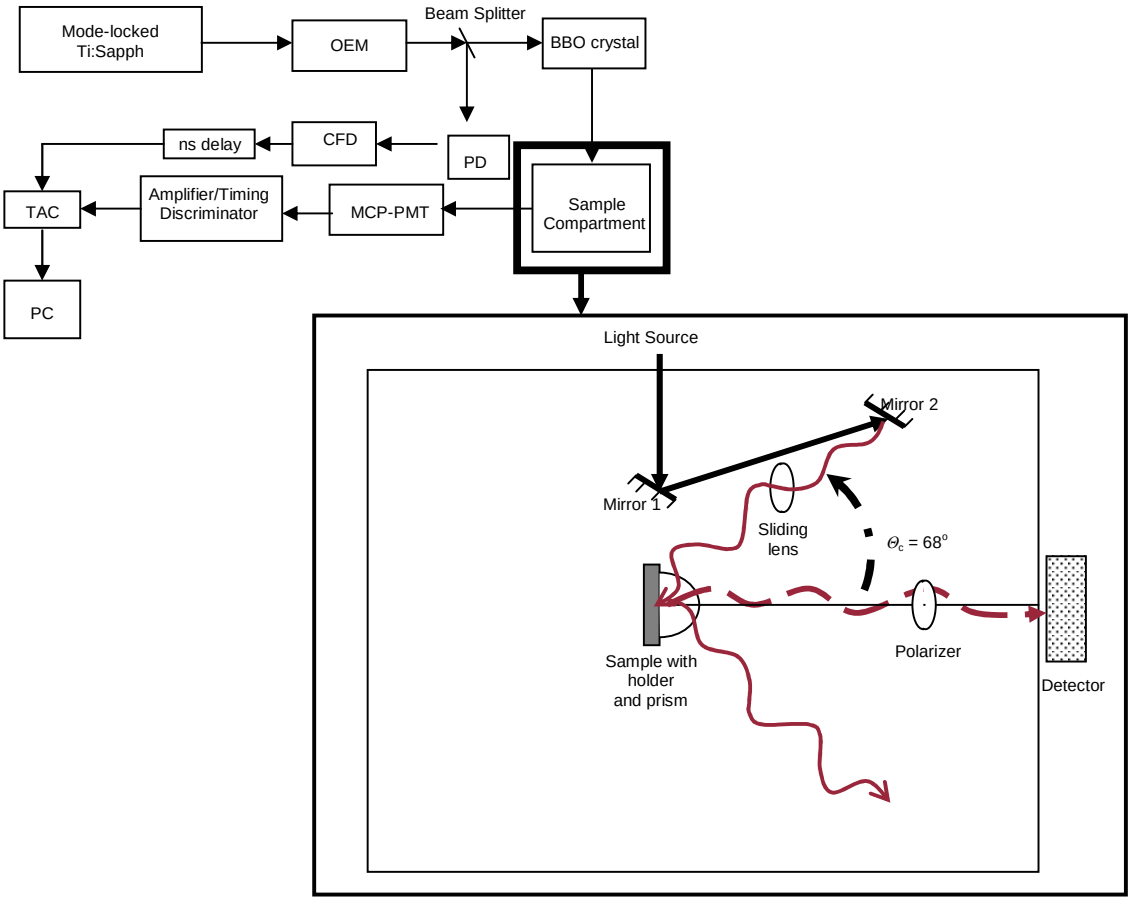

Figure 2.10. The block diagram of TCSPC –TIRF set up showing the modified arrangement of the sample compartment.

The instrument response function (IRF) is the primary factor determining the lower limit of lifetimes that can be measured. In the present set-up, the IRFs from bulk and surface measurements are 40 ps and 65 ps respectively. This result implies that measurements will fail to detect reliably any solvent reorganization processes that occur on timescales faster than the respective IRF limits. The focus of the present study is to examine how different solvent environment affect solute properties. The given instrumental constraint has little consequence for our results given that

fluorescence lifetimes range from 400 ps to ~5.00 ns. However, the reported IRFs do keep us from observing the effects of solvent relaxation in all solvents other than 1-decanol.

References

(1) Lakowicz, J. R.; *Topics in Fluorescence Spectroscopy*; Kluwer Academic / Plenum: New York, **1999**.

(2) Ingle, J.D.; Crouch, S.R. *Spectrochemical Analysis;* Prentice Hall: NJ, **1988.**

(3) Deak, J.C; Rhea, S.T.; Iwaki, L. K.; Dlott,D.D. *J. Phys. Chem. A*, **2000**, 104, 4866-4875

(4) Rosen, M.J., Surfactant and Interfacial Phenomena; *John-Wiley & Sons, Inc.: NJ,* **2004**

(5) Stock, K.;Sailer, R.; Straus, W. S. L.; Lyttek, M.; Steiner, R. Schneckenburger, H. *J. Microscopy-Oxford,* **2003**, 211, 19.

(6) O'Connor, D.V.; Phillips, D. *Time correlated single Photon Counting; Acad. Press:* London, 1984.

(7) Fleming, G.R.; *Chemical applications of ultrafast spectroscopy*, International series of Monongraphs on Chemistry 13; Oxford University Press: 91-95.

(8) Becker, W. Advanced time-correlated single photon counting techniques; *Springe*r: Berlin, Heidelberg, NY, **2005**.

(9) *What is TCSPC*? Technical Note by Edinburgh Instrument

(10) Why TCSPC for Fluorescence Lifetime Measurements? Technical Note by Edinburgh Instruments.

(11) Hamai, S.; Tamai, N.; Yanagimachi, M.; Masuhara, H. *Chem. Phys. Lett.* **1994,** *229,* 389-393.

(12) Pant, D.; Girault, H. H. *Phys.Chem. Chem.Phys.* **2005**, 7, 3457-3463.

(13) Hamai, S.; Tamai, N.; Masuhara, H. *J. Phys. Chem.*, **1995**, **99**, 4980.

(14) Ishizaka, S.; Ueda, Y.; Kitamura, N. *Anal. Chem.* **2004** 76, 5075-5079.

(15) Mirabelle, F.M. Jr. *Internal Reflection Spectroscopy Theory and applications;* Marcel Dekker, Inc.: New York, 1993.

Chapter 3. Decoupling Equilibrium and Time Dependent Solvation at a Solid/Liquid Interface

3.1. Introduction

Solvation in the most general sense describes the interactions of a solute with its surroundings. These interactions may be nonspecific and averaged over the entire solute cavity or specific and arise from localized, directional associations. One can also describe solvation in either an equilibrium or dynamic context. Here, equilibrium solvation refers to solute/solvent interactions that are time-averaged over a statistical distribution of local environments. In contrast, dynamic solvation probes a solute's time dependent response to fluctuating and changing local surroundings. Measurements probing different aspects of a solute's solvation environment usually lead to complementary descriptions of solute/solvent interactions. Occasionally, however, equilibrium and time-resolved experiments tell stories that are at odds with one another.[1-2] In these instances, one must reconsider solvation mechanisms and begin to reconcile the individual molecular properties measured by the different types of experiments. Findings presented in this chapter examine the equilibrium and time dependent fluorescence properties of two, primary amine coumarin dyes, Coumarin 151 and Coumarin 440 (Figure 3.1), in two solvents – methanol and decane – and adsorbed to the silica/methanol interface. Results from these experiments suggest that surfaces can decouple a solute's response to equilibrium solvation forces from its time dependent solvation behavior. C151 and C440 share the same structure except

for a $–CF_3$ (C151) or $–CH_3$ (C440) group at the molecule's 4-position and are ideal probes of equilibrium and dynamic solvation.[3-5]

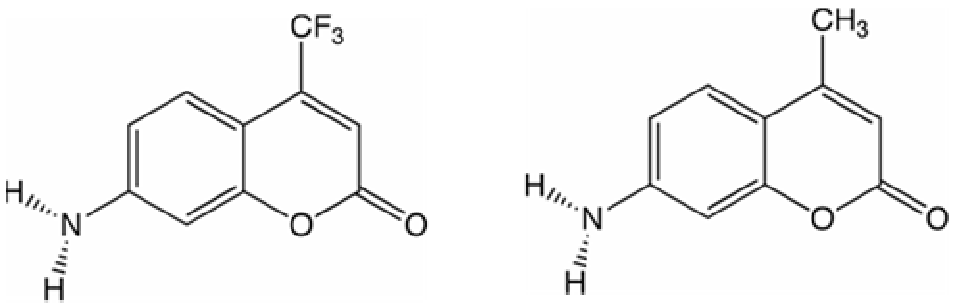

C151 **C440**

Figure 3.1. C151 and C440 ground state (S_0) structures.

In its ground electronic state (S_0) and when excited to its first excited (S_1) electronic state in nonpolar solvents, the amine in the 7-position retains its pyramidal geometry and sp^3 hybridization. Polar solvents, however, can stabilize a charge transfer (CT) state where the nitrogen adopts a planar (sp^2) geometry and the carbonyl oxygen assumes a formal negative charge.[6-8] The intramolecular potential of pyramidal structure for both solutes have a symmetric double well corresponding to the protons of the amine lying above or below the plane of the benzene ring, whereas the amine group of C151 and C440 in the CT state is subject to a single, shallow potential with a minimum when the amine is coplanar with the ring, as shown in Figure 3.2.[9] A schematic representation of the structures of C151 in its pyramidal and charge transfer (CT) state is shown with the potential energy curves in Figure 3.2. C440 will

have similar electronic structure, although the barrier to inversion will be at higher energy for C440 due to the weakly electron-donating $-CH_3$ group. [10-11]

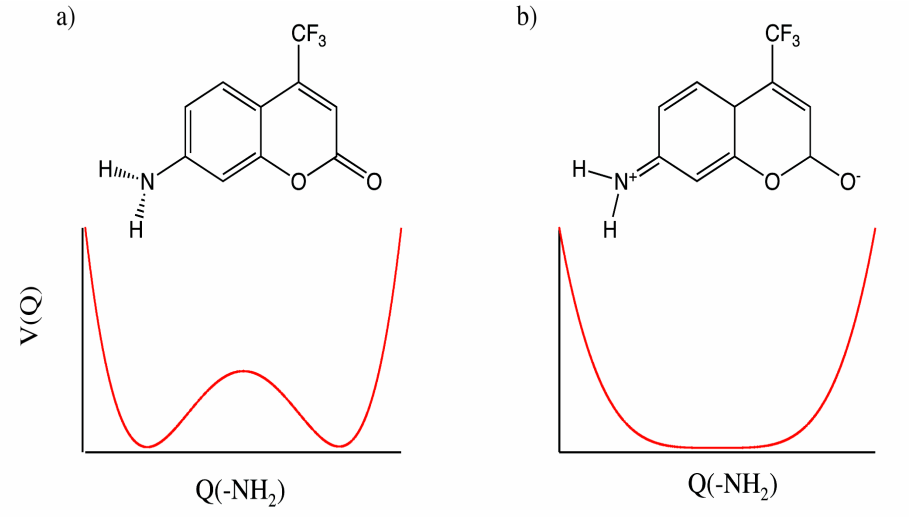

Figure 3.2. Structures of C151 in its pyramidal (a) and planar, charge transfer (CT) state (b). The potential curves below each structure illustrate qualitatively the intramolecular potential along the amine inversion coordinate (Q). Previous studies have calculated a barrier of ~ 4-8 kJ/mole separating the two minima in state (a) of C151.[12]

C151 and C440 both show strong solvatochromic shifts with emission maxima moving to longer wavelengths as solvent polarity increases.[4,13] (Figure 3.3.) Furthermore, the fluorescence lifetimes of both solutes in polar solvents show a single exponential decay arising from a charge transfer (CT) state, but in nonpolar environments, the decay is biexponential due to the emission from the pyramidal conformers and the intermediate CT state.[14]

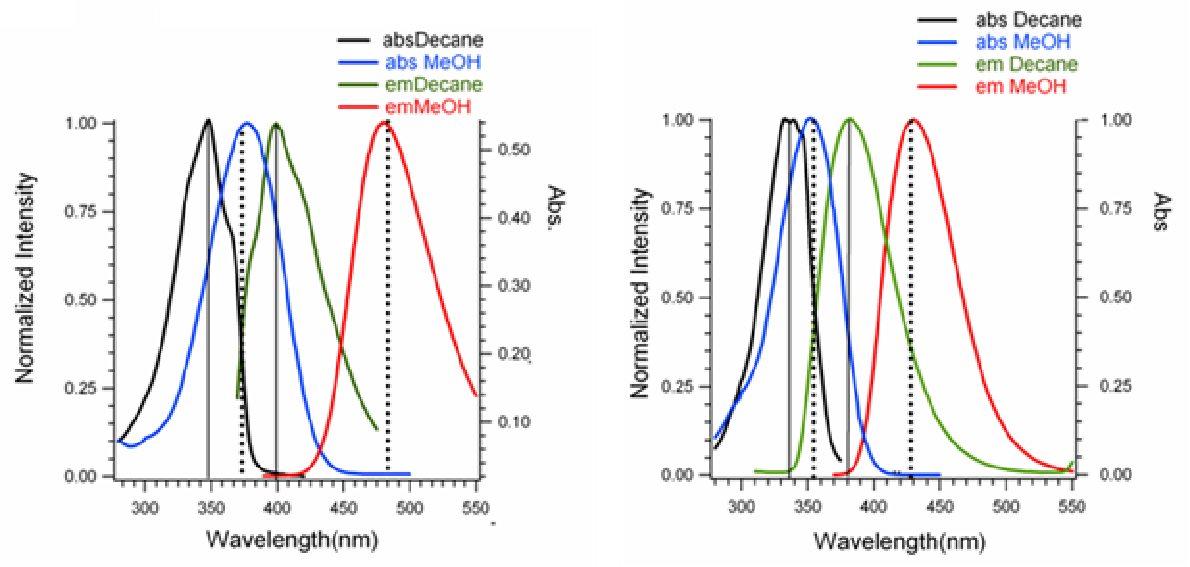

C151 **C440**

Figure 3.3. UV absorbance and steady state emission data for C151 (left) and C440 (right) in decane and methanol. Solute concentrations were ~30 -50 μMolar. Stoke's shifts are reported for for C151 in decane (~ 52nm) and MeOH (~100 nm) and for C440 in decane (~ 45 nm) and MeOH (~ 80 nm).

The surprising observation from findings reported in this chapter is that while the steady state spectra of both solutes adsorbed at silica interface sample a polar environment, the time resolved fluorescence is biexponential with a short lifetime component that matches the shorter lifetime of C151 and C440 in decane. We interpret these differences in terms of the hydrogen bond donating abilities of the silica surface. Solute-substrate hydrogen bonding leads to a polar solvation environment, but substrate rigidity and hydrogen bond donating ability inhibit the solute's ability to form a CT state following photoexcitation. These results illustrate how a surface can create local solvation environments different from bulk solution limits and highlight the ability of a surface to promote unanticipated solution phase surface chemistry.

3.2. Experimental Considerations

Laser grade C151 and C440 were purchased from Exciton and Aldrich, respectively and used as received. All solutions were made using spectral grade methanol (purity >99%). Steady state adsorption experiments were performed using hydrophilic silica slides as described in Chapter 2. Adsorption data were fit to Langmuir isotherms in order to determine free energies of adsorption ΔG_{ads}.[15]

Experiments measuring fluorescence lifetimes used the time-correlated single photon counting (TCSPC) assembly described in Chapter 2. Measurements of C151 and C440 in the near surface region of solid/liquid interfaces required using total internal reflection (TIR) geometry. For both bulk solution studies and TIR studies, the instrument response function measured ~ 40-65 ps (FWHM) and the data allowed for reliable measurements of lifetimes as short as 100 ps. Such constraints did not allow experiments to identify the fast, multi-exponential relaxation processes associated with methanol as a solvent. The excitation light was fixed at 370 nm and the fluorescence emission was collected using a 420 nm long pass filter to block light from the excitation pulse.

Time-resolved fluorescence decays were analyzed assuming multiple, independent exponential pathways following deconvolution with the instrument response function IRF:

$$F(t) = \sum_i a_i e^{-t/\tau_i} \qquad \text{Eq. 3.1}$$

Here *a* is the amplitude of the coefficient and τ is the lifetime of the fluorophore. The single and biexponential nature of fluorescence decays were determined by minimizing the χ^2 values and distribution of the weighted residuals.[16]

3.3. Result and Discussion

3.3.1. Steady State Adsorption Data

Steady state emission spectra of C151 and C440 in bulk methanol, the silica/vapor interface and decane, are shown in Figure 3.4. To acquire spectra from the silica surface, solutes were allowed to adsorb to the solid/vapor interface from a 50 μM methanol solution. Repeating this procedure for methanol solutions having different solute concentrations led to systematic changes in emission intensity (but not in emission wavelength). The peak intensities are plotted vs. bulk concentration in Figure 3.5 Fitting these data to a Langmuir isotherm led to calculated free energies of adsorption, ΔG_{ads}, of -25.7 ± 0.7 kJ/mole and – 24.0 ± 1.1 kJ/mole for C151 and C440 respectively as shown in Figure 3.5. The emission spectra of the solutes adsorbed at silica/vapor interface for different concentrations of bulk solutions are presented in Appendix C. Based on the emission spectra and the Langmuir isotherm, we infer that these primary amine coumarin solutes form monolayers at the silica/methanol interface, but these films do not promote additional adsorption. Furthermore, emission appears to come from monomers rather dimers or higher aggregates that often lead to features in emission spectra at much longer wavelengths.[17-19]

The emission spectra show wavelength maxima of 483 nm (C151) and 433nm (C440) in methanol; 470nm (C151) and 425 nm (C440) at the silica/vapor interface;

and 399 nm (C151) and 378nm (C440) in decane. The emission spectra of both solutes adsorbed to the silica surface correspond to an environment more polar than bulk acetonitrile, a polar non-hydrogen bonding solvent (λ^{C151}_{max} = 460 nm and λ^{C440}_{max} = 412 nm) and less polar than ethanol, a polar hydrogen bonding solvent (λ^{C151}_{max}= 477 nm and λ^{C440}_{max} = 432 nm). This observation is not surprising given that solvation chemistry at hydrophilic silica surfaces is dominated by the hydrogen bond donating properties of the surface silanol groups.[20-22] In principle the amine group on C151 and C440 can also donate hydrogen bonds, but hydrogen bonds donated from the amine solute to the silica surface are expected to be weak.[23]

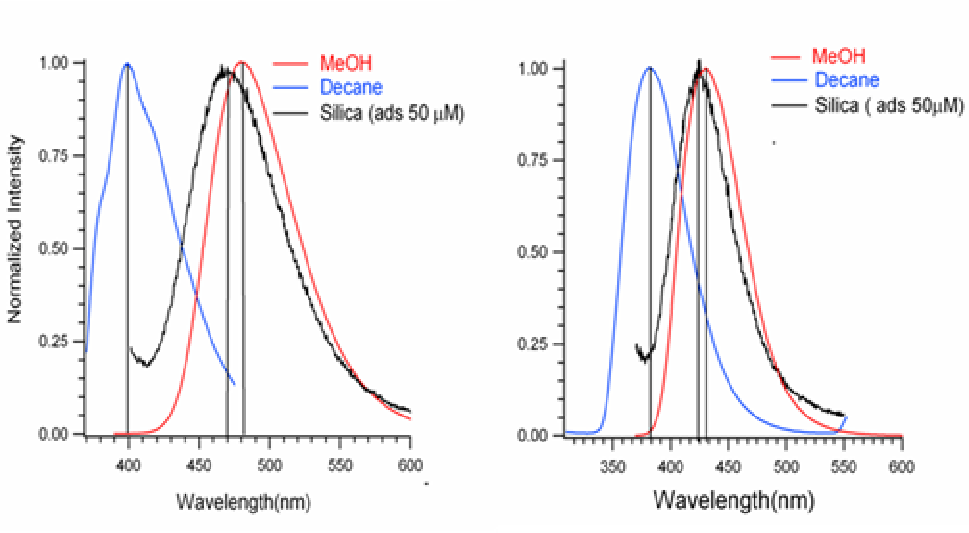

C151 **C440**

Figure 3.4. Emission spectra of C151 and C440 in methanol (red), adsorbed to the silica/vapor interface (black) and decane (blue). Methanol and silica/vapor emission spectra were acquired with an excitation wavelength of 370 nm and 350nm for C151 and C440 respectively. The decane emission was acquired with an excitation wavelength of 350 nm and 340 nm for C151 and C440 respectively. The silica surface was prepared as described in text.

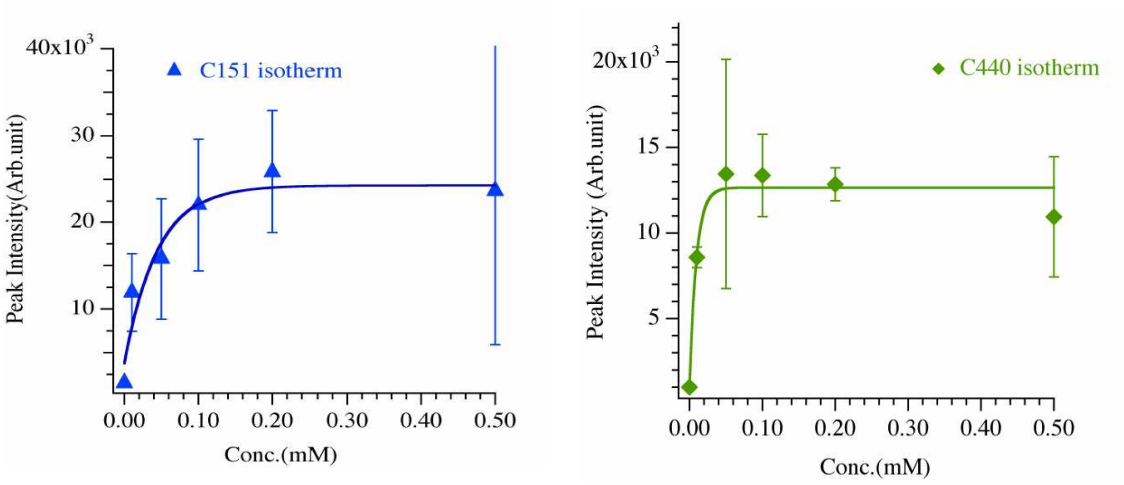

C151 **C440**

Figure 3.5. Adsorption isotherms resulting by plotting the peak emission intensities for different concentrations of C151 and C440 adsorbed at silica surface versus concentration ranging from 0.01mM to 0.5 mM

The results from steady state studies led us naturally to wonder how the time-dependent emission properties of adsorbed solutes would be affected by such strong anisotropy and motivated us to carry out the fluorescence measurements described in this chapter.

3.3.2. Time Resolved Measurements

Time resolved fluorescence experiments using time correlated single photon counting (TCSPC) show that in methanol, C151 and C440 decay with lifetimes of 5.26 ns and 4.00 ns respectively.(Figure 3.6, Table 3.1) These results agree well with previously published reports.[14] . TCSPC data acquired in a total internal reflection (TIR) geometry for the solutes adsorbed to the silica/methanol interface (50 μM) showed a biexponential decay with lifetimes of 1.15 ns (A_1 = 0.27) and 5.30 ns (A_2 = 0.73) for C151 and 1.42 ns (A_1 = 0.23) and 3.85ns (A_2 = 0.77) for

C440 respectively. The longer lifetime for each solute is assigned to those solutes that are either weakly associated with the surface or present in the ~70 nm depth sampled by the evanescent field of the excitation source. The shorter lifetime component is assigned to those solutes interacting directly with the surface.

In nonpolar solvents such as decane, both solutes show biexponential decay with lifetimes of 1.26 ns (A_1= 0.84) and 3.33 ns (A_2 = 0.16) for C151 and 1.08 ns (A_1= 0.15) and 3.45 ns (A_2 = 0.85) for C440 respectively. (Figure 3.7, Table 3.2) These two lifetimes are assigned to the sp^3 hybridized state (shorter lifetime) and the CT state (longer lifetime). Emission from C151 is dominated by the shorter lifetime whereas the longer lifetime is responsible for most of the emission from C440. The origin of this behavior is subtle and will be explored in much greater detail in Chapter 5. For the purpose of comparing C151 and C440 fluorescence in bulk decane with emission from solutes adsorbed to the silica/methanol interface, however, the important result is that significantly shorter lifetimes are characteristic of solvation in nonpolar environments. The shorter lifetime for the solutes in the double well potential likely reflects the effects of a nonradiative relaxation path as the solute interconverts between its two minima shown in Figure 3.2.

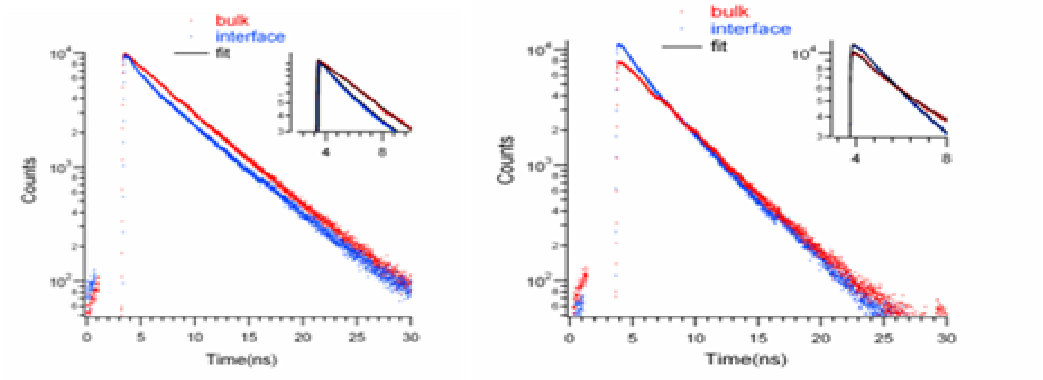

C151 **C440**

Figure 3.6. TCSPC data from C151 and C440 in methanol (red), and adsorbed to the silica/methanol interface (blue) from a 40 µM solution. The excitation wavelength was fixed at 370 nm for both the solutes. The insets represents the biexponential nature of the silica/methanol interface curve.

Table 3.1. Lifetimes and amplitudes of TCSPC decay traces shown in Figure 3.6. Uncertainties in lifetimes and amplitudes are ± 90 ps and ± 1%, respectively. Details about data acquisition and fitting can be found in Reference 24

Medium	Solute	A_1	τ_1 (ns)	A_2	τ_2 (ns)	χ^2
MeOH (Bulk)	C151	1.00	5.26	-	-	1.2
	C440	1.00	4.00	-	-	1.2
Silica/MeOH Interface	C151	0.27	1.15	0.73	5.30	1.1
	C440	0.23	1.42	0.77	3.85	1.3

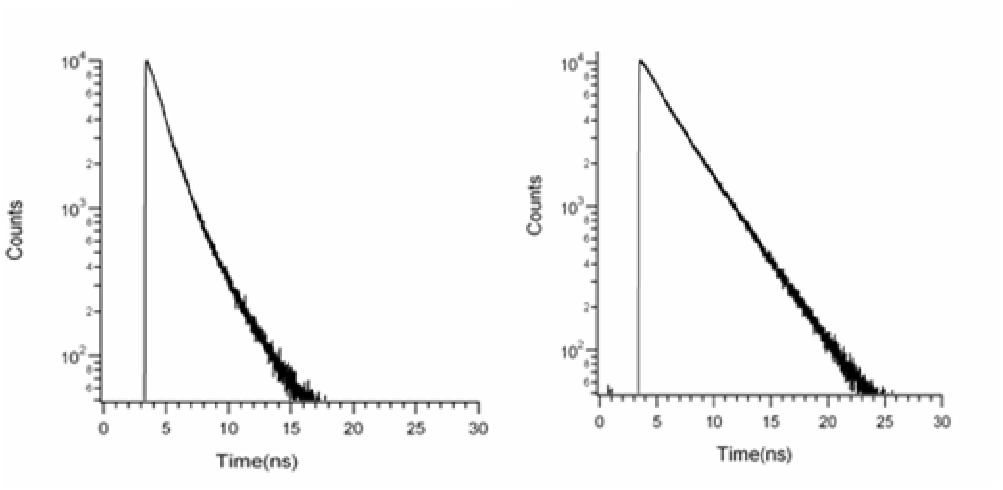

C151 **C440**

Figure 3.7. Fluorescence decay of C151 and C440 in bulk decane (10 μM). The excitation wavelength was fixed at 360 nm.

Table 3.2. Lifetimes and amplitudes of TCSPC decay traces shown in bulk decane. Uncertainties in lifetimes and amplitudes are ± 90 ps and ± 5%, respectively

Solute (Solvent)	Conc.	A_1	τ_1 (ns)	A_2	τ_2 (ns)	χ^2
C151 (Decane)	10μM	0.84	1.26	0.16	3.33	1.3
C440(Decane)	10μM	0.15	1.08	0.85	3.45	1.4

Here, χ^2 is used to measure the accuracy of the fit.

$$\chi^2 = \frac{1}{N}\sum_{i=1}^{N}\frac{(y_i - \alpha_i)^2}{\alpha_i} \qquad \text{Eq.3.2}$$

where y is the observed outcome, α is the expected outcome, and N is the number of observations.

The short lifetime observed in the TIR data is very close to the short lifetime component of the bulk decane decay, despite the fact that the solvent (methanol) and the surface (hydrophilic silica with terminated silanol groups) are both considered to

be polar.[25-27] Shortened fluorescence lifetimes are often ascribed to the introduction of new, nonradiative pathways that allow the excited state relaxation to the ground state.[28] However, previous studies have shown that surface-induced, nonradiative relaxation leads to non-exponential, quasi-continuous decays.[29-31] In contrast, the time dependent fluorescence observed from C151 and C440 in the TIR measurements is distinctly bi-exponential with very small residuals and a short lifetime component that matches almost exactly the short lifetimes of C151 and C440 in nonpolar, alkane solvents.

Similar behavior observed for C152 and C461 will be discussed in Chapter 4. Given the similarities between emission behavior at the silica/methanol interface and emission in bulk decane *and* the apparent generality of this phenomenon for both primary and tertiary 7AC species, we believe that any mechanism specifically invoking surface quenching of excited adsorbed solutes is unlikely. Rather, we believe that strong hydrogen bond donation from the surface silanol groups to the adsorbed fluorophores keeps the species trapped in a double-well potential and unable to form the CT state generally observed in polar media. Previous work investigating coumarin solutes adsorbed to silica surfaces has shown strong bonding between hydrophilic silica surfaces and the adsorbed coumarin solutes resulting in modifying the time resolved properties of the dye molecule.[32]

Any spectroscopic experiment carried out in a total internal reflection (TIR) geometry will necessarily probe molecules at the surface as well as those molecules in the "bulk" solution that fall within the distance spanned by the evanescent wave. The data reported in Figure 3.6 and in Table 3.1 can contain contributions from both

species - bulk *and* adsorbed. Given that under TIR conditions the evanescent wave of the excitation light extends ≥ 50 nm into the methanol solution, we assign the longer-lived component observed in the TIR data to those solutes either solvated in bulk methanol or solutes that are interacting only weakly with the silica surface. The shorter-lived component assigned to sp^3 hybridized solutes interacting directly with the surface are likely accepting hydrogen bonds from the surface silanol groups. The short lifetime observed in the TIR data is very close to the short lifetime component of the bulk decane decay leads us to conclude that those C151 and C440 solutes interacting directly with the polar silica/methanol interface are subject to excited state photophysics similar to those experienced in a nonpolar solvation environment. At the silica surface amines are known to be active participants in interfacial acid-base chemistry with the surface silanol groups serving as Lewis acids.[33] Calorimetry experiments with model amines (not coumarins) measure adsorption energies as large as 65 kJ/mole.[33] Such strong binding will create a polar equilibrium environment but will also constrain adsorbed C151 and C440 to a pyramidal geometry about the amine even after photoexcitation. Fluorescence decay, then, will reflect a surface stabilized conformation in polar surroundings that has the amine restricted to a (less polar) nonplanar conformation.

In summary we propose that specific substrate/solute hydrogen bonding decouples the equilibrium from the time dependent solvation behavior of C151 adsorbed to the silica/methanol interface. The high dipole density formed by the surface silanol groups renders the interface polar (as evidenced in a large Stokes shift in the adsorbed C151 emission). However, these same hydrogen bonding moieties are

not mobile and hydrogen bonding to the C151 and C440 solutes (through the amine lone pair) keeps the molecular conformation restricted to a sp^3 geometry after photoexcitation. The observed time dependent fluorescence reflects this constraint with a measured lifetime that is more consistent with solvation in a nonpolar environment. In this way, the steady-state and time-resolved data do not have to be (and appear not to be) correlated. Experiments probing C151 and C440 solvation at silica surfaces show that solutes sample apparently contradictory environments depending on whether the property of interest corresponds to equilibrium or time-dependent behavior. A hydroxyl terminated silica surface and bulk methanol – can create an environment that induces dynamic behavior of adsorbed solutes representative of nonpolar environments. These results can be reconciled with each other but only after considering explicit solute-surface and solute-solvent interactions. The findings presented above do not support a model that includes strong solute-solute interactions.

3.4. Conclusions

Steady state and time-resolved fluorescence measurements have been carried out to compare the interfacial solvation behavior of C151 and C440 in bulk methanol solution and adsorbed to polar silica surfaces. Steady state data revealed that solutes adsorbed to the silica/vapor interface is subject to a moderately polar environment but the time-dependent properties of the adsorbed solutes favored a nonpolar environment. The biexponential fluorescence decay we observe from C151 and C440 adsorbed to a silica/methanol interface decay matches the lifetime of the solutes in a

nonpolar solvent reflecting the constraints of the surroundings. These findings are expressed in terms of ability of silica surface to donate hydrogen bonds that keeps the amine groups constrained to a pyramidal geometry, despite the fact that in bulk polar environments, the planar geometry corresponding to a charge transfer state is favored. Strong hydrogen bonding from the substrate and the inability of the substrate to move limits the conformational freedom of the adsorbed solute making the CT state inaccessible at the surface. Taken together, these results motivate the need to study further localized interfacial effects on solution-phase photochemistry and isomerization.

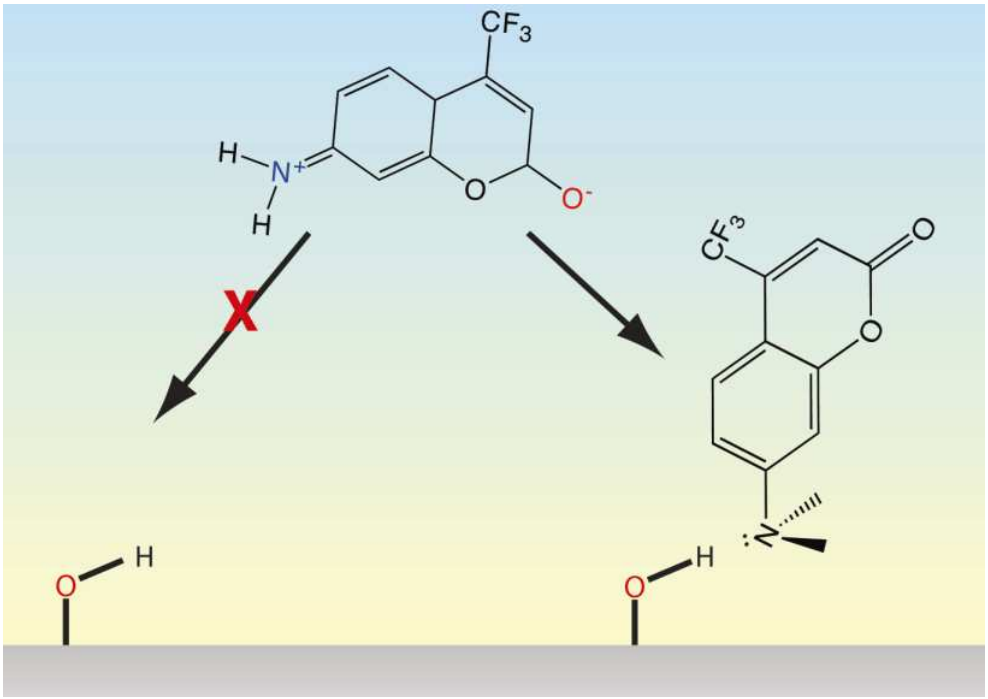

Figure 3.8. A schematic picture illustrating Coumarin 151 in its excited charge transfer (CT) state. Polar solvents (such as methanol) stabilize this excited state conformation. However, a polar, hydrophilic silica surface stabilizes the pyramidal (non-CT) state of C151 adsorbed directly to the interface. Steady state emission indicates that solute adsorbed to the surface experiences a polar environment but time-resolved emission suggests a dynamic solvation environment that resembles that created by nonpolar alkanes.

References

(1) Horng, M. L.; Gardecki, J. A.; Papazyan, A.; Maroncelli, M. *J. Phys. Chem.* **1995**, 99, 17311-17337.

(2) Horng, M. L.; Gardecki, J. A.; Maroncelli, M. *J. Phys. Chem. A* **1997,** 101, 1030-1047.

(3) Rechthaler, K.; Kohler, G. *Chem. Phys.* **1994,** 189, 99-116.

(4) Sharma, V. K.; Saharo, P. D.; Sharma, N.; Rastogi, R. C.; Ghoshal, S. K.; Mohan, D. *Spectrochim Acta Part a-Mol. and Biomol. Spect.* **2003,** 59, (6), 1161-1170.

(5) Nemkovich, N. A.; Reis, H; Baumann,W. *J. Lumin.* **1997**, 71, 255-263

(6) Satpati, A.; Senthilkumar, S.; Kumbhakar, M.; Nath, S.; Maity, D. K.; Pal, H. *Photochem. Photobio.* **2005,** 81, 270-278.

(7) Nad, S.; Kumbhakar, M.; Pal, H. *J. Phys. Chem. A* **2003,** 107, (24), 4808-4816.

(8) Barik, A.; Nath, S.; Pal, H. *J. Chem. Phys.* **2003,** 119, (19), 10202-10208.

(9) Daisuke, K.; Arora, P.; Nakayama, A.; Noro, T.; Gordon, M.S.; Taketsugu,T. *International. J. Quant. Chem.* **2009,** 109, 2308-2318.

(10) Belostoskii, A.M.; Aped. P.; Hasner, A. ; *J.Mol. Struct. (Theochem)* **1997,** 398-399, 427-434.

(11) Oki, M. *Application of Dynamic NMR spectroscopy to Organic Chemistry; VCH: Deerfield Beach*, **1985**.

(12) Cave, R. J.; Burke, K.; Castner, E. W. *J. Phys. Chem. A* **2002**, 106, 9294-9305.

(13) Arbeloa, T. L.; Arbeloa, F. L.; Arbeloa, I. L. *J. Lumin.* **1996,** 68, 149-155.

(14) Nad, S.; Pal, H. *J. Phys. Chem. A* **2001,** 105, 1097-1106.

(15) Rosen, M.J. *Surfactant and Interfacial Phenomena*; *John-Wiley & Sons, Inc.: NJ*, **2004.**

(16) O'Connor, D.V.; Phillips, D. *Time correlated single Photon Counting; Acad. Press:* London, **1984.**

(17) Lindrum,M.; Glismann, A.; Moll, J.; Daehne, S. *Chem. Phys*. **1993**, 178,423-432.

(18) Moll, J.; Daehne, S.; Durrant, J. R.; Wiersma, D. A. *J Chem Phys.* **1995,** 102, (16), 6362-6370.

(19) Ichino, Y.; Minami, N.; Yatabe, T. *J. Lumin.* **2000,** 87-9, 727-729.

(20) Brindza, M.R.; Walker, R.A. *J. Am. Chem. Soc.* **2009**, 131, 6207-6214.

(21) Suratwala, T.; Gardlund, Z.; Davidson, K.; Uhlmann, D. R.; Watson, J.; Peyghambarian, N. *Chem Mater.* **1998,** 10, (1), 190-198.

(22) Hair, M. L.; Hertl, W. *J. Phys. Chem.* **1969,** 73, (12), 4269-4276.

(23) Carlson, H. A.; Nguyen, T. B.; Orozco, M.; Jorgensen, W. L. *J. Comp. Chem.* **1993,** 14, 1240- 1249.

(24) Grimes, A. F.; Call, S. E.; Vicente, D. A.; English, D. S.; Harbron, E. J. *J. Phys. Chem. B* **2006** , 110, 19183-19190.

(25) Avnir, D.; Levy, D.; Reisfeld, R. *J. Phys. Chem.* **1984,** 88, (24), 5956-5959.

(26) Avnir, D.; Kaufman, V. R.; Reisfeld, R. *J. Non-Crys. Solids* **1985,** 74, (2-3), 395- 406.

(27) Knobbe, E. T.; Dunn, B.; Fuqua, P. D.; Nishida, F. *App. Optics* **1990,** 29, (18), 2729-2733.

(28) Turro, N. J. *Modern Molecular Photochemist;*University Science Books: **1991.**

(29) Lee, M.; Kim, J.; Tang, J.; Hochstrasser, R. M. *Chem. Phys. Lett.* **2002**, 359, 412-419.

(30) Ambrose, P. W.; Goodwin, P. M.; Martin, J. C.; Keller, R. A. *Science* **1994** 265, 361-364.

(31) Wang, H.; Harris, J.M. *J. Phys. Chem*. **1995**, 99, 16999-17004.

(32) Gu, G.; Ong, P.P.; Li, Q. *J. Phys. D.: Appl. Phys.* **1999,** 32, 2287-2289

(33) Cook, W.G.; Ross, R. *A Canadian Journal of Chemistry* **1972**, 50, 1666 -1674.

Chapter 4: Surface Induced Changes in Coumarin Isomerization at Polar Solid/Liquid Interfaces

4.1. Introduction

Few families of molecules have had their photochemistry examined more closely than the substituted coumarins.[1-15] Motivating this attention are several properties common to most coumarin molecules: coumarins tend to be photochemically stable with high quantum yields making them suitable for use as laser dyes and markers in fluorescence assay experiments.[3-5] Furthermore, certain coumarin dyes undergo large changes in permanent dipole upon photoexcitation making these molecules very sensitive probes of solvent polarity and solvation dynamics.[8-10,16-19] Finally, the basic coumarin structure can be easily modified in a number of locations and with a variety of functional groups leading to solvatochromic shifts of excitation and emission wavelengths by more than 100 nm across the visible and near-UV regions of the optical spectrum.[1,7, 15]

Of the different types of coumarins, the 7-aminocoumarin family (7AC) is particularly popular as a probe of solvation.[9,16-19] 7-aminocoumarins can form several different resonance structures upon photoexcitation including a charge transfer (CT) state with the nitrogen adopting a planar (sp^2 hybridized) geometry provided that the amine is not conformationally restricted. The electronic state having charge transfer character also places a formal negative charge on the carbonyl oxygen at the 2-position. These CT states typically have high quantum yields, longer fluorescent lifetimes and are most stable in polar solvents. An exception to this pattern occurs

when formation of a CT state is also accompanied by large amplitude, intramolecular conformational changes. Based on time resolved fluorescence and transient absorbance measurements, Nad[11] *et al.* proposed the existence of a non-fluorescent, twisted intramolecular charge transfer (TICT) state for some 7AC dyes having a $–CF_3$ group in the 4-position. A $–CF_3$ group increases the electron withdrawing character of the heterocyclic ring and can stabilize charge transfer and TICT states following photoexcitation especially in polar solvents where dipolar interactions can also serve to stabilize the cationic amino group.[2,20] Cave and Castner's *ab initio* studies of different 7ACs in their ground and excited electronic states provide additional insight into the dependence of electronic state structure on molecular structure and functional group composition.[21, 22] Based on energetic considerations these computational results indicated that TICT formation is unlikely following photoexcitation in the gas phase, but the presence of explicit aqueous solvents stabilized a planar geometry for 7AC species in the S_1 excited state.

The present study examines how polar silica surfaces can affect the photophysical behavior of two different 7AC solutes, Coumarin 152 (C152) and Coumarin (C461). Both solutes are N, N dimethyl substituted tertiary amines. C152 has an electron withdrawing $–CF_3$ group in the 4 position while C461 has a weakly electron donating $–CH_3$ group in the same position. (Figure 4.1) In general, coumarin photochemistry at surfaces has received less attention than solvation in bulk. Studies of solvation dynamics around coumarins adsorbed to the surfaces of reverse micelles revealed that water relaxation following coumarin photoexcitation is much slower than in bulk.[23] Similar results were inferred by Zimdars, *et al.* who measured

reorientation times of coumarins adsorbed to an aqueous/air interface.[24] These latter studies employed resonance enhanced, second harmonic generation (SHG) to quantify how in-plane vs. out-of-plane solute reorientation rates differed for C314 adsorbed to an air-water interface. These studies found that surface reorientational times are slower than bulk orientational diffusion times. Time-resolved fluorescence spectroscopy was used by Yamashita and coworkers to examine solvation dynamics of coumarin 343 at a water/mica interface. Data again showed that the solvent relaxation at the water/mica interface was much longer than observed in bulk solution.[25]

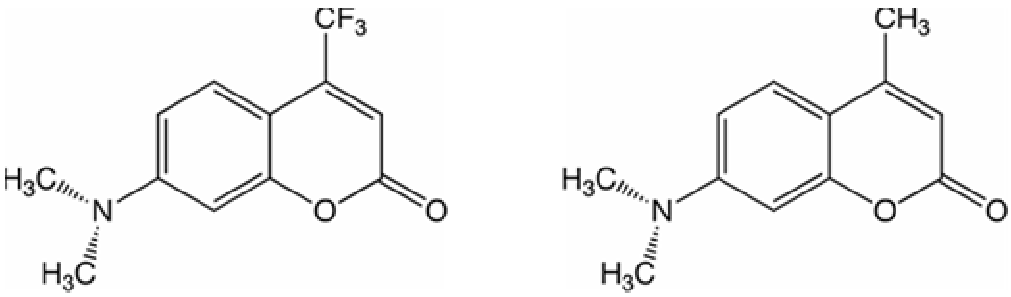

C152 **C461**

Figure 4.1. Structure of C152 and C461

While these findings provide detailed insight into reorientation of coumarins and surrounding solvent molecules, they do not address directly whether or not the photophysical properties of the adsorbed coumarins themselves change as a result of interfacial anisotropy. Such concerns may not be relevant for rigid 7AC species such as C314 or C343 (See, Chapter 7) but for unrestricted 7ACs that can undergo facile

inversion about the amino group, electronic structure and relaxation should be extremely sensitive to local asymmetry. Differences between bulk and interfacial solvation can have dramatic changes on solute properties where a transition state might be rendered inaccessible due to steric constraints *or* stabilized by surface mediated solvent-solute interactions. For example, using time resolved SHG Shi[26] *et al.* explored the photoisomerization of malachite green at air/aqueous, alkane/aqueous and silica/aqueous interfaces. The isomerization dynamics were 3-5 fold slower at air/aqueous and alkane/aqueous interfaces in comparison to bulk aqueous environments. The same solute isomerization rate was slower by an order of magnitude at a silica/aqueous interface compared to the bulk water limit. The slower isomerization dynamics at the silica/aqueous interface were attributed to the structure imposed on the interfacial solvent by the silica surface.

Experiments described below examine the steady state and time dependent photophysical behavior of C152 and C461 in bulk methanol solution and adsorbed to silica/methanol surfaces. Steady state and time-resolved fluorescence methods are used to examine the spectroscopic and lifetime properties of these two 7AC solutes in bulk methanol solutions and adsorbed to silica/vapor and silica/methanol interfaces. Results from bulk solution measurements show that despite similar steady-state emission behaviors in methanol, C152's fluorescence lifetime is markedly shorter than that of C461 indicating that nonradiative pathways play a larger role in the electronic relaxation of the $-CF_3$ substituted solute. At silica surfaces, C152 exhibits markedly different behavior compared to both C461 (bulk and surface) and C152 in bulk methanol. At surface coverages in excess of 1 monolayer, C152 emission shows

a second feature in the steady state spectrum at longer wavelengths consistent with the formation of extended surface aggregate structures. Such features are absent from the C461 emission spectra at all surface coverages. The lifetime of C152 solutes emitting at long-wavelength is similar to that of monomers solvated in a polar environment where TICT formation is the dominant (nonradiative) pathway. In contrast molecules adsorbed directly to the silica/methanol surface show a 5-fold longer fluorescence lifetime characteristic of solvation in nonpolar media, indicating that the surface sterically hinders C152 isomerization in the excited state. In contrast, the time-resolved emission of C461 adsorbed to the silica surface is virtually indistinguishable from that observed in bulk solution.

4.2. Experimental Considerations

Laser grade C461 and C152 were purchased from Exciton and Aldrich, respectively and used as received. All solutions were made using spectral grade methanol (purity >99%). The bulk, steady state absorption spectra were recorded using a Hitachi U-3010 UV/vis spectrophotometer and steady state fluorescence spectra were recorded using Jobin-Yvon Horiba Fluorolog 3 FL3-11 (Figure 4.2). The values are listed in Table 4.1.

Adsorption data were fit to Langmuir isotherms[27] in order to determine free energies of adsorption (ΔG_{ads}). Experiments measuring fluorescence lifetimes used a time-correlated single photon counting (TCSPC) assembly described in Chapter 2.[28] Measurements of C152 and C461 in the near surface region of solid/liquid interfaces required using a total internal reflection (TIR) geometry. For both bulk solution

studies and TIR studies, the instrument response function measured ~ 40-65 ps (FWHM) and the data allowed for reliable measurements of lifetimes as short as 100ps Such constraints did not allow experiments to identify the fast, multi-exponential relaxation processes associated with methanol as a solvent.[17] Time-resolved fluorescence decays were analyzed assuming multiple, independent, single exponential pathways following deconvolution with the instrument response function IRF:

$$F(t) = \sum_i a_i e^{-t/\tau_i} \qquad \text{Eq. 4.1}$$

The IRF was obtained from a dilute scattering solution. The single and bi-exponential nature of fluorescence decays were determined by minimizing the χ^2 values and distribution of the weighted residuals.[29]

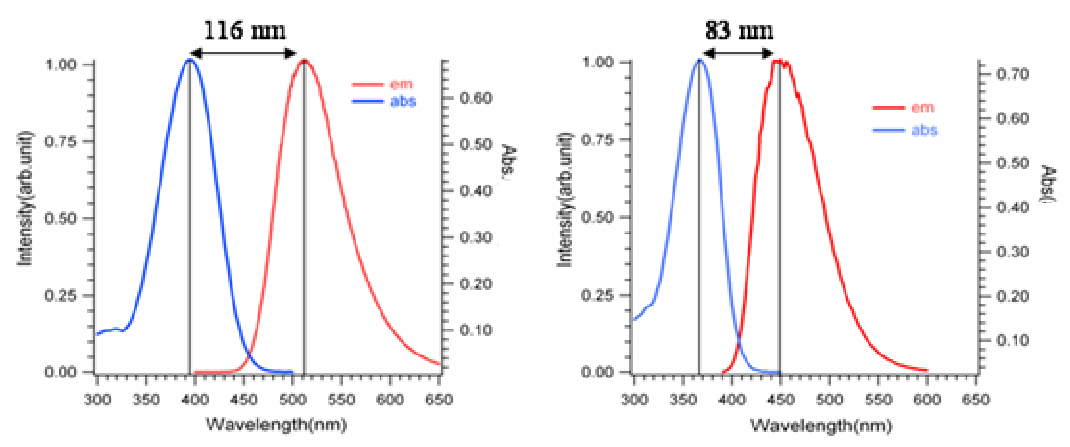

C152 **C461**

Figure 4.2. Absorption and emission spectra of C152 and C461 in bulk methanol

Table 4.1: Spectral data of C152 and C461 in bulk methanol

Probe	Solvent	Absorption peak wavelength (nm)	Emission peak wavelength (nm)	Stokes shift (cm^{-1})
C152	MeOH	395	511	5800
C461		367	450	5000

4.3. Results

4.3.1. Steady State Adsorption Spectra and Langmuir Isotherms

Figure 4.3 shows the emission spectra of C152 and C461 adsorbed to hydrophilic silica/vapor surfaces from solutions having different concentrations. Several observations stand out. First, at low concentrations both C152 and C461 emissions are characterized by single features centered at 495 nm and 448 nm, respectively. These emission wavelengths correspond to polar media having effective dielectric constants similar to those of short chain alcohols. Second, emission intensities reach a plateau at bulk concentrations above ~15 μM before rising again at concentrations ≥ 100 μM. (Figure 4.4). Third, emission shifts to longer wavelengths with increasing surface coverage, suggesting that increased adsorption creates an even more polar environment within the adsorbed film. Fourth, at higher concentrations the C152 spectra show a second feature appearing at a much longer wavelength (~574 nm). In contrast, the C461 spectra from films formed in high concentration solutions continue to be characterized by a single emission wavelength.

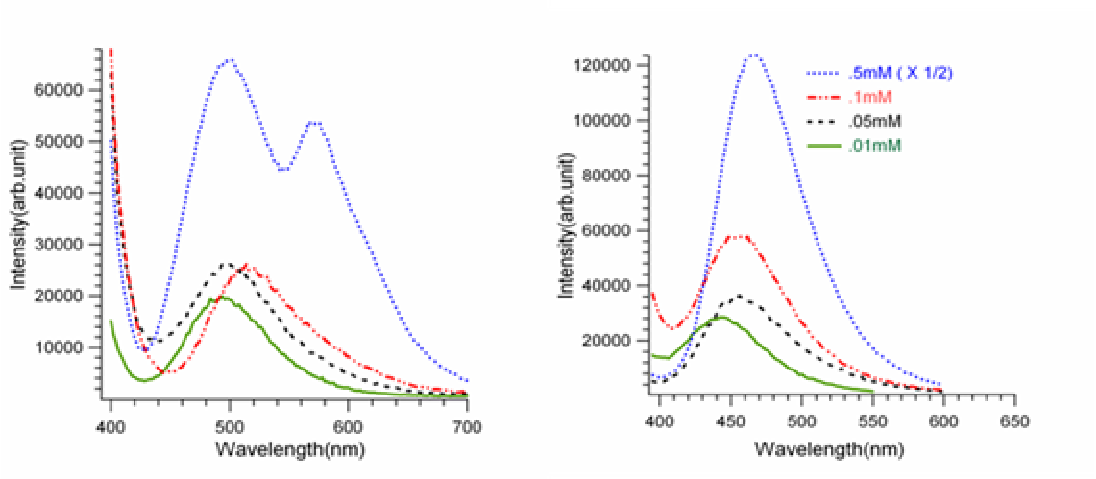

C152 **C461**

Figure 4.3. The emission intensities for different concentrations of C152 and C461 adsorbed at silica surface. Figure in left displays the intensities of C152 concentration ranging from 0.01mM to 0.5mM, and Figure in right displays the intensities of C461 concentration ranging from 0.01mM to 0.5mM. Note that the 0.5mM intensities have been multiplied by 0.5 to be placed on the same scales as the lower concentration data. The silica/vapor emission spectra were acquired with an excitation wavelength of 390 nm and 375nm for C152 and C461 respectively.

Given the structural similarities between C152 and C461, one might expect that both solutes should demonstrate similar adsorption behavior at interfaces. Both C152 and C461 have sizable ground state dipole moments of ~ 6D and both are capable of accepting hydrogen bonds through the carbonyl group and/or the tertiary amine group in the 7-position.[30] Neither solute can donate hydrogen bonds. Peak intensities of the emission spectra were used to determine the adsorption isotherms shown in Figure 4.4. Assuming that emission intensity from the coumarin adsorbed to quartz slides scales linearly with surface coverage, plotting the emission intensity as a function of bulk concentration allows one to determine relative solute surface activities and free energies of adsorption. The low concentration ($\leq$ 100 μM) peak

intensity data for both C152 and C461 were fit to Langmuir isotherms leading to ΔG_{ads} of -29.0 ± 1.7 kJ/mole and -30.8 ± 1.0 kJ/mole for C152 and C461, respectively. Given experimental uncertainties, these two values imply that C152 and C461 adsorb to silica through similar mechanisms, with surface silanol groups donating hydrogen bonds to the carbonyl and/or the tertiary amine of the adsorbed solutes.[31-36]

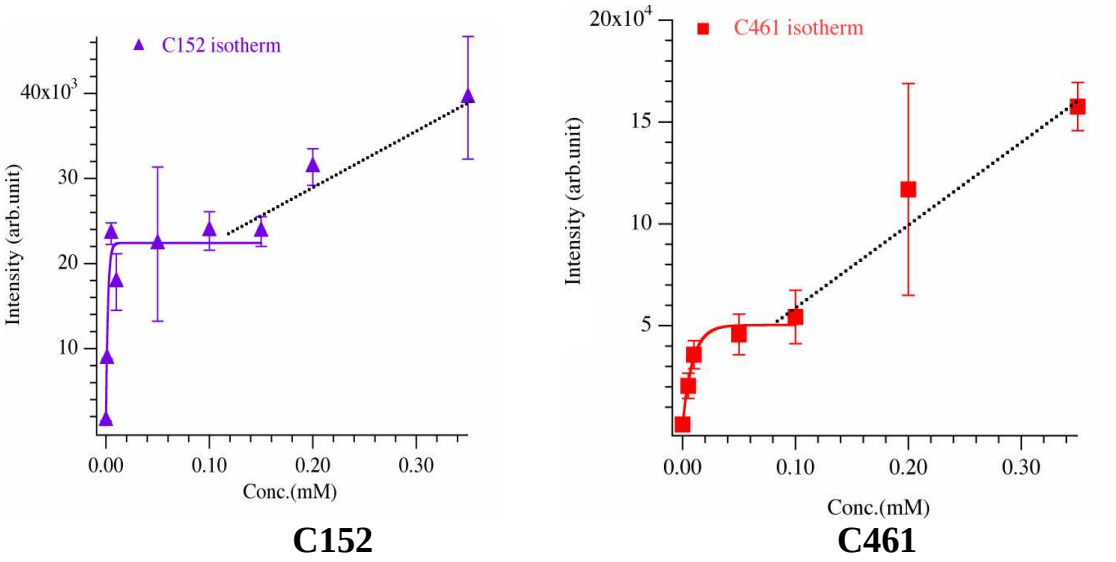

Figure 4.4. An adsorption isotherm from emission spectra of C152 and C461 adsorbed to hydrophilic silica from MeOH solution of varying bulk solute concentrations up to 0.35mM. The Y-axis represents the peak intensity associated with each concentration. In the case of C152 at higher concentrations, peak intensity corresponds to the short wavelength feature. The low concentration data (< 0.10 mM) are fit to Langmuir isotherms. The straight line through the high concentration data is provided as a guide to the eye.

Despite similar adsorption energetics, the steady state emission behaviors of C152 and C461 show clear differences as surface coverages increase beyond the monolayer limit. Again, the sole structural difference between the two solutes is the identity of the methyl group in the 4-position. The $-CF_3$ group of C152 is electron

withdrawing whereas the $-CH_3$ of C461 is weakly electron donating. In bulk solution this difference in functional group composition leads to enhanced Stokes shifts for C152 and reflects a larger change in permanent dipole following photoexcitation compared to C461. Rechthaler[30] calculated $\Delta \mu_{S0\text{-}S1}$ for C152 and C461 to be 8.4 D and 7.7 D, respectively. Similar results can be inferred from the calculations of Cave and Castner.[21,22] A second effect of having the $-CF_3$ group in the 4- position is that the orientation of the C152's permanent dipole will experience very little change upon photoexcitation. The change in dipole orientation following photoexcitation of C461 is expected to be larger. For a pair of related 7ACs – C151 and C120 are the primary amine analogs to C152 and C461 – Cave and Castner[22] calculated the orientational change in permanent dipole between the S_0 and S_1 states of C151 and C120. These calculations showed that C151's permanent dipole reorients slightly ($\Delta\theta = 8.9^0$) upon photoexcitation whereas C120's permanent dipole undergoes a 2-fold larger change in direction ($\Delta\theta = 18.6^0$). A large change in permanent dipole orientation following photoexcitation can disrupt long range order in adsorbed multilayers leaving observed emission to be dominated by solute monomers (as appears to be the case of C461). In contrast, if photoexcitation leads primarily to a change in dipole magnitude but not orientation, solute excitation can be delocalized over multiple, preferentially aligned monomers leading to a pronounced red shift in emission as electronic states become delocalized over two or more monomers.

4.3.2. Fluorescence lifetime Measurements

4.3.2.1. In Bulk Methanol

Figure 4.5 shows the fluorescence decays of C152 and C461 in bulk methanol. The relevant lifetime components are reported in Table 4.2. The fluorescence decays of C152 and C461 in bulk methanol (10 μM) were fit to single exponential functions having lifetimes of $\tau = 0.90 \pm 0.02$ ns and 3.22 ± 0.01 ns respectively. These results compare favorably with previously published data.[11,30] The radiative lifetime will depend inversely on the radiative rate constant (k_{rad}) and rate constants associated with any nonradiative processes (k_{nonrad}):

$$\tau = \frac{1}{k_{rad} + k_{nonrad}} \qquad \text{Eq. 4. 2}$$

In nonpolar solvents such as long chain alkanes, C152 and C461 have similar fluorescent lifetimes of 4.00 ns and 3.45 ns, respectively. (Fluorescence decays from both solutes in decane are shown in Appendix A.4.2). Consequently, we attribute the difference in fluorescence lifetimes observed in bulk methanol to C152 having a nonradiative relaxation mechanism that is unavailable to C461. Several reports have cited the existence of a nonradiative charge transfer state in photoexcited C152.[11,37,38] Such a state would be stabilized in polar solvents such as methanol but not in nonpolar solvents. The possibility of TICT formation depends both on the presence of intramolecular electron donor and acceptor groups and on solvent polarity.[2,20] The presence of an electronegative substituent ($-CF_3$) at the 4-position inductively facilitates charge transfer from the electron donating dimethylamino group to the coumarin ring and allows the formal negative charge to be shared between the carbonyl oxygen and the $-CF_3$ group.[1,20] The fact that the TICT state formation is not

inferred from the time resolved emission of C461 implies that the electron donating character of the $–CH_3$ group in the 4-position destabilizes this very polar conformer, regardless of the local dielectric environment.

4.3.2.2. Silica/Methanol Interface

The time dependent, photophysical properties of C152 and C461 near the silica/methanol interface were meaured using TCSPC fluorescence emission in TIR geometry. Figure 4.5 shows the fluorescence decays of C152 and C461 at a silica/methanol interface and lifetime values are reported in Table 4.2. Concentrations of both solutions were 10 μM. This concentration corresponds to approximately full monolayer coverage according to the adsorption data shown in Figure 4.4. In the case of C152, this concentration should not lead to a significant population of the second species responsible for the long-wavelength emission observed in Figure 4.3. The TIR data for C461 are virtually equivalent to data in bulk solution (τ = 3.23 ns), but C152 in the interfacial region shows clear evidence of a second, long-lived emissive state (τ_2 = 5.20 ns) in addition to a shorter lived species (τ_1 = 1.00 ns) assigned to the monomer in bulk solution.

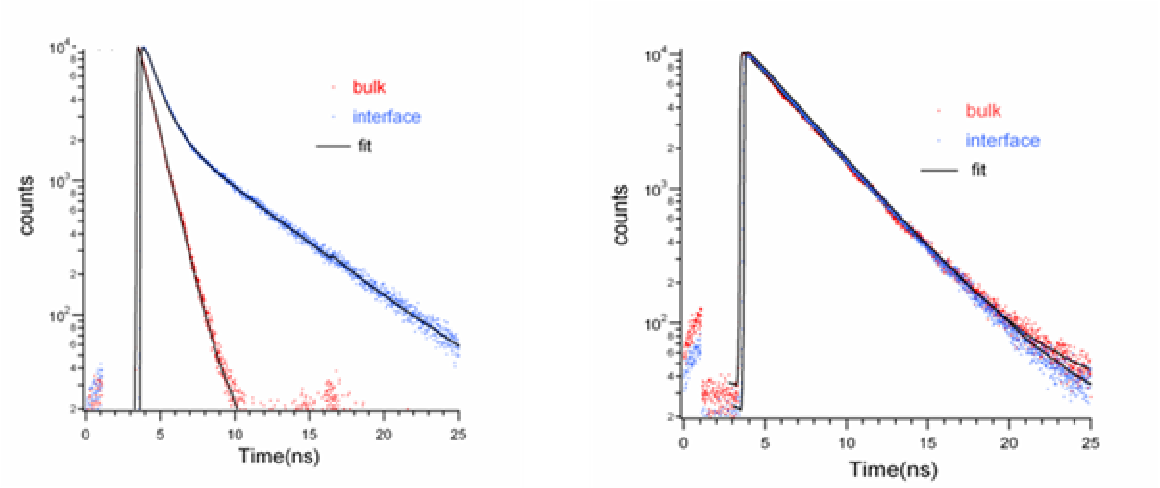

C152 **C461**

Figure 4.5. Fluorescence decay curves of C152 (red dotted) and C461 (red dotted) in bulk methanol of 10 µM. Fluorescence decay curve of C152 (blue dotted) C461 (blue dotted) at solid/methanol interface having conc. 10 µM. The solid line denotes the best fit. The fluorescence data were collected using 420 long pass filter (LPF). The excitation wavelength were fixed at 390 nm and 375 nm for C152 and C461 respectively.

Table 4.2. Fluorescence lifetime of C152 and C461 in bulk methanol and at silica/methanol interface using 420 long pass filter (LPF). Uncertainties in lifetimes and amplitudes are ± 40 ps and ± 1%, respectively.

Medium	Solute	A_1	τ_1 (ns)	A_2	τ_2 (ns)	χ^2
MeOH (Bulk)	C152	1.00	0.90	NA	NA	1.2
	C461	1.00	3.22	NA	NA	1.3
Silica/MeOH	C152	0.77	1.00	0.23	5.20	1.1
Interface	C461	1.00	3.23	NA	NA	1.5

To explore further the properties of C152 emission from solutes in the interfacial region, we used a series of filters to determine whether the distinct fluorescence lifetimes corresponded to emission from the short and long wavelength

regions of the C152 emission profile. A 420 nm long-pass filter was used to detect the total emission and filter out residual excitation light. An additional 512 nm short-pass filter discriminated against contributions to the decay from the long wavelength portion of the spectrum. In a separate experiment a 550 nm long-pass filter was used to capture only emission from the red edge of the emission spectrum. Results from these experiments are shown in Figure 4.6. The fluorescence decay curves were fit without any constraints and results are presented in Table 4.3. The first striking observation is that both lifetimes remain virtually unchanged regardless of the spectral window being sampled. However, the amplitudes of the coefficients vary in a systematic manner. Using the 512 nm short-pass filter, we observe that the longer lifetime component makes a more significant contribution to the measured decay (A_2 = 0.40 with 512 nm short-pass filter compared to 0.23 from the total emission data collected using the 420 nm long-pass filter) whereas the 550 nm long-pass filter emphasizes the short-lifetime component (A_1 = 0.90 with 550 nm long-pass filter compared to 0.77 using 420 nm long-pass filter).

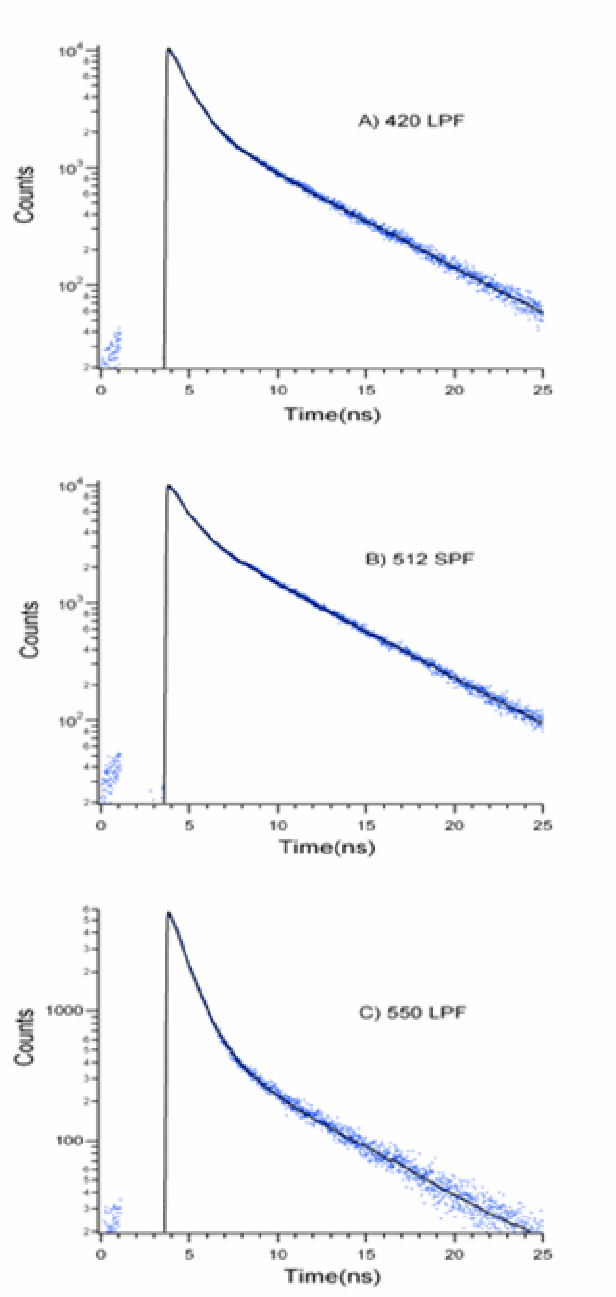

Figure 4.6. Fluorescence decay curve of C152 (blue dotted) at solid/methanol interface of conc. 10 µM. (A) 420nm long pass filter (B) 512nm short pass filter (C) 550nm long pass filter. The solid line denotes the best fit to a double exponential decay.

Table 4.3: **Fluorescence lifetime of C152 at silica/methanol interface using three different filters, e.g. 420nm long pass filter (LPF), 512nm short pass filter (SPF), 550nm long pass filter (LPF). Uncertainties in lifetimes and amplitudes are ± 50 ps and ± 3%, respectively.**

Medium	Filters	A_1	τ_1 (ns)	A_2	τ_2 (ns)	χ^2
Silica/MeOH interface	420 LPF	0.77	1.00	0.23	5.20	1.1
	512 SPF	0.60	1.00	0.40	5.20	1.2
	550LPF	0.90	0.95	0.10	5.20	1.1

4.4. Discussion

The data presented in Figures 4.3 – 4.6 raise a host of interesting questions regarding the observed differences in photophysical behavior between C152 and C461 both in bulk methanol and adsorbed to the silica/methanol interface. As noted earlier, differences in C152 and C461 time dependent behavior in bulk methanol solution can be traced to C152's ability to form a TICT state upon photoexcitation.[11] In the proposed TICT state, the $-CF_3$ group of C152 is strongly electron withdrawing allowing the carbonyl group to be more electronegative than it would be with a simple, electron-donating alkyl group in the 4-position. This induced change in electron affinity stabilizes the charge transfer state in a manner that can not be accomplished in C461.

What is less clear is how this change in molecular and electronic structure leads to the pronounced differences observed when these two solutes are adsorbed at polar silica surfaces. Several issues need to be addressed: first, what is the origin of the long-wavelength feature in the steady-state emission spectra of C152 adsorbed from solutions having bulk concentrations $\geq$ 400 μM? Second, how does the silica

surface introduce the long-lifetime component to the fluorescence decay of C152 but leave the fluorescence decay of C461 unchanged? This question is particularly intriguing given that longer lifetimes of C152 are generally associated with nonpolar environments, but the steady state emission experiments from adsorbed C152 show clearly that the surface is quite polar. Third, why is the long-wavelength feature observed in the high surface coverage steady-state data associated with the short-lived excited state of C152 and the short wavelength feature associated more with the long-lived excited state?

With regards to observed differences in steady-state emission between adsorbed C152 and C461, we assign the long wavelength feature in the high surface coverage C152 data to the formation of aggregates in multilayers. Previous work examining adsorption of other dyes on silica surfaces have observed similar effects arising from a variety of aggregate structures.[39,40,41] Given the comparable linewidths of the emission features at 505 nm and 574 nm observed in Figure 4.3 we do not believe that C152 forms aggregates having special, well defined geometries such as J-aggregates.[42] What is clear, however, is that high surface coverages of C152 lead to a newly emissive eigenstate whose wavelength implies a delocalized wavefunction spread over multiple associated monomers.

As with C152, the adsorption isotherm for C461 shown in Figure 4.4 suggests strongly that this solute also forms multilayers at silica surfaces. However, high C461 surface coverages result only in increased intensity in a single emission feature (at ~ 468 nm), not in the appearance of a new emission feature at longer wavelengths. Both C152 and C461 are anticipated to have similar ground state dipole moments [30]

and both are able only to accept hydrogen bonds. These similarities lead to the similar adsorption energies calculated from the adsorption data. The most pronounced difference in electronic structure between these two species is the change in permanent dipole *orientation* in the S_1 excited states of C152 and C461. As mentioned above, both solutes have relatively large changes in dipole *magnitude* ($\Delta\mu$ = 8.4 D for C152 and 7.7 D for C461 [30]), but the *orientation* of the C461 S_1 dipole is expected to rotate more than twice as much compared to C152. Based on the *ab initio* calculations performed by Cave and Castner[22], we propose that a similar pattern in the dipole moment's directional change is responsible for the observed differences in fluorescence behavior between C152 and C461.

The adsorption data imply that both C152 and C461 form multilayers at concentrations above ~100 μM. Upon excitation, the increase in molecular dipole magnitude should strengthen the interactions between adsorbed species both for C152 *and* C461. If, however, the molecular dipoles change orientation as well as magnitude, then any interactions arising from a self assembled structure will be weakened leaving the molecules to behave as decoupled monomers rather than as a collection of associated multimers. For C152, we propose that the change in dipole orientation following photoexcitation is not large enough to disrupt the intermolecular interactions between adsorbed species, thus one observes a second, longer wavelength emission at higher (aggregated) surface coverages. In contrast, a larger change in C461's dipole orientation will drive molecules in multilayers to lose correlation with one another and emit as monomers rather than as aggregates. Given the large change in permanent dipole following photoexcitation ($\Delta\mu \sim 8$ D), correlated monomers in

adsorbed multilayers will be energetically stabilization. The greatest stabilization will occur if dipole orientation does not change ($\Delta\theta = 0^0$ where $\Delta\theta$ is the change in the angle between the ground and the excited state dipole). If the dipole orientation does change then this stabilization will be weakened according to the following expression.[43]

$$w(r) = -\mu_1\mu_2[2\cos\theta_1\cos\theta_2 - \sin\theta_1\sin\theta_2\cos\varphi]/4\pi\varepsilon_r r^3 \qquad \text{Eq. 4.3}$$

where w(r) is the dipole-dipole interaction energy. μ_i the dipole moment of molecule i, θ_i is the change in the dipole orientation of molecule i, φ is the dihedral angle and r is the intermolecular distance. To estimate the importance of dipole reorientation we assume that monomers start perfectly aligned ($\theta = 0^0$, $\varphi = 0^0$) and closely packed. (r ~ 5Å). Using the change in dipole orientation calculated by Cave and Castner[22] for C151 (8.9^0) and C120 (18.6^0) we estimate that the large change in orientation for C120 leads to a corresponding 20% reduction in the energetic stabilization that would result from photoexcitation if $\Delta\theta = 0^0$. The smaller change in dipole orientation for C151 lowers w(r) by less than 2%

The second and third questions posed above focus on differences in the fluorescence lifetimes of C152 near a polar, silica interface compared to bulk solution limits. The shorter lifetime of C152 in bulk methanol solution has been assigned to the formation of a TICT state following photoexcitation. In nonpolar solvents the TICT state can not be stabilized and the fluorescence lifetimes of C152 and C461 are very similar. (See Supporting Information, Figure A.4.2. for fluorescence decay curves of C152 and C461 in bulk decane. Figure A.4.1. shows the steady state absorption and emission data for both solutes in decane). The longer lifetime

observed for C152 in the TIR measurements at the methanol/silica interface is assigned to C152 monomers interacting directly with the silica surface. Surfaces introduce anisotropy that can restrict molecular motion both through changes in local solvent density *and* through specific solute-substrate interactions.[24, 26, 31] Strong associations between the solute and substrate can limit the ability of a solute to undergo large amplitude motion.[44] We believe that this effect – solute-substrate interactions – is responsible for the difference between C152 fluorescence emission in bulk methanol solution and emission observed in TIR measurements carried out at the methanol/silica interface. We base this assignment on several considerations. First, adsorption experiments show that C152 adsorbs relatively strongly to the silica/methanol interface. Second, resonance enhanced SHG experiments have shown that solvation at hydrophilic silica surfaces is dominated by strong hydrogen bond donating sites that do not have any conformational flexibility.[31,33,34] If the silica surface donates hydrogen bonds to C152 through the solute's nitrogen lone-pair, then the surface will restrict the C152's ability to form the TICT state following photoexcitation. Thus, although the silica surface presents adsorbed solutes with a very polar environment, the surface itself can inhibit the ability of these adsorbed solutes to undergo large amplitude structural transformations and the time dependent emission will resemble that of monomers dissolved in less polar solvents. Third, the observed behavior of C152 at the silica methanol interface appears to be general given similar observations made with C151, the primary amine analog of C152. In the case of C151, the sp^3-hybridized conformer has a relatively short lifetime (~ 1.00 ns) compared to the CT conformer (~5.00 ns) and TIR fluorescence measurements

show that the silica surface stabilizes the C151 conformer having the *shorter* lifetime, despite the silica/methanol interface being decidedly polar.

A final basis for assigning the long-lived C152 species observed in the TIR measurements to solutes adsorbed directly to the silica surface comes from using different filters to discriminate the time dependent behavior of the red and blue edges of the overall emission profile. From the data shown in Figure 4.6 and analyses reported in Table 4.2.2 one readily sees that the long 5.20 ns lifetime is more pronounced in the short wavelength emission (collected using the 512 nm short pass filter). Again, a longer lifetime is associated with C152 solutes unable to undergo large amplitude motion to form the TICT state. The long wavelength emission (collected with the 550 nm long pass filter) has a lifetime (0.95 ns) characteristic of C152 that can form a nonradiative charge transfer state. An important consideration is that these experiments were carried out with relatively low C152 concentrations (10 μM) to lessen the contributions from solutes in bulk solution within the ~60 nm probed by the evanescent field of the excitation laser. Those solutes sampled in the experiment that do not interact directly with the surface *should* have emission profiles and lifetimes similar to those observed in the bulk solution. (Figure 4.5) The fact that the TIR measurements carried out with the 512nm short pass filter emphasize the *long-lived* C152 population bolsters confidence that these solutes are, in fact, adsorbed directly to the silica surface.

The last remaining question is how to interpret the long wavelength, short-lived feature attributed to C152 that appears at high surface coverage. The long wavelength implies dimer or higher aggregate formation. This inference is consistent

with results from adsorption experiments that show the integrated intensity of the entire emission spectrum grows linearly for concentrations above 100 μM. Such behavior is consistent with the formation of multilayers at the liquid/solid interface. The short lifetime inferred from data in Figure 4.5 suggests that species contributing to this emission can relax via one or more nonradiative pathways. The collective behavior of C152 contrasts with that of C461 where C461 species in multilayers retain their monomeric photophysical properties. The small red shift in the C461 high surface coverage emission spectra reports a slightly more polar environment for those molecules in multilayers compared to those adsorbed to the surface, but the emission maximum still falls within the solvatochromic window of C461 and the single exponential fluorescence lifetime of 3.23 ns is virtually identical to that measured in bulk methanol solution.

Taking into account all of these observations, we propose that the unusual behavior observed for C152 adsorbed to the silica/methanol interface is due to the formation of multilayers composed of monomers, which can either isomerize or relax through one or more nonradiative processes thus shortening the fluorescence lifetime from the 5.20 ns observed for monomers adsorbed directly to the silica surface. Furthermore, monomers within these aggregate assemblies must be able to interact cooperatively allowing for fluorescence emission at a wavelength much longer than that observed for isolated monomers even in the most polar solvation environments. Such interactions can arise from C152's unique structure, namely the close proximity of two electronegative groups in the molecule (the carbonyl group and the $–CF_3$ group at 4-position). Resultant charge separation inside a monomer stabilized by the

electronegative substituents will drive monomers to form close packed aggregates due to strong coulomb interactions.

Further support for this picture comes from time resolved experiments that were carried out with films formed at the solid/vapor interface using procedures identical to those used to prepare the films responsible for the adsorption data shown in Figures 4.3-4.4. The two lifetimes observed at the solid/vapor interface are comparable to those observed at the solid/methanol interface possibly indicating that two species at solid/vapor interface have similar characteristics than at solid/methanol interface. The decay trace for the solid/vapor interface is presented in the Appendix D Figure A.4.3.

4.5. Conclusions

Steady state and time-resolved fluorescence measurements for C152 and C461 in bulk methanol and adsorbed to the methanol/silica surfaces show that interfaces can change significantly the photophysical properties of adsorbed solutes, but that interfacial effects depend sensitively on solute structure. Analysis of adsorption data revealed that the $\Delta G_{adsorption}$ of C152 and C461 is insensitive to solute structure. However, the small difference in the solute structure at the 4-position does strongly influence the photophysical properties of the adsorbed monolayer.

Steady state fluorescence measurements indicate the presence of a second fluorescent excited state for adsorbed C152, when bulk solution concentrations exceed ~ 400 μM; films for adsorbed C461, on the other hand, show no such behavior. The influence of the given substituent is also apparent in the measured

fluorescence lifetimes of bulk and surface species. In bulk methanol C152's fluorescent decay profile is single exponential with a lifetime of 0.90 ns while the fluorescence decay profile of C461 is also single exponential with a lifetime of 3.22 ns, where the value is comparable to lifetimes observed in nonpolar solvents (Supporting Information Figure A.4.2). The reduction in the C152 lifetime is attributed to the formation of a nonradiative twisted intramolecular charge-transfer state that is stabilized in polar solvents.

The TIR fluorescence decay of C152 adsorbed to silica/methanol interface shows significantly different properties from bulk methanol. In contrast the fluorescence decay of C461 at the silica/methanol interface was similar as that in bulk solution. C152 fluorescence decay at the same solid/methanol interface shows a double exponential decay with lifetimes of 5.20ns and 1.00ns respectively. The longer lifetime was assigned to the silica surface's ability to inhibit the formation of a TICT state upon photoexcitation. In contrast, the shorter lived species retains the monomer properties similar to those in bulk. Based on correlations between measured lifetimes and emission wavelengths we assign the short wavelength emission in C152 spectra to those species interacting directly with the silica surface whereas those C152 solutes adsorbed in multilayers are responsible for the long wavelength emission and are associated with the short lifetime observed in fluorescence decays. For C461 the unchanged fluorescence lifetime and the emission profile that shows only a small red shift with increasing surface coverage indicate that C461 retains monomer-like properties at high coverages.

References

(1) Arbeloa, T. L.; Arbeloa, F. L.; Arbeloa, I. L. *J. Luminescence* **1996**, 68, (2-4), 149-155.

(2) Arbeloa, T. L.; Arbeloa, F. L.; Tapia, M. J.; Arbeloa, I. L. *J. Phys. Chem.* **1993**, 97, (18), 4704-4707.

(3) Atkins, R. L.; Bliss, D. E. *J. Org. Chem.* **1978**, 43, (10), 1975-1980.

(4) Jones, G.; Jackson, W. R.; Halpern, A. M. *Chem. Phys. Lett.* **1980**, 72, (2), 391-395.

(5) Jones, G.; Jackson, W. R.; Choi, C.; Bergmark, W. R. *J. Phys. Chem.* **1985**, 89, (2), 294-300.

(6) Bank, A.; Kumbhakar, M.; Nath, S.; Pal, H. *Chem. Phys.* **2005**, 315, (3), 277-285.

(7) Atkins, R. L.; Bliss, D. E. *J. Org. Chem.* **1978,** 43, (10), 1975-1980.

(8) Satpati, A.; Senthilkumar, S.; Kumbhakar, M.; Nath, S.; Maity, D. K.; Pal, H. *Photochem. and Photobio.* **2005**, 81, (2), 270-278.

(9) Kahlow, M. A.; Jarzeba, W.; Kang, T. J.; Barbara, P. F. *J. Chem. Phys.* **1989**, 90, (1), 151-158.

(10) Senthilikumar, S.; Nath, S.; Pal, H. *Photochem. and Photobio.* **2004**, 80, (1), 104-111.

(11) Nad, S.; Kumbhakar, M.; Pal, H. *J. Phys. Chem. A* **2003**, 107, (24), 4808-4816.

(12) Kim, T. G.; Topp, M. R. *J. Phys. Chem. A* **2004**, 108, (38), 7653-7659.

(13) Nag, A.; Bhattacharyya, K. *Chem. Phys. Lett.* **1990**, 169, (1-2), 12-16.

(14) Nad, S.; Pal, H. *J. Phys. Chem. A* **2001**, 105, (7), 1097-1106.

(15) Sharma, V. K.; Saharo, P. D.; Sharma, N.; Rastogi, R. C.; Ghoshal, S. K.; Mohan, D. *Spectrochim Acta Part a-Mol. and Biomol. Spect.* **2003**, 59, (6), 1161-1170.

(16) Rosenthal, S. J.; Jimenez, R.; Fleming, G. R.; Kumar, P. V.; Maroncelli, M. *J. Mol. Liq.* **1994**, 60, (1-3), 25-56.

(17) Horng, M. L.; Gardecki, J. A.; Papazyan, A.; Maroncelli, M. *J. Phys. Chem.* **1995**, 99, (48), 17311-17337.

(18) Jimenez, R.; Fleming, G. R.; Kumar, P. V.; Maroncelli, M. *Nature* **1994**, 369, (6480), 471-473.

(19) Jin, H.; Baker, G. A.; Arzhantsev, S.; Dong, J.; Maroncelli, M. *J. Phys. Chem. B* **2007**, 111, (25), 7291-7302.

(20) Chu, G.; Yangbo, F. *J. Chem. Soc., Faraday Trans, 1*,**1987**, 83, 8, 2533-2539.

(21) Cave, R. J.; Castner, E. W. *J. Phys. Chem. A* **2002**, 106, (50), 12117-12123.

(22) Cave, R. J.; Burke, K.; Castner, E. W. *J. Phys. Chem. A* **2002**, 106, (40), 9294-9305

(23) Riter, R. E.; Willard, D. M.; Levinger, N. E. *J. Phys. Chem. B* **1998**, *102, (15*), 2705-2714.

(24) Zimdars, D.; Dadap, J. I.; Eisenthal, K. B.; Heinz, T. F. *J. Phys. Chem. B* **1999**, *103, (17),* 3425-3433.

(25) Yamashita, T.; Amino, Y.; Yamaguchi, A.; Teramae, N. *Chem. Lett.* **2005**, 34, (7), 988-989.

(26) Shi, X.; Borguet, E.; Tarnovsky, A. N.; Eisenthal, K. B. *Chem. Phys.* **1996**, *205, (1-2), 167-178.*

(27) Rosen, M.J., Surfactant and Interfacial Phenomena; *John-Wiley & Sons, Inc.: NJ*, **2004**

(28) Grimes, A. F.; Call, S. E.; Vicente, D. A.; English, D. S.; Harbron, E. J. *J. Phys. Chem. B* **2006**, 110, (39), 19183-19190.

(29) O'Connor, D.V.; Phillips, D., *Time correlated single Photon Counting; Acad. Press: London,* **1984**.

(30) Rechthaler, K.; Kohler, G. *Chem. Phys.* **1994**, 189, (1), 99-116.

(31) Brindza, M.R.; Walker,R. A. *J. Am. Chem. Soc* **2009**,131(17) 6207-6214.

(32) Kovaleski, J. M.; Wirth, M. J. *J. Phys. Chem. B* **1997**, 101, (28), 5545-5548.

(33) Wirth, M. J.; Legg, M. A. *Ann. Rev. Phys. Chem.* **2007**, 58, 489-510.

(34) Wong, A. L.; Harris, J. M. *J. Phys. Chem.* **1991**, 95, (15), 5895-5901.

(35) Hair, M. L.; Hertl, W. *J. Phys. Chem.* **1969**, 73, (12), 4269-4276.

(36) Al-Abadleh, H. A.; Voges, A. B.; Bertin, P. A.; Nguyen, S. B. T.; Geiger, F. M. *J. Am. Chem. Soc.* **2004**, 126, (36), 11126-11127.

(37) Dahiya, P.; Kumbhakar, M.; Mukherjee, T.; Pal, H. *Chem. Phys. Lett.* **2005**, 414, (1-3), 148-154.

(38) Choudhury, S. D.; Kumbhakar, M.; Nath, S.; Pal, H. *J. Chem. Phys.* **2007**, 127, (19), 194901(1)-194901(11).

(39) Ohline, S. M.; Lee, S.; Williams, S.; Chang, C. *Chem. Phys. Lett.* **2001,** 346, (1-2), 9-15.

(40) Heinz, T. F.; Chen,C. R.; Ricard, D.; Shen Y. K. *Phys. Rev. Lett.* **1982**, 48 , (7), 478 – 481.

(41) Higgins, D.A.; Byerly, S.K.; Abrams, M. B.; Corn, R. M. *J. Phys. Chem.* **1991**, 95 (18),6984–6990

(42) Moll, J.; Daehne, S.; Durrant, J. R.; Wiersma, D. A. *J. Chem. Phys.* **1995**, 102, (16), 6362-6370.

(43) Israellachvili, J. N, *Intermolecular & Surface Force; Acad. Press: London,* **1991**.

(44) Jones, G.; Yan, D. X.; Hu, J. Q.; Wang, J. D.; Xia, B.; Vullev, V. I. *J. Phys. Chem. B* **2007**, 111, (24), 6921-6929.

Chapter 5: Time Resolved Fluorescence of 7-Aminocoumarins in Decane and at Decane/Silica Interface: Correlating Aggregation Tendencies with Solute Structure

5.1. Introduction

Coumarins are the derivatives of a general class of molecules known as benzopyrones. Because coumarins tend to be photochemically stable with high quantum yields, derivatives of these molecules are often used laser dyes in the short wavelength region of the visible spectrum.[1-3] Coumarins substituted with amino groups at the 7-position are of special importance in this regard. 7-amino-coumarins (7AC) (Figure 5.1.1) dyes have high chemical stability and very high quantum yields, often close to unity [4,5], and a majority of these 7AC dyes show a substantial change in permanent dipole following excitation from S_0 to S_1. This property leads to large Stokes shifts that are sensitive to solvent polarities, and have been exploited to probe local solvation effects in heterogeneous environments.[6-10] The experiments described in this chapter examine the photophysical behavior of several related 7AC solutes in order to better understand how solute structure and local solvation effects in *nonpolar* media change the electronic structure of the solutes themselves. More specifically, steady state and time resolved fluorescence behaviors of Coumarin 152 (C152), Coumarin 461 (C461), Coumarin 151 (C151) and Coumarin 440 (C440) in decane are discussed in the chapter. Some of the schemes developed from this work are tested with the two additional 7AC solutes, Coumarin 445 (C445) and Coumarin 450 (C450).

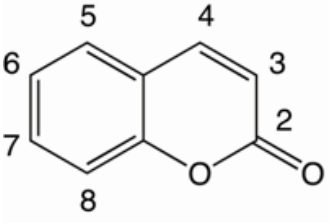

Figure 5.1.1. Structure of 1, 2 benzopyrone

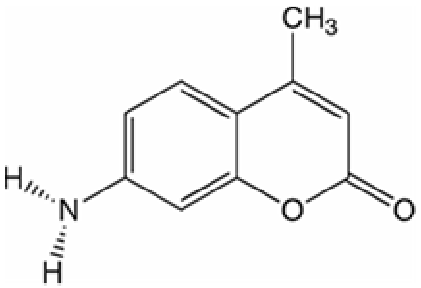

C440

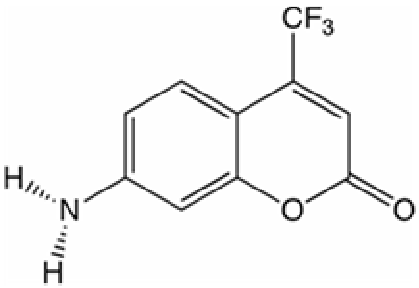

C151

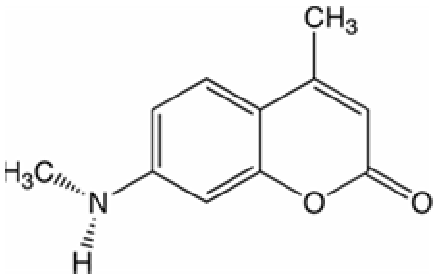

C445

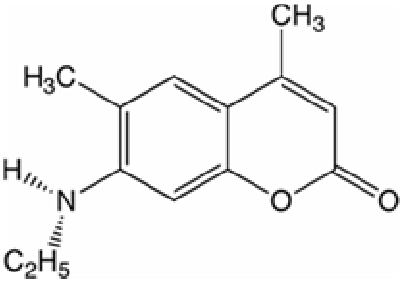

C450

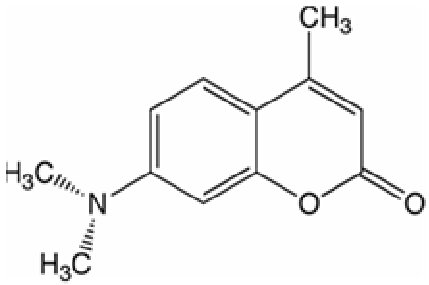

C461

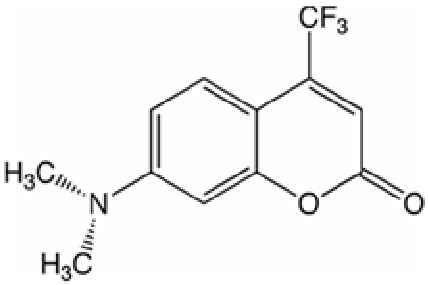

C152

Figure 5.1.2. Structures of 7-aminocoumarins dyes

Additional experiments identify differences in solute emissive behavior in bulk decane solution and at the anisotropic solid/liquid boundary formed between silica and decane. Studies described in this chapter focus on the roles played by solute structure, concentration and solvation environment in determining the equilibrium and dynamic solvation properties of structurally related solutes. Results provide clear evidence that subtle changes in solvent structure can have dramatic impact on phenomena such as nonradiative decay rates and the tendency of solutes to aggregate in solution or at/near surfaces. These results stand in contrast to those reported in Chapters 3 and 4 where the solvent was polar and aggregation in solution was never a concern, but aggregation near surfaces strongly influenced the emissive behavior of selected 7AC species. When the solvent is nonpolar, surface aggregation appears inhibited and dimers of the 7ACs with tertiary amines are much more likely to form in bulk decane. The 7ACs having primary amines show no such tendency.

The four coumarin solutes used in these studies are shown in Figure 5.1.2. All have a common 7AC structure and differ solely in the nature of substituents in the 7- and 4- positions. C152 and C151 both have a $-CF_3$ group in the 4- position while this both C461 and C440 have a methyl ($-CH_3$) substituent in this same position. C152 and C461 are tertiary amines with methyl groups attached to the 7- position amine. C151 and C440 are both primary amines. Throughout this work, these solutes are referred to as tertiary coumarins (C152 and C461) and primary coumarins (C151 and C440). All four solutes have two low-lying excited electronic states resulting from n- π^* or π- π^* transition and the charge localized in the benzopyrone ring.[11,12]

Several different 7AC solutes have been used extensively to characterize solvation dynamics in a wide variety of solvents. Coumarin 343 and Coumarin 314 are tertiary amines but – unlike C152 and C461 – the nitrogens in C343 and C314 are locked into large, conformationally hindered fused ring systems (See chapter 7). In contrast, C152 and C461 are free to undergo inversion about the amine in solution and all of the 7AC solutes used in this work are capable of forming charge transfer (CT) states upon photoexcitation. In a CT state the amine in the 7- position assumes a planar geometry (sp^2 hybridization) with the rest of the aromatic ring. This geometry also places a formal positive charge on the nitrogen and a formal negative charge on the carbonyl group in the 2-position.[13] Previous work have noted that 7AC CT states are stabilized in polar solvents but not in nonpolar solvents.[13-15] As a result, the photophysics of unhindered 7AC solutes can be complicated given the proximity of two different excited states.

Work presented in Chapters 3 and 4 show solute structure and changes in solute properties that accompany photoexcitation can result in significantly different emission behaviors both in bulk solution and at silica/methanol interfaces. An important finding from this work was that the ability of a polar environment to stabilize a CT state did not necessarily transfer to polar surfaces where hindered functional group mobility restricted the conformations available to adsorbed solutes. A second observation was that tertiary coumarins (C461 and C152) formed multilayers whereas the primary coumarins (C440 and C151) did not. A final observation was that the change in dipole moment *direction* upon photoexcitation appeared to play a large role in controlling the solute's ability to form associated

aggregates at surfaces. With these considerations in mind, we have chosen C152, C461, C151 and C440 to probe solvation in environments where the solvent is nonpolar. By comparing these results to those observed for the same solutes in methanol, we are able to learn about which photophysical properties of the solutes are general and which depend on solvent choice.

Compared to the properties of the coumarin solutes in polar, protic solvents such as methanol, observations of coumarin photophysical behavior in nonpolar decane solutions are surprising. Tertiary coumarins appear to form dimers at higher concentrations, but primary coumarins do not. Such behavior is considered in light of differing barriers to amine inversion between the tertiary and primary coumarins. In contrast to bulk solution behavior, tertiary coumarin solutes adsorbed to silica surfaces appear to emit as monomers regardless of bulk (and surface) concentrations. These differences are explored further using 7AC solutes having secondary amines in the 7- position.

An important aspect of the studies presented in this work is the correlation between solute structure, nonpolar solvation and solute photophysical properties. Additional experiments examining how these properties are altered by surface anisotropy reinforce the notion that solute photophysics reflects a complicated interplay between nonspecific dipolar forces and localized, directional interactions such as hydrogen bonding and/or individual dipole-dipole interactions. Data presented in this work attempt to categorize each of these contributions to the ground and excited state behaviors of solutes in solution.

The remainder of this chapter is organized as follows: Section 5.2 describes experimental considerations. Section 5.3 presents results in two subsections. The section begins by comparing and contrasting steady sate emission data from these solutes in bulk decane. Fluorescence lifetime measurements in bulk and the silica/decane interface are described in the subsection 5.3.2. Section 5.4 discusses the steady state and time-resolved results and explores possible mechanisms and interfacial interactions that lead to observed differences between the interfacial and bulk solvation. Section 5.5 has the concluding remarks. Our findings show that primary coumarins (C440 and C151) in decane have fluorescence lifetimes characterized by biexponential decays. Both the lifetimes and the relative amplitudes are concentration independent. The two distinct lifetimes are assigned to different excited state conformers. The tertiary coumarins show single exponential emission at low concentrations but at higher concentrations (>100 μM) a second contribution to the emission decay begins to grow in with a negative amplitude. We assign this second, concentration dependent process to dissociation of pre-formed, ground-state dimers that are photoexcited by the incident laser pulse but then fall apart to leave an excited state monomer that then fluoresces. The silica/decane interface inhibits formation of dimers and higher aggregates by adsorbed tertiary 7AC, in contrast to the behavior observed at the silica/methanol interface. Primary coumarins also showed an unusual behavior at silica/decane interface by stabilizing the excited state charge transfer (CT) conformer which was destabilized in bulk decane.

5.2. Experimental Considerations

Laser grade coumarin 461, coumarin 440, coumarin 445, coumarin 450 were purchased from Exciton and coumarin 152 and coumarin 151 were purchased from and Aldrich. All solutes were used as received without any additional purification. The solvent used was spectral grade decane(>99%). The fluorescence lifetimes were measured using a time-correlated single photon counting (TCSPC) assembly described in Chapter 2. A total internal reflection (TIR) geometry was employed to measure the lifetimes of C151 and C440 at solid/liquid interface. A block diagram of the TCSPC assembly including the TIR geometry appears in Chapter 2. All data analyses were carried out using routines written in Igor Pro and provided by Dr. Castner from Rutgers University.

5.3. RESULTS

5.3.1. Steady State Characteristics

Absorption and fluorescence spectra of all four coumarins were recorded in bulk decane and are shown in Figure 5.2. Table 5.1 lists the absorption and peak fluorescence wavelength and their respective Stokes shift values. Solute concentrations were kept constant at 50 μM. Both the absorption and fluorescence spectra show modest Stokes shifts consistent with previous results reported by Nad *et al.*[16, 17] The approximate "mirror symmetry" in the vibronic structure of the absorption and emission spectra of C151 and C152 imply that these dyes in their excited state retain a geometry reminiscent of the ground state structure with a sp^3 geometry about the amine in the 7-position. For C440 and C461, however, the

absorption spectra show some vibronic structure but the emission spectra are relatively featureless indicating some degree of large amplitude motion or fast conformational changes following excitation.

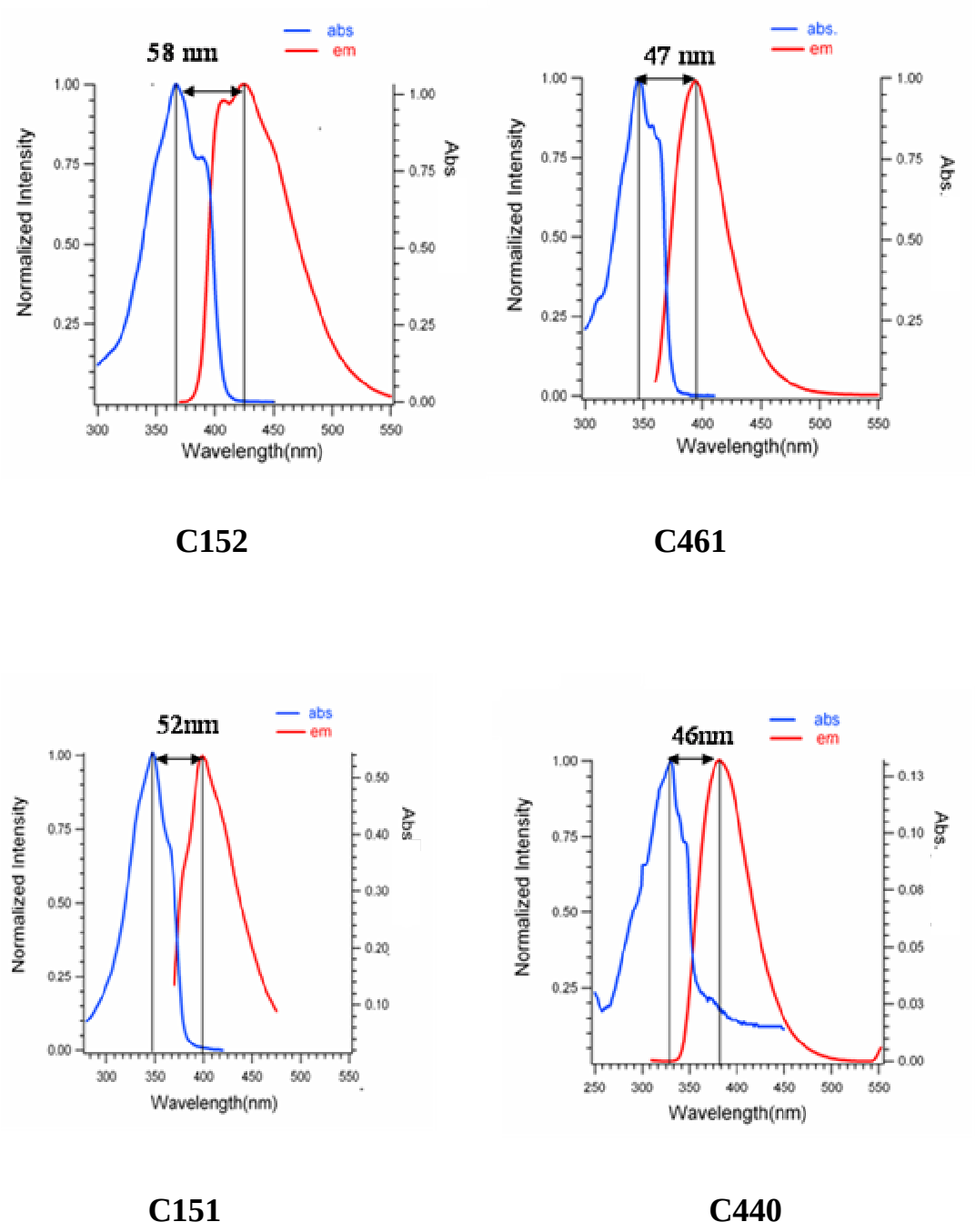

Figure 5.2. Steady state spectra for 7-aminocoumarins in bulk decane

Table 5.1. Spectral data for 7- aminocoumarins in bulk decane

Solute	Absorption peak (nm)	Emission peak (nm)	Stoke's shift (cm^{-1})
C152	367	425	3720
C461	348	395	3420
C151	348	400	3736
C440	332	378	3670

5.3.2 Fluorescence Lifetime Measurements

5.3.2.1 C152/C461 in Bulk Decane

Figure 5.3.1 shows the time resolved fluorescence decays of C152 and C461 in bulk decane. Results are reported in Table 5.2.1. As noted in the introduction, the sole structural difference between these two solutes is the identity of the substituent in the 4-position. The $–CF_3$ group at the 4-position of C152 is electron withdrawing whereas the $–CH_3$ at the 4-position of C461 is weakly electron donating. In polar solvents, the $-CF_3$ functional group on C152 stabilizes a twisted charge transfer state (formally placing a positive charge on the nitrogen and a negative charge on the carbonyl) that can decay nonradiatively shortening the observed fluorescence lifetime ($\tau \sim$ 0.90 ns in methanol).[14] C461, in contrast, fluoresces with a longer lifetime ($\tau \sim$ 3.22 ns in methanol) and is thought to retain a pyramidal structure about the amine group. In decane, the fluorescence decays for these solutes in low-concentration solutions (~10 μM) show single exponential decays with time constants of 3.85 ns and 3.33 ns for C152 and C461, respectively. These results imply that the

low-dielectric alkane solvent can not stabilize a planar excited electronic state having charge transfer character.

At higher bulk concentrations ($\geq$ 500 μM), the decay profiles of both C152 and C461 in decane show a second time constant having negative amplitude and a lifetime comparable to that of the first time constant. The two lifetimes observed for C152 are 4.54 ns (A_1 = +0.60) and 3.85 ns (A_2 = -0.40); similarly, the lifetimes observed for C461 are 3.85 ns (A_1 = +0.60) and 2.08 ns (A_2 = -0.40), respectively. The experimental effect of the second, negative amplitude component is to diminish the fluorescence intensity at early time. This negative amplitude (also called a rise time) is often associated with aggregate and/or excimer formation.[18] Simple physical considerations lead us to believe that the data reflect the presence of dimers (or larger aggregates) that form in solution prior to photoexcitation. We propose that the growth of a rise time in the emission decay is due to ground state dimers and not excited state excimer formation based on concentration considerations. If monomers are randomly distributed throughout solution, then the average separation between monomers is ~3.5 μm for a 500 μM solution. Assuming a diffusion coefficient of coumarin in decane of ~5 x 10^{-6} cm^2/s [19], excited monomers travel only ~0.04% of their mean separation distance within their 4.00 ns excited state lifetime. In contrast, for these solutes to form excimers in bulk solution, concentrations >1 M is required. In fact, the emission spectra of C152 don't show any secondary emission characteristic of excimer or aggregate formation until bulk concentration exceeds 0.5 mM. In the kinetic model discussed below, we propose that the polar solutes form weakly associated ground state dimers in nonpolar solvents. Photoexcitation leads first to

dimer dissociation and then radiative relaxation of an excited state monomer. The rise time reflects the dissociation of excited state dimers into excited state and ground state monomers and the experiment then detects emission from the monomer. Wurthner and coworkers showed that such a dimerization process is very sensitive to solvent polarity. For low polarity solvents dimerization of merocyanine dyes begins to occur at concentrations as low as 30 μMolar.[20]

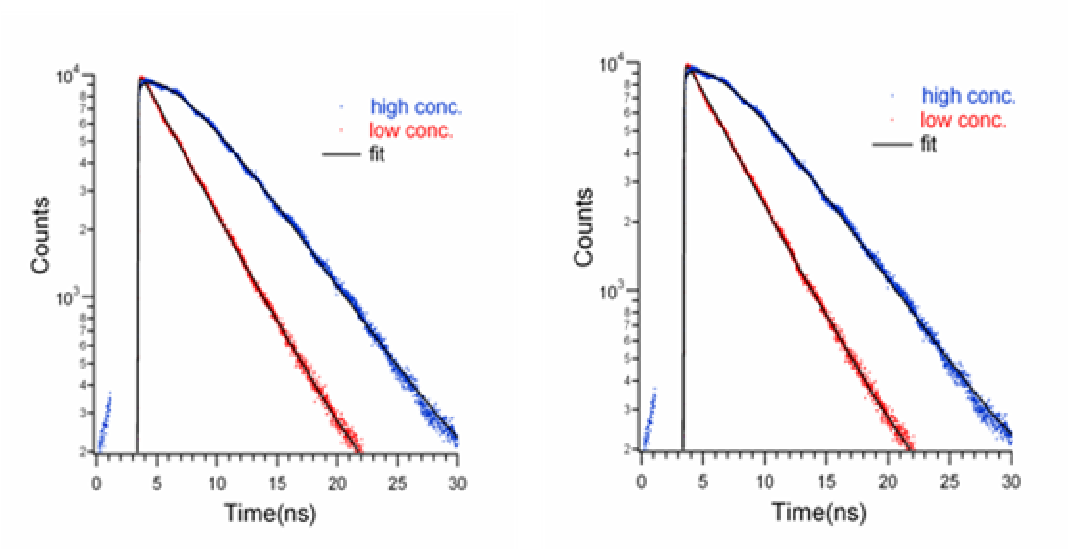

Figure 5.3.1. Fluorescence decay profile of C152 and C461 in high and low concentration of bulk decane. The excitation wavelength was fixed at 360 nm and the fluorescence emission was collected using a 420 nm long pass filter (LPF).

Table 5.2.1. Fluorescence lifetime values of C152 and C461 in bulk decane. Uncertainties in lifetimes and amplitudes are ± 90 ps and ± 1%, respectively. The low concentration data reported in the table were fitted with double exponential to reduce the χ^2 value, but no significant change was noticed. For the high concentration data the χ^2 values are high as the decay traces are not smooth as the low concentration data.

Solute in Solvent	Conc.	A_1	τ_1 (ns)	A_2	τ_2 (ns)	χ^2
C152 in Decane	50μM	1.00	3.85	-	-	1.4
	500μM	1.00	4.54	-0.70	3.84	
C461 in Decane	50μM	1.00	3.33	-	-	1.5
	500μM	1.00	3.85	-0.65	2.08	

5.3.2.2. C152/C461 at the Silica/Decane Interface

The time dependent, photophysical properties of C152 and C461 near the silica/decane interface were measured using TCSPC fluorescence emission in a TIR geometry. Figure 5.3.2 showed the decay traces and results are reported in Table 5.2.2. Unlike in bulk decane the fluorescence lifetimes of C152 and C461 remain virtually unchanged for different concentrations in the TIRF experiments. As bulk concentrations varied from 50 μM to 1mM the lifetime of C152 remained single exponential with a decay constant of ~ 4.00 ns. This result matches the observed lifetime of C152 in low concentration decane solutions and is assigned to monomers constrained to a nonplanar geometry with a sp^3 hybridized nitrogen. Similarly, the lifetime of C461 measured in the TIRF experiments averages ~3.4 ns and again coincides with results from C461 in low concentration bulk solution. From these results, we deduce that whatever process is responsible for the risetime observed in high concentration bulk solution is restricted at the silica/decane interface. Given the

strong hydrogen bonding opportunities available at the silica surface, we propose that adsorbed solutes interact so strongly with the interface that they do not form dimers or larger, extended structures that are inferred from rise time observed in the high concentration bulk solution measurements. Furthermore, we also believe that the low polarity of the solvent *destabilizes* any surface aggregation such as that observed for C152 adsorbed to silica/methanol interfaces. (See Chapter 4.)

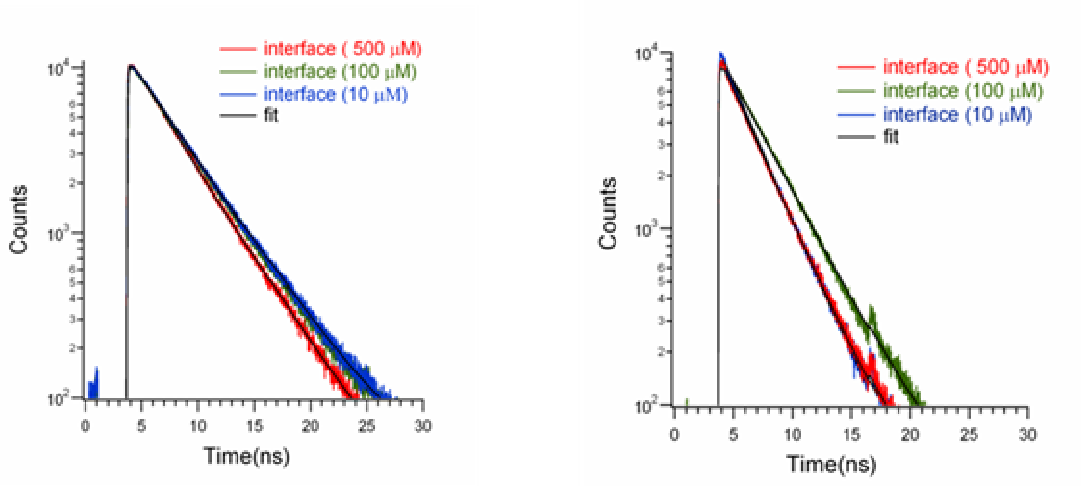

Figure 5.3.2. Fluorescence decay profile of C152 and C461 in high and low concentration at silica/ decane. The excitation wavelength was fixed at 360 nm and the fluorescence emission was collected using a 420 nm long pass filter (LPF).

Table 5.2.2. Fluorescence lifetime values of C152 and C461 at silica/decane interface. Uncertainties in lifetimes is ± 30 ps. The C461 data were tried to fit with double exponentials but showed no significant change.

Solute	Conc.	A_1	τ_1 (ns)	A_2	τ_2 (ns)	χ^2
C152 (Silica/Decane)	10μM	1.00	4.16	-	-	1.1
	100μM	1.00	4.00	-	-	1.1
	500μM	1.00	4.34	-	-	1.2
C461(Silica/Decane)	10μM	1.00	3.70	-	-	1.6
	100μM	1.00	3.70	-	-	1.6
	500μM	1.00	2.85	-	-	>2

5.3.2.3 C151/C440 in Bulk Decane

C151 and C440 are the primary amine analogs of C152 and C461, respectively. A consequence of having two protons rather than two methyl groups attached to the 7-position amine is that inversion becomes much more facile. (The gas-phase barrier to inversion shrinks by almost ~ 40 % when comparing a primary amine to its N, N-dimethyl tertiary equivalent.[21] In bulk decane, both solutes show fluorescence decays that can be fit quite accurately with two lifetimes: ~3.5ns and 1.26ns for C151 and 3.45 ns and ~0.80 ns for C440. These lifetimes are largely insensitive to 100-fold changes in concentration and, in contrast to the tertiary coumarins C152 and C461, both amplitudes remain positive. The primary difference between C151 and C440 is that the short lifetime component accounts for almost 67 % of the total integrated intensity measured in the C151 decay but only ~ 5 % of the total integrated intensity measured for C440. Based on previously reported results as well as our own experiments studying the fluorescence behavior of these solutes in

methanol, we assign the short lifetime to radiative relaxation from a non-planar excited state having a fast nonradiative decay channel. The long lifetime is assigned to decay from an excited state having a degree of charge transfer character and a planar sp^2 hybridized amine[15] For both C151 and C440 the fluorescence lifetimes remain largely unchanged over a 100-fold increase in concentration; measured lifetimes are reported in Table 5.3.1.

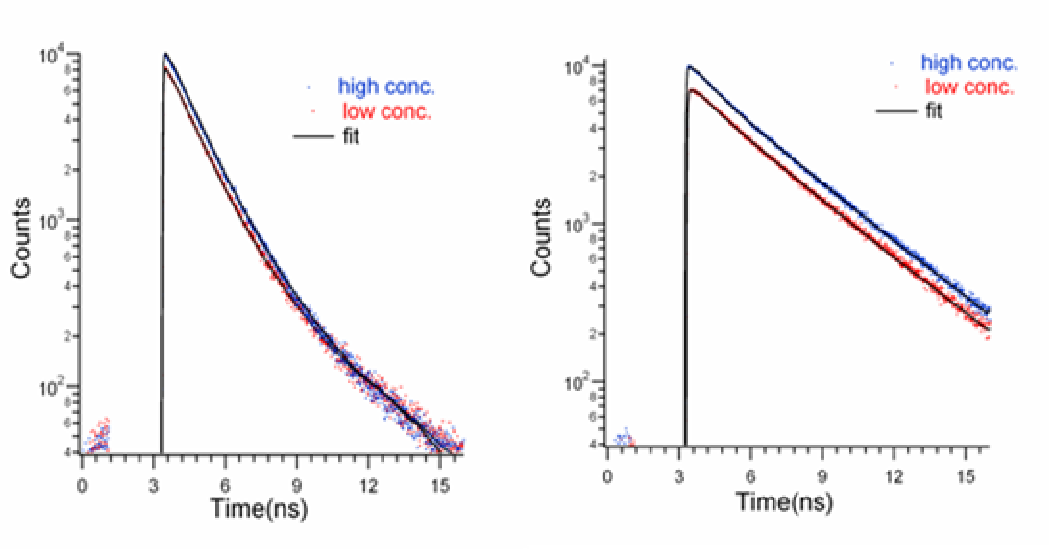

C151 **C440**

Figure 5.4.1. Fluorescence decay profile of C151 and C440 in high and low concentration of bulk decane. The excitation wavelength was fixed at 360nm and the emission was collected using a 400 nm long pass filter (LPF).

Table 5.3.1. Fluorescence lifetime values of C151 and C440 in bulk decane. Uncertainties in lifetimes and amplitudes are ± 90ps and ± 5% respectively.

Solute in Solvent	Conc.	A_1	τ_1 (ns)	A_2	τ_2 (ns)	χ^2
C151 in Decane	10μM	0.84	1.26	0.16	3.33	1.3
	500μM	0.92	1.23	0.08	3.57	1.3
	1mM	0.92	1.23	0.08	3.33	1.3
C440 in Decane	10μM	0.15	1.08	0.85	3.45	1.1
	500μM	0.18	0.63	0.82	3.45	1.2
	1mM	0.16	0.77	0.83	3.45	1.2

5.3.2.4 . C151/C440 at the Silica/Decane Interface

Figure 5.4.2 shows the results of TIRF experiments measuring the fluorescence decays of C151 and C440 at the silica/decane interface. The corresponding lifetime values of C151 at silica/decane interface are reported in Table 5.3.2. The TIR data for the range of C440 concentrations studied (10 μM,100 μM,500 μM) are virtually indistinguishable from bulk decane limits. The TIR data from C151 in the interfacial region show a more prominent contribution from the longer lived state relative to bulk solution limits. Based on comparisons with C151 time resolved fluorescence in bulk polar solvents, the longer lifetime is assigned to a planar, CT state. Unlike in bulk decane where the long lifetime contributes to only ~33% of the total observed fluorescence intensity, at the silica/decane interface, the long lifetime component is responsible for ~65% of the total integrated intensity. Furthermore, this contribution remains constant over a 50-fold change in concentration (10 μM to 500 μM) indicating that the surface is saturated, a result that is consistent with the observed adsorption behavior (See Chapter 3). At the silica/decane interface C151's CT state is stabilized by the more polar environment. C440 fluorescence from the silica decane/interface shows little difference from bulk solution limits indicating that a charge transfer state remains relatively inaccessible at the polar solid surface following photoexcitation.

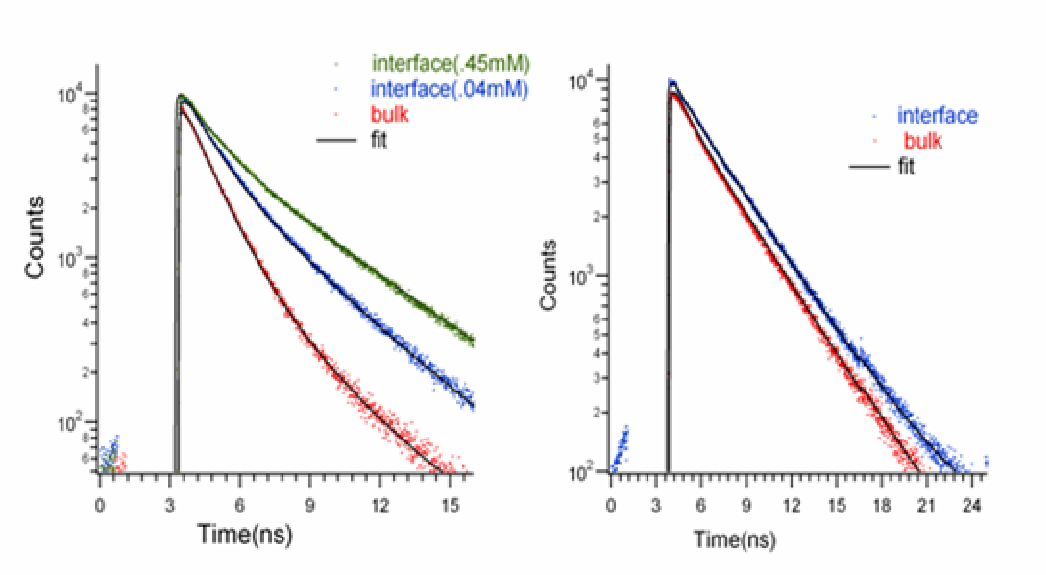

C151 **C440**

Figure 5.4.2. Fluorescence decay profile of C151 and C440 at silica/decane interface. The excitation was fixed at 360 nm and the fluorescence emission was collected at 400 nm long pass filter (LPF).

Table 5.3.2. Fluorescence lifetime values at silica/decane interface. Uncertainties in lifetimes and amplitudes are ± 80 ps and ± 1% respectively.

Solute	Conc.	A_1	τ_1 (ns)	A_2	τ_2 (ns)	χ^2
C151 at silica/Decane	40μM	0.60	1.20	0.40	3.33	1.2
	100μM	0.60	1.30	0.40	3.53	1.1
	450μM	0.62	1.15	0.38	4.34	1.3
C440 at silica/Decane	40μM	0.14	0.83	0.86	3.33	1.3
	100μM	0.13	0.96	0.87	4.30	1.5
	450μM	0.10	0.80	0.90	3.70	1.4

5.4. Discussion

When considering the properties of the different coumarins in bulk decane and adsorbed to the silica/decane interface, several questions stand out. First, what

is the origin of the rise time that appears in the time resolved emission from high concentration tertiary coumarins? Second, why is such behavior observed neither for C152 and C461 at the silica/decane interface nor for the primary coumarins (C151 and C440) in bulk solution? Third, why do the two primary coumarins, C440 and C151, show such different behavior relative to each other when solvated in bulk decane? Finally, why does the silica/decane interface appear to stabilize the planar, CT state of photoexcited C151 but not C440?

The behavior of the tertiary 7-aminocoumarins is, perhaps, easiest to understand. At low concentrations in decane, both solutes are characterized by single exponential fluorescence decays and in both cases, the measured lifetimes are consistent with a nonplanar, sp^3 hybridized amine in the 7-position. At higher concentrations in bulk decane, the time resolved data from both solutes show evidence of a second lifetime having negative amplitude. We attribute the negative amplitude feature at the higher C152 and C461 concentrations to the formation of solute dimers in solution. Dimers that are loosely associated in bulk solution can separate upon photoexcitation with one of the monomers remaining excited and then fluorescing with a lifetime characteristic of monomers in solution. Such a scheme would lead to continued buildup of excited state monomers in solution even after the laser pulse has passed through. This kinetics would manifest them as a second process observed in the time resolved emission and this process would have negative amplitude (meaning that the process would continue to create excited state monomers) long after the original laser excitation. This scheme is illustratedin the following page:

Scheme for dimer dissociation

In this scheme both ground state monomers and ground state dimers are present at high concentration solutions (> ~500μM). The ~100 fs optical pulse excites both species. The excited monomers will relax with an excited state lifetime equivalent to that of monomers in low concentration solutions. The excited dimers can relax nonradiatively (and remain associated as dimers), dimers can dissociate nonradiatively to form two ground state monomers or dimers can dissociate and still retain the excitation energy that resulted from absorption of a photon. In this last instance, one of the monomers will be in its ground state, but the other monomer will remain in its excited state and thus decay radiatively with the characteristic monomer emission lifetime. The important part of this mechanism is that it provides a way for the excited state monomer population to continue to grow long after the original excitation pulse has passed through the sample.

Further support of the proposal that the monomers in solution form dimers comes from steady state emission spectra from 1 mM concentrations of C152 in alkanes. Figure 5.5 shows the absorption and emission spectra from high and low concentration solutions of C152 in hexane. In addition to the primary feature centered at 425 nm from monomer fluorescence, the emission spectrum also shows a very weak but distinct band at ~520 nm. We assign this emission to weak fluorescence from those dimers in solution that remain associated following excitation. Absorption spectra of high concentration solutions showed no significant change with respect to the low concentration data, indicating that the loosely formed dimers have no addition electronic state.

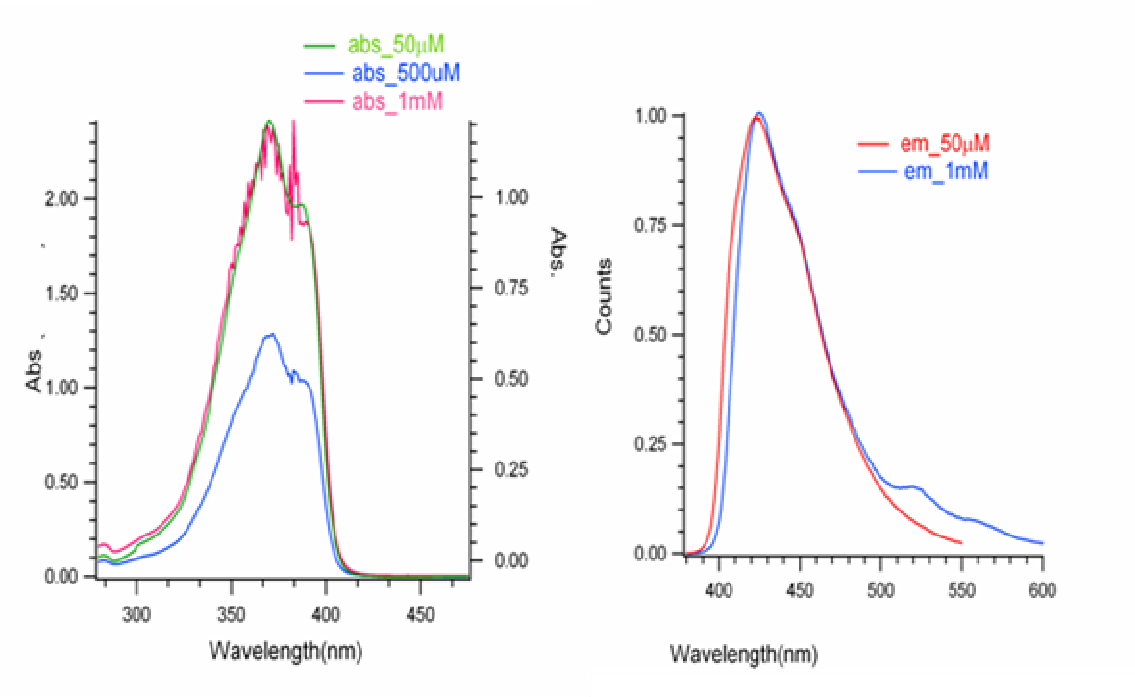

Figure 5.5. (Left) Absorption spectra and (Right) Emission spectra of C152 in bulk hexane. High concentrations absorption spectra were taken with a cell having pathlength 1mm.

Given the consistency of the proposed scheme with experimental observations and prior reports from the literature, [22] one can wonder about the structure of the proposed C152 dimer that forms at higher bulk concentrations. Both C152 and C461 are tertiary amines and are unable to donate hydrogen bonds. However, these monomers do have relatively large ground state dipole moments that can pair either in a head-to-tail fashion or with an anti-parallel geometry. We believe that the data presented in this work are most consistent with an anti-parallel arrangement. We base this conclusion on several considerations. First, explicit intermolecular hydrogen bonding can not be important given that the rise time is observed at high concentrations for the tertiary amines but not for the primary amines. (The tertiary

amines cannot donate hydrogen bonds.) Second, both the tertiary and primary amines have similar ground state dipole moments,[23-25] so simple energetic arguments based on dipole-dipole pairing would predict that the tertiary and primary coumarins should behave in a similar manner contrary to experimental observation. (The excited state tertiary and primary coumarins also have similar dipole moments, so the argument that monomer association following excitation (or excimer formation) is also unable to account for the diference between the primary and tertiary coumarins.) The most important structural difference between the tertiary and primary coumarins is the barrier to inversion about the amine. This barrier is ~2-3 fold lower for primary amines compared to the tertiary amines,[21] meaning that C151 and C440 will be undergoing large amplitude conformational changes more often than C152 and C461. Inversion about the amine will not change significantly the magnitude or the direction the ground state dipole, but such motion *will* affect the minimum separation between polar solutes that might otherwise try to dimerize in nonpolar solvents. We propose that rapid inversion disrupts the ability of C151 and C440 to form strongly associated dimers in solution and thus not exhibit the distinctive rise time in the time resolved fluorescence observed for C152 and C461 at higher bulk concentrations.

Further support for the idea that dimer dissociation is responsible for the rise time observed in the emission from high concentration solutions of C152 and C461 comes from the behavior of these solutes adsorbed to the silica/decane interface. TIR measurements of C152 adsorbed to the silica/decane interface show fluorescence decay that is single exponential characterized by a lifetime (~ 4.00 ns) that matches almost exactly the lifetime of C152 in low concentration decane solutions. This result

is independent of bulk solution concentration. In bulk decane the long lifetime of C152 is assigned to an excited electronic state where the amine retains its pyramidal, sp^3 geometry. We interpret results from the silica/decane interface first in terms of the silica surface's ability to restricts C152's ability to form a charge transfer state (with a correspondingly short, ~0.90 ns lifetime in polar solvents) [14] and in terms of the surface's ability to hinder C152 dimer formation (given the absence of a measurable risetime in the fluorescence decay regardless of bulk solution concentration). C461 shows similar behavior adsorbed to the silica/decane interface. Given that the all of the coumarin solutes adsorb strongly to the silica surface from methanol solutions, (ΔG_{ads} ~-25-30 kJ/mole), we expect that the reduced conformational mobility would favor the formation of head-to-tail dimers over anti-parallel dimers due to steric considerations.[26] Nevertheless, the TIRF measurements do not provide any evidence of dimer formation at any concentration.

The third question raised at the start of this section focuses on the differences in emission behavior between the two primary coumarins, C151 and C440, in decane. Time resolved fluorescence from both solutes show biexponential decay in decane. For each solute the long lifetime is ~ 3.50 ns and the short lifetime is ~1.00 ns. The long lifetimes of these primary amines is associated with a planar, charge transfer excited state while the shorter lifetime is typically associated with the sp^3 hybridized amine with a double-well potential. In the case of C151, the short lifetime (τ_1) component dominates the time resolved emission (A_1 ~ 0.85) whereas for C440, the long lifetime (τ_2) is the dominant pathway for radiative relaxation (A_2 ~0.85). Previous studies by Nad and Pal reported that the photophysical properties of C151 in

nonpolar solvents change dramatically from those of C151 in moderate to higher polarity solvents.[16,17] In particular, the quantum yield of C151 in alkanes drops from ~0.5 to ~0.2 as solvent polarity changes from that of DMSO or ACN to that of hexane or branched pentanes. Transient absorption measurements identify a nonradiative state having absorbance wavelength maxima at ~525 nm and 700 nm.[16] If we assign the dominant, short lifetime component observed for C151 fluorescence in decane to rapid conversion to a nonradiative state, then we are led to conclude that optically excited C440 does not cross over to the nonradiative state as readily and the observed fluorescence results from a state having more charge transfer character

The origin of this difference between C151 and C440 emission is not obvious, although experimental constraints may play a role. The steady state spectrum of C440 in bulk decane (Figure 5.2) has a distinct maxium at 332nm (See Table 5.1.), but our excitation laser is limited to producing light at 360 nm on the long wavelength side of the spectrum. At the excitation wavelength, we estimate that only 15% of the solutes are excited and those solutes that are excited do not have significant excess vibronic energy in the excited state. In contrast, the excitation maximum of C151 in decane falls at 348 nm and our excitation wavelength can excite close to 40% of the solutes in solution. If excess energy in the excited state is responsible for rapid inversion about the amine and nonradiative decay, we would expect that the shorter lifetime would be emphasized for C151 and the longer lifetime would be emphasized for C440 given these specific experimental conditions.

Time resolved measurements of C151 and C440 adsorbed to the silica/decane interface continued to show biexponential decay as observed in bulk decane, the

lifetimes measured in the TIRF experiments matched closely those measured in bulk solution. In the case of C440, even the relative amplitudes associated with the short and long lifetimes were unchanged. For C151 we observed an increase in the relative amplitude assigned to the long-lived CT state. In bulk decane, ~ 90% of the C151 fluorescence comes from the shorter lived electronic state. In contrast, the contribution to the fluorescence decay from the short lived states of those solutes probed in a TIRF experiment is only 60%. (See Table 5.3.2). These data imply that the polar silica surface is able to better stabilize the long lived, planar CT state of C151. For C440 the TIR data showed no significant change with respect to the bulk data indicating that the weakly electron donating $-CH_3$ group of C440 is unable to help stabilize a planar conformation of the excited state solute, but due to experimental constraints mentioned above the fluorescence will be detected from the CT state.

Many of the differences between the bulk solution photophysical behavior of tertiary and primary coumarins have been assigned intramolecular motion about the amino group in the 7-position. At low bulk concentrations, the tertiary coumarins (C152 and C461) both show single exponential fluorescence decays. At higher concentrations, the emission data show a distinctive rise time consistent with the dissociation of pre-formed dimers in solution. The primary coumarins (C151 and C440) show biexponential decays (with positive amplitudes) associated with emission from two distinct electronic states. These decays remain invariant regardless of solute concentration and the different weightings of the short and long lived states are

attributed to the amount of excess vibrational energy each solute has following photoexcitation.

To test these ideas we conducted several experiments examining the steady state (Figure 5.6.1) and time resolved fluorescence properties of two coumarins having *secondary* amines at 7-position (Figure 5.6.2). Coumarin 445 (C445) is equivalent to C440 and C461 except that C445 has a single $-CH_3$ group attached to the amine. Coumarin 450 (C450) has an ethyl group ($-C_2H_5$) group attached to the amine and a methyl group attached to the aromatic ring at the 6 position. In terms of inversion about the amine, barriers in 2˚ amines are intermediate between the primary and tertiary amine limits.[21]

The steady state emission behaviors of both solutes in bulk decane were similar to that of the other 7-aminocoumarins. The time resolved emission from both solutes at low concentrations showed single exponential behavior (similar to the tertiary amines) but the emission behavior remained invariant with solute concentration (similar to the primary amines). (Figure 5.6.2 and Table 5.4) From these observations, we conclude the following: First, the single exponential decay shows that these photoexcited secondary amines in decane decay from one electronic state, not two. In this respect, the secondary coumarins have photophysical properties similar to the tertiary coumarins. However, the absence of a rise time that appears in higher bulk concentrations signifies the absence of dimmer formation for these secondary coumarins, much like the primary coumarins. Due to the presence of single methyl group for C445 and ethyl group for C450 present at the 7-position the

inversion motion around the secondary amine group is restricted [21] but for high concentration there is no evidence of dimer formation much alike primary coumarins.

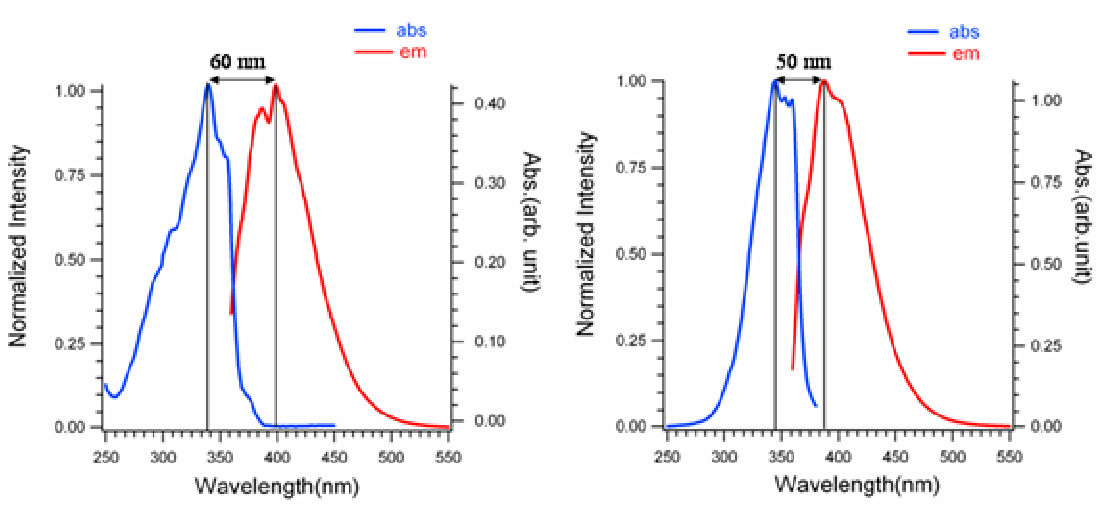

C445 **C450**

Figure 5.6.1. Steady state spectra of C445 and C450 in bulk decane

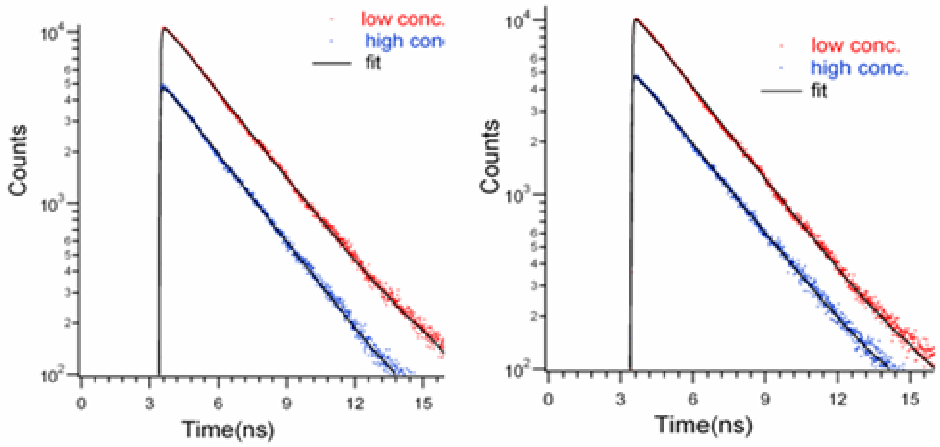

C445 **C450**

Figure 5.6.2. Fluorescence decay profile for C445 and C450 in bulk decane.

Table 5.4. Fluorescence lifetime value of C445 and C450 in bulk decane. Uncertainties in lifetimes is 100 ps

Solute in Solvent	Conc.	A_1	τ_1 (ns)
C445 in	10μM	1.00	2.56
Decane	1mM	1.00	2.70
C450 in	10μM	1.00	2.43
Decane	1mM	1.00	2.50

5.5. Conclusions

The experiments described in this chapter compared the steady state and time resolved fluorescence data acquired for a family of related 7-aminocoumarin derivatives solvated in bulk decane and adsorbed at a silica/decane interface. The absorbance and steady state fluorescence emission spectra exhibited small Stokes shifts in comparison to polar solvents which is in agreement with previous bulk solution results.[16,17] The time correlated single photon counting (TCSPC) data suggests that the substitution pattern of the solute and the concentration in bulk decane determine the solutes' fluorescence decay kinetics. For instance, the data show that the 7-aminocoumarins with tertiary amines are characterized by a single exponential time constant at low concentration. At high solute concentration, the fluorescence emission showed a distinctive rise time (or negative amplitude) characteristic of dimer or excimer formation in solution. Primary amine analogs, contrastingly showed biexponential decays as their lifetimes and relative amplitudes remained unchanged with changes in solute concentration. Physical considerations imply that tertiary amines are more likely to form ground state dimers rather than

excimers after photoexcitation, at least at the low concentrations sampled in this work. The dimers can dissociate upon photoexcitation leading to a continued growth of an excited state monomer population, which fluoresces with characteristic single exponential decay. Tertiary amine coumarins adsorbed at a silica/decane interface probed with TCSPC in total internal reflection geometry showed no such aggregation at any concentration most likely due to the hydrogen bond donating properties of the hydrophilic surface silanol groups.

In contrast, the primary coumarins show no aggregate formation in nonopolar solvents. These findings are discussed in terms of the ability of solute to undergo rapid inversion about the nitrogen that likely affects dimer formation in solution. The silica/decane interface study of C151 ($-CF_3$ at the 4 position), a primary coumarin, showed that the planar CT state was stabilized in comparison to the bulk decane limits. Bulk experiments with secondary coumarins showed intermediate behavior with these solutes showing single exponential fluorescence decay (similar to the tertiary coumarins) but with no evidence of aggregate formation at higher concentrations (similar to the primary coumarins).

References

(1) Atkins, R. L.; Bliss, D. E. *J. Org. Chem.* **1978,** 43, (10), 1975-1980.

(2) Halstead, J. A.; Reeves, R. R. Optics Communications **1978,** 27, (2), 273-276.

(3) Fletcher, A. N. *Appl. Phys.* **1977**, 14, 295- 302.

(4) Chu, G.; Yangbo, F. *J. Chem. Soc. Fard. Trans* **1987**, *83*, 2533-2539.

(5) Jones, G., Jackson, W. R., Choi, C.; Bergmark, W. R. *J. Phys. Chem.* **1985**, *89*, 294-300.

(6) Nemkovich, N. A.; Reis, H; Baumann,W. *J. Lumin.* **1997**, 71, 255-263

(7) Parkanyi, C. ; Antonious, M. S;Aaron, J. J.; Buna, M.;Tine, A.;Cisse, L. *Spectrosc.Lett.* **1994**, 27, 439-449

(8) Samanta, A.; Fessenden, R. W. *J. Phys. Chem. A* **2000,** 104, 37, 8577-8582.

(9) Tominaga, K.; Walker, G.C. *J. Photochem. Photobio. A: Chem*, **1995**, 87,127-133

(10) Gardecki, J.A.; Maroncelli, M. *J.Phys.Chem.***1999**,103, 1187-1197.

(11) Demelo, J. S. S.; Becker, R. S.; Macanita, A. L. *J. Phys. Chem.* **1994,** 98, (24), 6054-6058.

(12) Song, P.S.; Gordon (III), W.H. *J. Phys. Chem.*, **1970**, 74 (24), 4234–4240

(13) Satpati, A.; Senthilkumar, S.; Kumbhakar, M.; Nath, S.; Maity, D. K.; Pal, H. *Photochem. Photobio.* **2005,** 81, (2), 270-278.

(14) Nad, S.; Kumbhakar, M.; Pal, H. *J. Phys. Chem. A* **2003,** 107, (24), 4808-4816.

(15) Barik, A.; Nath, S.; Pal, H. *J. Chem. Phys.* **2003,** 119, (19), 10202-10208.

(16) Nad, S.; Pal, H., *J. Phys. Chem. A* **2001,** 105, (7), 1097-1106.

(17) Pal, H.; Nad, S.; Kumbhakar, M. *J. Chem. Phys.* **2003,** 119, (1), 443-452.

(18) Yamazaki, I.; Tamai, N.; Yamazaki, T., *J. Phys. Chem.* **1987,** 91, 3572-3577

(19) March, N.H.; Toshi, M.P. *Introduction to Liquid State Physic;*, World Scientific: NJ, **2002**.

(20) Wurthner, F.; Yao, S.; Debaerdemaeker, T.; Wortmann, R. *J. Am. Chem.l Soc.* **2002,** 124, (32), 9431-9447.

(21) Belostoskii, A.M. ; Aped. P. ; Hasner, A. *J.Mol. Struct. (Theochem)* **1997,** 398-399, 427-434.

(22) Forster, T. *Laboratorium fur physicalische Chemie, Technische Hochshule;* Stuttgart, Deutschland

(23) Cave, R. J.; Castner, E. W. *J. Phys. Chem. A* **2002,** 106, (50), 12117-12123.

(24) Cave, R. J.; Burke, K.; Castner, E. W. *J. Phys. Chem. A* **2002,** 106, (40), 9294-9305.

(25) Rechthaler, K.; Kohler, G. *Chem. Phys.* **1994,** 189, (1), 99-116.

(26) Martinez, V. M.; Arbeloa, F. U.; Prieto, J. B.; Lopez, T. A.; Arbeloa, I. L. *J. Phys. Chem. B* **2004,** 108, 20030- 20037.

Chapter 6. Competition between Polar and Nonpolar Solvation Mechanism

6.1. Introduction

Experiments described in earlier chapters probed the steady-state and time-dependent photophysical properties of 7-aminocoumarins (7-AC) in a polar, protic solvent (methanol), in a nonpolar solvent (decane), and adsorbed to a polar silica surface from both solutions. A surprising result was that the silica surface appeared to stabilize a conformation of excited state coumarins that was less polar than expected. Specifically, the time dependent fluorescence emission from C151, C440, and C152 adsorbed to the silica/methanol interface all exhibited lifetimes more consistent in a nonpolar solvation environment. We attributed this behavior to the silica surface's ability to donate strong hydrogen bonds to the amino group thereby favoring a pyramidal, sp^3 hybridization. In bulk methanol solution, the solvent was mobile enough for excited state coumarin solutes to adopt a planar, CT geometry (or a nonplanar TICT structure in the case of C152) with the amine adopting a sp^2 hybridization.

These studies showed that solute-substrate and solute-solute interactions played important roles in promoting unexpected surface chemistry. Additional experiments using decane as a solvent clarified further the roles played by solvent-solute and substrate-solvent solvent interactions in controlling interfacial solvation. Tertiary-7AC solutes showed a tendency to aggregate in bulk decane solution at

concentrations above ~ 1 mM. For these coumarin species in decane solutions, however, a silica surface appeared to inhibit the formation of dimers (or larger aggregates) and the time resolved emission data were consistent with the surface promoting emission from the polar, excited state conformer. Given the very different effect of polar and nonpolar solvents on the interfacial photophysical properties of these solutes, one can wonder what effects an amphiphilic solvent will have on the steady state and time resolved properties of solutes at surfaces.

1-decanol has characteristics of both decane (a 10-carbon aliphatic chain) and methanol (a –OH group in the 1-position). Experiments described in this chapter examine the steady state and time resolved emission properties of different 7AC solutes both in bulk solution and adsorbed to silica/1-decanol interfaces. The simplest question that can be asked is will solvation in decanol resemble solvation in decane or methanol or will evidence of both nonpolar and polar solvation environments be observed? Alternatively, will decanol solvate the coumarin solutes in bulk solution and at interfaces in unique ways that can not be described by some combination of nonpolar and polar environments? What affect the surface have on interfacial solvation in decanol solutions? To answer these questions we measure both steady-state and time-dependent fluorescence emission of primary and tertiary 7AC solutes using instrumentation described in Chapter 2.

Previous works in our own group and by others provide a basis for anticipating results. Maroncelli and coworkers determined the solvation timescale of Coumarin 153 in variety of alcohols.[1] Flourescence upconversion experiments showed that hydrogen bond donating properties of the alcohols provide an additional

solvation mechanism with a characteristic timescale that is considerably longer than other aprotic solvents.[1] In a separate effort Eisenthal and coworkers also probed the solvation timescale in different alcohols. They observed that solvation timescales slowed down for long chain alcohols and proposed that solvent relaxation times depend on alcohol chain-length due to the effect of the hydroxyl liberational motion and translational motion of the alcohol molecules.[2] Extending these studies into interfacial solvation, Yanagimachi *et al.* probed solvent relaxation at the sapphire/1-butanol interface and observed that the relaxation became slower in the interfacial region due to the hydrogen bonding interactions between solvent and substrate.[3]

To further investigate the effect of solvent-substrate and solute-substrate interactions earlier work from our own group used nonolinear optical methods to probe polarity at two different interfaces: a weakly interacting silica/cyclohexane interface, and a strongly associating silica/1-octanol interface. Results showed that at the weakly interacting silica/alkane interface, solutes sampled a more polar environment than in bulk. In contrast, the silica/octanol interface showed evidence of heterogeneity with two distinct dielectric regions: one that was more polar and the one that was less polar than bulk solution.[4] These studies were sensitive to the orientation and environment surrounding adsorbed solutes in their electronic ground state. These studies also motivated us to explore how altered solvation environments at interfaces influence the properties of these same solutes in their excited states. To accomplish this goal, we carried out TIRF-TCSPC measurements of solutes solvated at the silica/decanol interface. Of particular interest was whether or not these experiments would show evidence of both the polar and nonpolar environments

inferred from non linear optical measurements of solvent polarity at strongly associating, silica/*n*-alcohol interfaces.

In this chapter we first report the steady state and time-resolved emission of 7-AC solutes dissolved in bulk *n*-decanol. The solutes used are the same as those that were featured in Chapters 3-5 of this thesis, namely Coumarins 151 (C151), Coumarins 152 (C152), Coumarin C440 (C440), and Coumarin 461 (C461). (Figure 6.1) All solutes were used as received without any additional purification. The solvent used for all of these studies was spectral grade decanol (>99%, Aldrich) that again was used as received.

Results presented in this chapter address how hydrogen-bonding properties of the solvents can affect solute emission dynamics.[5-13] For the first time, we observe effects on solute emission behavior that can be assigned to solvent reorganization following excitation. For smaller solvents like methanol, such dynamics were too fast to be measured with our instrumentation. For 1-decanol, however, Maroncelli and co-workers reported solvation dynamic times as long as 250 ps around 7AC solutes including C153.[14] In the data presented below, we see evidence of this reorganization reflected in the measured lifetimes of emitting solutes. Following photoexcitation, hydrogen bonds between the solute and solvent break in order for the solvent to stabilize the new electron distribution.[15-18] In decanol such motion is slow and, consequently, the solute exists first in a partially solvated (non-hydrogen bonded) state following photoexcitation before the solvent fully reorganizes around the solute re-establishing hydrogen bonds and any additional dipole-dipole and dipole-induced dipole interactions.

For C152 and C151 we observe fluorescence from these two states distinctly and the origin of the two lifetimes will be discussed in detail below. Unlike C152 and C151, the fluorescence decay behavior of C461 and C440 showed a distinctive rise time that is assigned to the inertial solvent motion resulting from solvent reorganization. For C461 and C440 the solvent reorganization is most pronounced as the solute molecules undergo a relatively large change in the dipole direction compared to C152 and C151.[19] The change in $\Delta\theta$ is almost two-fold greater for C440 and C461 than for C151 and C152 as described in detail in Chapter 4. This change requires a greater degree of solvent motion in order to stabilize the newly excited electron distribution. Results from bulk solution were compared with those obtained from the silica/decanol interface, but the interfacial data showed little significant change from the bulk limit implying that at the silica/decanol interface solutes do not interact as strongly with the surface and see a consistent, bulk solution environment.

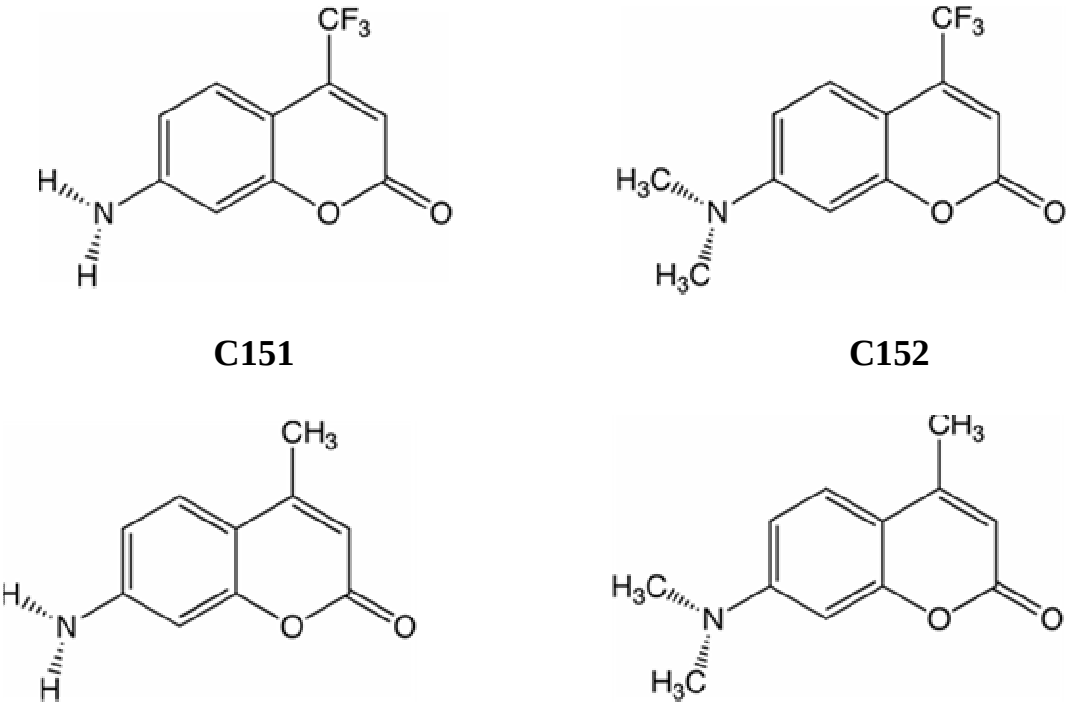

Figure 6.1. Structures of the 7-aminocoumarins

6.2. Results

Figure 6.2 shows the absorption and emission of the 7AC solutes in decanol. Previous results in this thesis showed that the Stoke's shift is larger in the polar hydrogen donating solvents than nonpolar non-hydrogen bonding solvents. (See Figure A.6.1 in the Appendix-6).[20-22] The values of the Stoke's shift are reported in Table 6.1. From the steady state results of n-decanol it was observed that the Stoke's shifts were smaller compared to MeOH and larger compared to decane. From these results we infer that steady state solvation behavior in n-decanol is intermediate between MeOH and decane which reflects a balance between the hydrophobic and hydrogen bonding solvation mechanism. Furthermore, the similarities between C440

and C461 indicate that steric hindrance about the amine does not impact significantly the local solvation environment.

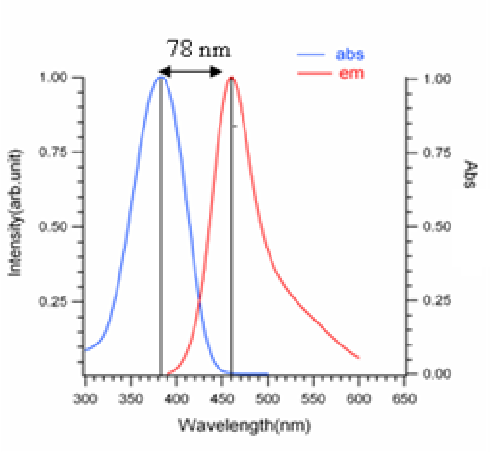

C151

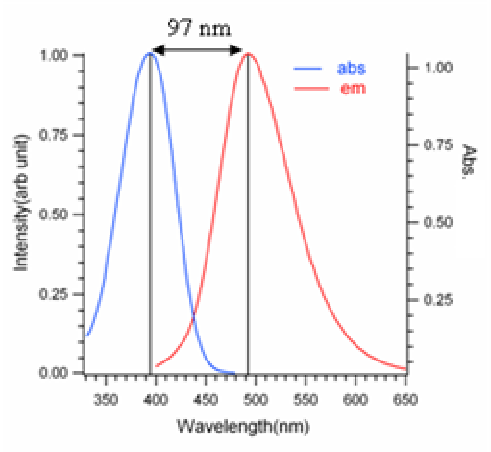

C152

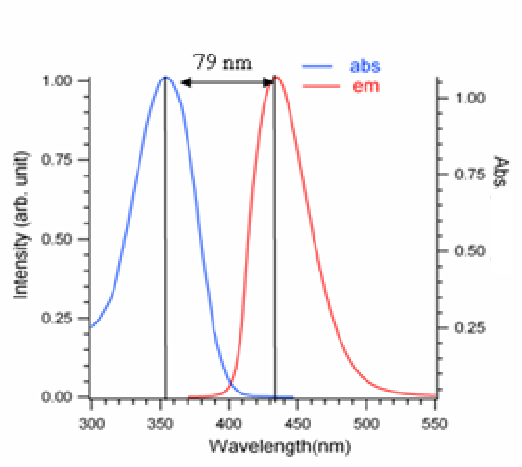

C440

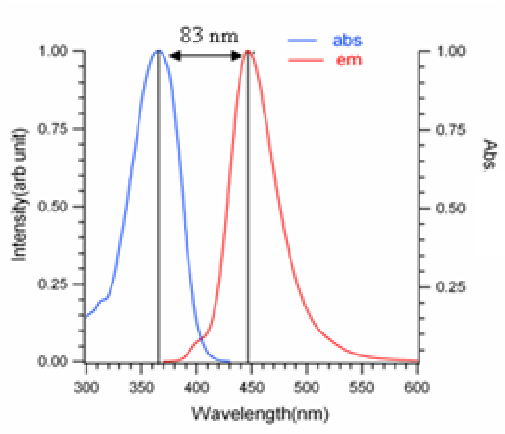

C461

Figure 6.2. Spectra of 7-aminocoumarins in bulk decanol

Table 6.1. Spectral data in bulk decanol

Solute	Absorption Peak (nm)	Emission Peak (nm)	Stoke's Shift (cm^{-1})
C151	382	460	4440
C152	392	492	5190
C440	355	432	5020
C461	365	445	5030

In order to determine whether polarity and hydrogen bonding properties of the solvent play an important role in defining time dependent solute-solvent interactions, emission lifetimes were measured using the TCSPC instrumentation described earlier. Figure 6.3.1 shows fluorescence decay traces of the four coumarins in bulk decanol. The fluorescence lifetime measurements were made with ~ 100 μM concentrations. For both C151 and C152, the decays are distinctly biexponential. The longer lifetimes of C151 and C152 are characterized by time constants ranging ~ 4.00 to 5.00 ns with both amplitudes being positive. The shorter lifetimes for C151 and C152 are on the order of ~ 500 ps and contribute ~10% - 15% to their emission intensity**.** In contrast to these two solutes that have the -CF_3 group at the 4-position, the decay data of C461 and C440 in decanol could only be fit if a rise time (indicated by a negative preexponential factor [23]) was added to the exponential decay at a ~ 4.00 ns (Figure 6.3.1). The value of the rise time for the two solutes varies between 200 ps-300 ps and the negative amplitude accounts for ~13%-20% of the total intensity. The relevant lifetime values are reported in Table 6.2.1 and Table 6.2.2 respectively. It is

important to note that all experiments were carried out with an excitation wavelength of 380 nm and emission was measured with a 420 nm LPF to discriminate against scattered light from the excitation pulse. Given that the absorption and emission peaks for the four solues are different for each of these coumarins, experiments begin with different amounts of excess internal energies in their excited states.

To further explore the origin of the two lifetimes associated with the fluorescence decay of C152 and C151, we employed combinations of short pass filters (SPF) and long pass filters (LPF) to examine separately the short and long wavelength contributions to the emission spectra. In addition to the 420 LPF we used a 512 SPF and 550 LPF. The 512 nm SPF discriminated against contributions to the decay from the long wavelength portion of the spectrum and the 550 nm long-pass filter was used to capture only emission from the red side of the emission spectrum. Using the 512 nm SPF, we observe that the contribution of the shorter lifetime (~ 400 -500 ps) component to the measured decay for both C152 and C151 increases by 2-3 fold (A_1= 0.3), whereas with a 550 LPF the observed fluorescence for C152 showed an evidence of rise time with a time constant of almost ~ 500 ps. (See Figure 6.3.2). For C151, using 550 LPF yielded no significant signal as the steady-state emission spectrum has virtually no intensity at 550 nm.

Results for C151 and C152 solvated in bulk decanol were compared to time-resolved results from the silica/decanol interface. For bulk solution measurements, concentrations were kept low (10 μM) but these were increased serially to 100 μM for the TIRF measurements. Regardless of bulk solution concentration, fluorescence lifetimes of these coumarin species at silica/decanol

interface remained virtually unchanged compared to bulk limits. The fluorescence decay profiles are shown in Figure 6.4.and amplitudes/lifetimes are reported in Table 6.3.

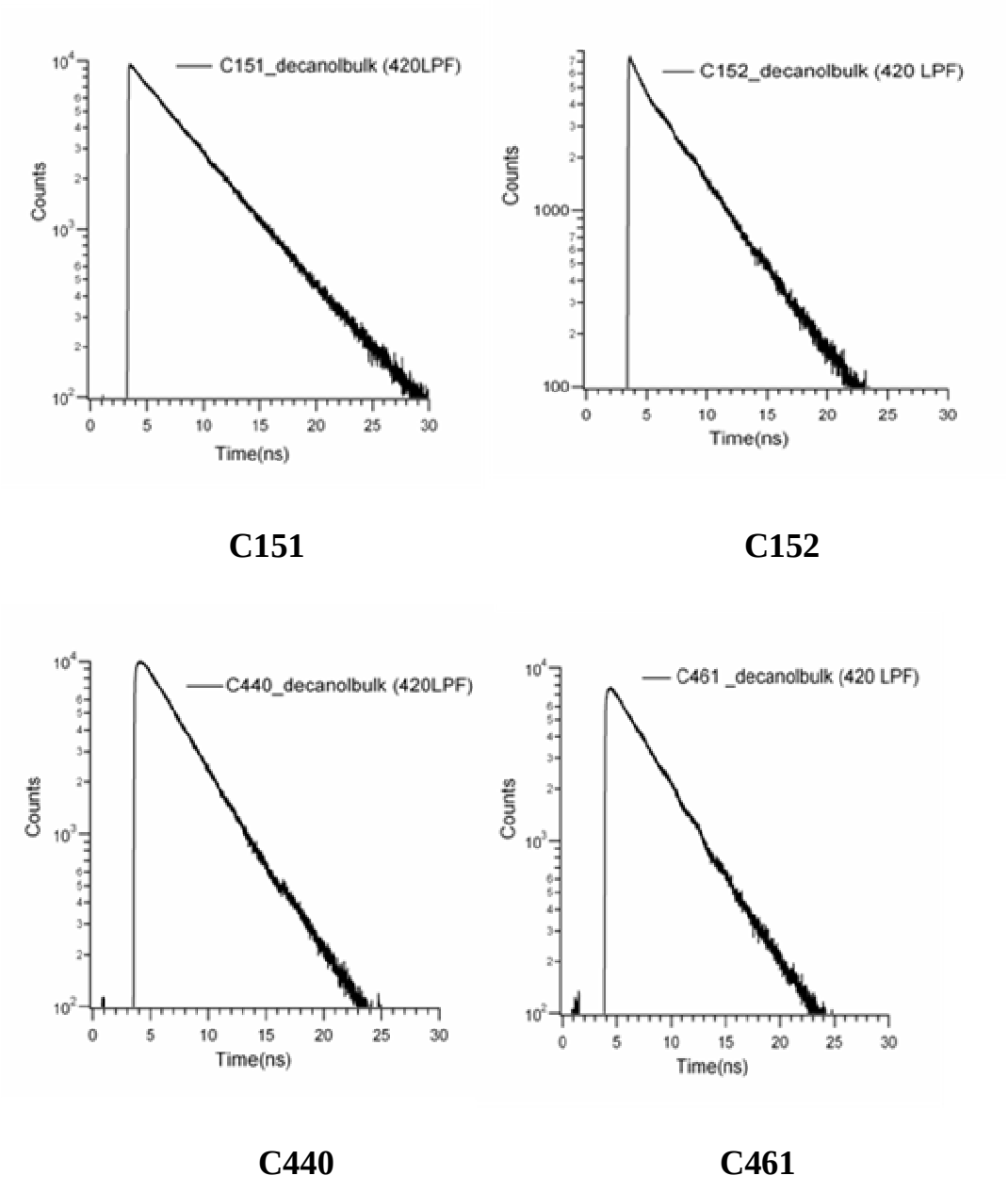

Figure 6.3.1. Fluorescence decay of 7-aminocoumarins used in the present study in bulk decanol. The excited wavelength was fixed at 380nm for C151 and C152; whereas for C461 and C440 the excited wavelength was 365 nm. The fluorescence emissions were collected using a 420 long pass filter (LPF).

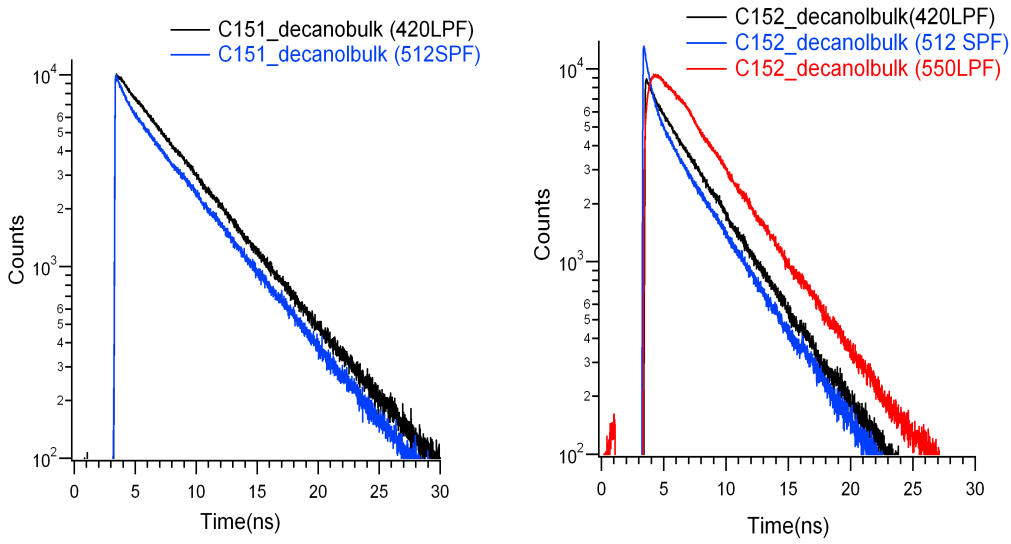

C151 **C152**

Figure 6.3.2. Fluorescence decay of 7-aminocoumarins used in the present study in bulk decanol using three different filters to collect emission for C151 and C152.

Table 6.2.1. Fluorescence lifetime in bulk decanol. Uncertainties in lifetime and amplitude are ± 60 ps and ± 8% respectively.

Solute	Filter	A_1	τ_1 (ns)	A_2	τ_2 (ns)	χ^2
C151	420 LPF	0.10	0.40	0.90	5.55	1.3
	512 SPF	0.30	0.41	0.70	5.55	1.4
	550 LPF		*Signal very low*			
C152	420 LPF	0.17	0.55	0.83	4.34	1.2
	512 SPF	0.26	0.55	0.74	5.30	1.1
	550 LPF	1.00	4.34	-0.65	0.50	1.6

Table 6.2.2 Fluorescence lifetime in bulk decanol. Uncertainties in lifetime and amplitude are ± 60 ps and ± 3% respectively.

Solute	Filter	A_1	τ_1 (ns)	A_2	τ_2 (ns)	χ^2
C440	420 LPF	1.00	4.00	-0.20	0.28	1.4
C461	420 LPF	1.00	4.00	-0.13	0.21	1.1

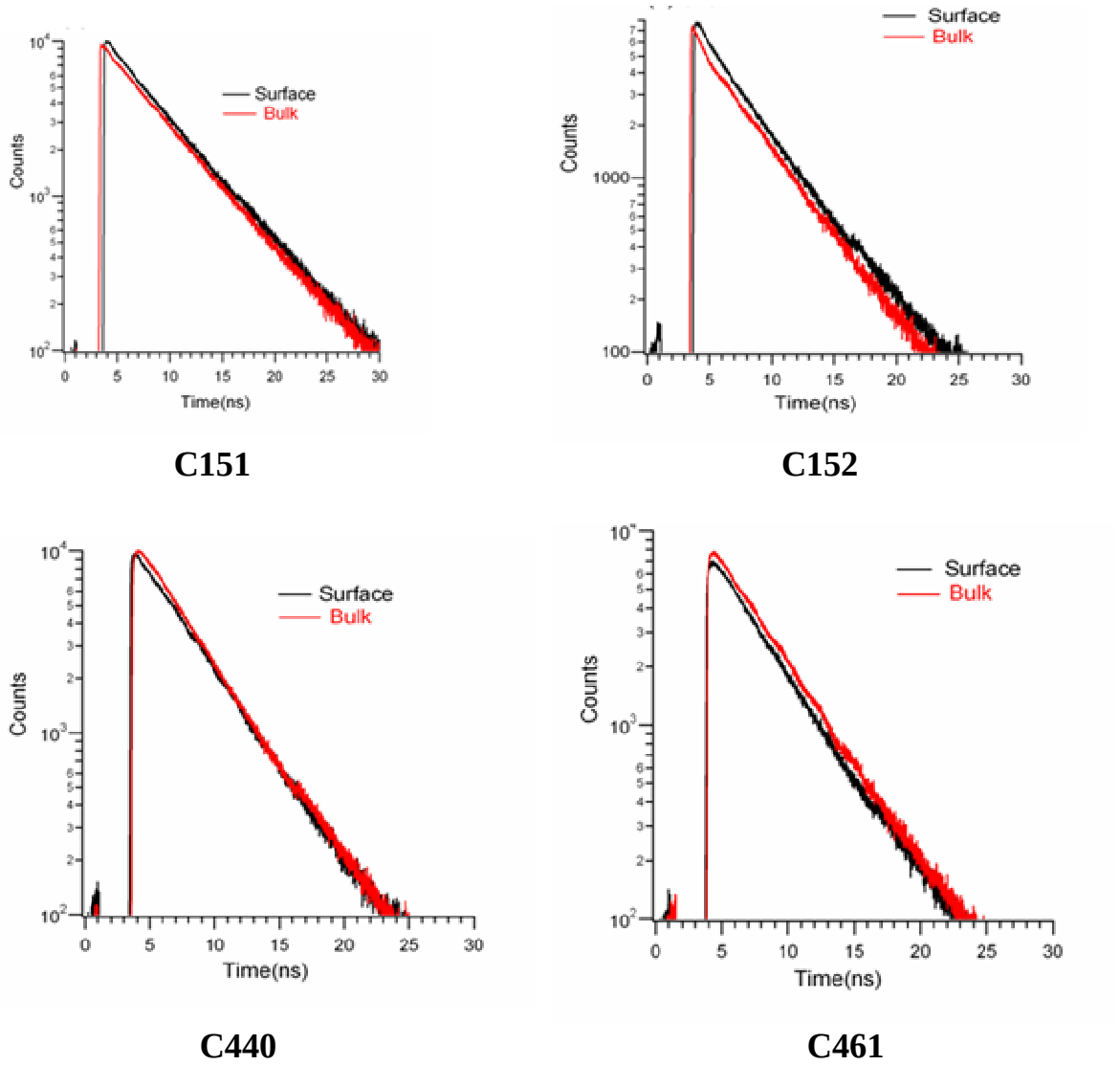

Figure 6.3.3. Fluorescence decay profile of 7-aminocoumarins at silica/decanol interface. The excited wavelength was fixed at 380nm for C151 and C152; whereas for C461 and C440 the excited wavelength was 365 nm. The fluorescence emissions were collected using a 420 long pass filter (LPF).

Table 6.3. Fluorescence lifetime at silica/decanol interface. Uncertainties in lifetime and amplitude are ± 30 ps and ± 3% respectively

Solute	Filter	A_1	τ_1 (ns)	A_2	τ_2 (ns)	χ^2
C151	420 LPF	0.16	0.50	0.84	5.27	1.3
	512 SPF	0.35	0.47	0.65	5.27	1.5
	550 LPF	*Signal very low*				
C152	420 LPF	0.33	0.48	0.67	4.16	1.4
	512 SPF	0.60	0.47	0.40	4.16	1.5
	550 LPF	1.00	4.06	-0.60	0.52	1.1
C440	420 LPF	1.00	3.84	-0.30	0.31	1.4
C461	420 LPF	1.00	4.00	-0.20	0.30	1.2

6.3. Discussion

Studies described in this chapter examine the photophysical behavior of different 7-AC solutes in decanol solutions and adsorbed to the silica/decanol interface. These studies build upon work presented earlier that characterized the fluorescence emission of these solutes in methanol, a polar protic solvent, and decane, a nonpolar, saturated alkane. Decanol has both polar and nonpolar characteristics and can provide insight into which solvation mechanisms – polar or nonpolar – control a solute's behavior when both mechanisms are viable. Our results indicated that the primary and tertiary 7ACs with $-CF_3$ at 4-positions (C151 and C152) behave similarly. However, in C151 the dominant long lifetime indicates the stablization of CT state, but the dominant long lifetime of C152 indicates a nonplanar sp^3 conformation.

The decay profiles of 7ACs with $-CH_3$ groups at the 4-position (C440 and C461) appeared similar to each other but different from those of C151 and C152.

With these comparisons in mind, we conclude that the identity of the substituent at 4-position appears is the primary factor controlling 7AC solvation in decanol. This result contrasts with the behaviors of these same solutes in decane where the identity of the amine (primary or tertiary) played the dominant role in controlling solvation behavior. The decanol results also contrast in part from those observed for these solutes in methanol solutions. Methanol stabilized the polar conformation of all 7AC solutes studied, regardless of the actual functional groups or substitutents present.[24,25] Unlike in methanol, both C151 and C152 in decanol showed biexponential decays indicating that two excited states – not one – contributed to the observed emission.

To explain differences between solvation in 1-decanol and methanol, we begin by assuming that all solutes in their electronic ground states are hydrogen-bonded to decanol in a manner similar to methanol. Following photoexciation the electronic structure of the solute changes and (solute) functional groups that participated in ground state hydrogen bonding may be more (or less) electronegative. The solvent will reorganize itself to accommodate this new charge distribution leading to some hydrogen bonds being broken and new ones being formed.[9,10] In short chain alcohols like methanol this reorganization is fast (< 20 ps) and is can not be observed with our instrumentation. Reorganization in 1-decanol, however, is slow ($\geq$ 200 ps),[14] and we are able to detect emission from the excited state prior to the excited solute being fully stabilized by the surrounding solvent.

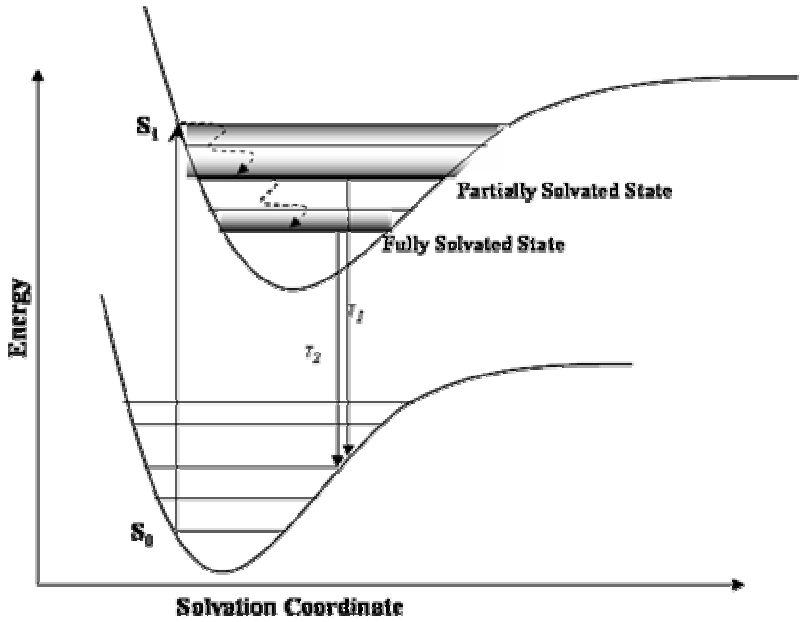

Figure 6.4. Scheme depicting the hydrogen bond mediated solvation mechanism. Here S_0 is the ground state and S_1 is the first electronic energy state populated by the solutes immediately after photoexcitation (before the H-bond dissociates).

We assign the shorter lifetime (~ 400 ps) observed for C151 and C152 in decanol to the intermediate non-hydrogen bonded state. The longer lifetime of C151 (5.00 ns) and C152 (4.00 ns) in decanol are assigned to the fully solvated excited solutes. As noted above, the longer lifetime of C151 in decanol appears similar to that in bulk methanol, whereas the longer lifetime of C152 appears to be the same as in bulk decane. We, therefore propose that the fully solvated C151 state in decanol experiences a *polar* environment leading to a planar CT state. Conversely the fully solvated C152 in decanol appears to adopt a non-planar *nonpolar* conformation as in bulk decane. The origin of this difference is not clear, but is likely due to steric considerations. C151 with its primary amine may have a CT state more accessible to be stabilized by the –OH groups of decanol. In contrast, the TICT state of C152 may

not be as easily stabilized because of the methyl groups on the amine *and* the bulky C_{10} chain on the solvent.[26-28]

Dissecting the emission spectra from these two solutes using the 512 SPF and 550 LPF helps clarify these ideas. From the original experiments (collecting all of the emission using only a 420 nm LPF), fluorescence was dominated by the longer lifetime (~ 4.00 – 5.00 ns) component implying that most of the solutes sampled in this spectral window were emitting from the fully stabilized excited electronic state; whereas the 512 nm SPF led to enhanced contribution from shorter-lived species. From these findings we surmise that the emission from the shorter-lived species comes from excited state solutes that have not been fully stabilized by the decanol solvent. Next, a 550 nm LPF was used probing C152 to collect emission from the red tail on the emission spectrum. This experimental configuration discriminated against contributions from the shorter-lived species emitting at a shorter wavelengths. With the 550 LPF we were unable to observe any emission from C151, but the C152 emission from longer wavelengths showed the distinct growth of a rise time (with a negative amplitude). This result reinforces the idea that the ~0.50 ns lifetime observed for these solutes in decanol reflects the effects of solvent relaxation. With the 550 LPF, we can only detect emission from those solutes that have been sufficiently stabilized so that they lie at the minimum of the excited state potential energy surface. The rise time observed in the C152 emission would then correspond to the duration of the reorganization before the emitting solutes fall into the "window" where the fluorescence can be observed.

Decay from C440 and C461 with the $-CH_3$ group at 4-position is characterized by a single emission mechanism coupled with a second process having a negative amplitude or rise time. We propose that this phenomenon can be attributed to the fact that the 7AC solutes with a $-CH_3$ at 4-position undergoes a larger dipole orientation orientation ($\Delta\theta$),[19] compared to 7AC solutes having a $-CF_3$ group. In the case of C151 and C152, excitation leads to a change in dipole magnitude, but not orientation, meaning that long range solvent structure does not need to change significantly and that reorganization will be affected by local interactions. The change in dipole *orientation* that accompanies excitation of C440 and C461 will require not only that local structure changes but also that the surroundings also adapt to the new dipole orientation. One important point to note is that all the decay profiles of all 7ACs in decanol were sampled using 420 LPF. Using a 420 LPF we collect emission towards the red-edge in the steady state emission spectra for C461 and C440. Therefore, it could be possible that any fluorescence from wavelength shorter than 420 nm is not detected in this present experiment, and the fluorescence from the partially solvated non-hydrogen bonded complex was not sampled using a 420 LPF. This last hypothesis represents a clear line of investigation that can be pursued in future investigations.

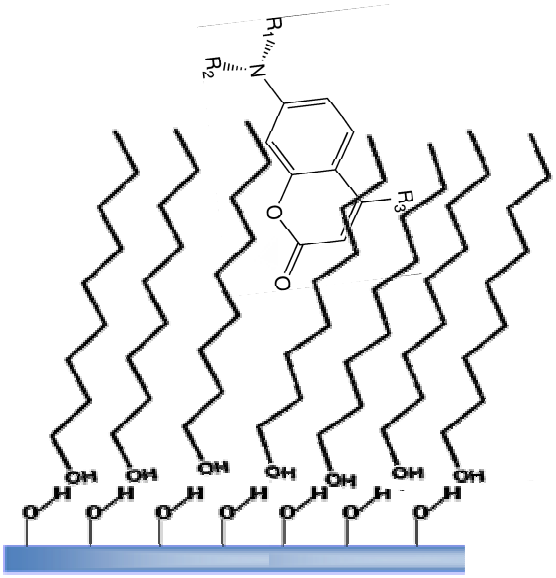

Figure 6.5. A representation of silica/decanol interface

The last experiments conducted compared the results from these solutes in bulk decanol to those from solutes adsorbed to the silica/decanol interface. The surface data showed no significant difference from the bulk limits. For C151 and C152, we observed a bi-exponential decay similar to bulk solutions (with similar coefficients). For C440 and C461, a fast rise time was observed again, like the bulk data, along with a long lived decay. These results may mean that the solvation environment sampled at the silica/decanol interface differs little from bulk decanol *or* that these solutes do not adsorb to the silica interface to an appreciable degree from decanol solution and that all of the signal detected in the TIRF experiments comes from those solutes probed by the evanescent wave. A lack of surface activity could be due intermolecular interaction solutes as long chain alcohols force to make their way to the surface (illustrated schematically in Figure 6.5).

References

(1) Maroncelli, M.; Fleming, G.R. *J. Chem. Phys.* **1987**, 86 (11), 6221-6239.

(2) Shi, X.; Long, F.H.; Lu, Hong.; Eisenthal, K.B. *J. Chem. Phys.* **1995**, 99(18), 6917-6922.

(3) Yanagimachi, M., Tamai, N. and Masuhara, H.*Chem. Phys. Letts* **1992**, *200*, 469-474.

(4) Zhang, X.; Steel, W.H.; Walker, R.A. *J. Phys. Chem. B* **2003**, 107, 3829-3836.

(5) Negrerie, M.; Gai, F.; Bellefeuille, S. M.; Petrich, J. W. *J. Phys. Chem.* **1991,** 95, 8663-8670.

(6) Moog, R.S.; Maroncelli, M. *J. Phys. Chem*. **1991**, 95, 10359-10369.

(7) Schwartz, B.J.; Peteanu, L.A.; Harris, C.B. *J. Phys. Chem*. **1992,** 96, 3591-3598.

(8) Barbara, P.F.; Walsh, P.K.; Brus, L. E. *J. Phys. Chem*. **1989,** 93, 29-34.

(9) Marcus,Y. *J. Sol.Chem.* **1991 ,**20, 929- 944.

(10) Reid, P.J.; Alex, S.; Jarzeba,W.; Schlief, R.E.; Johnson, A.E.; Barbara, P.F. *Chem. Phys. Lett.* **1994**, 22, 93 – 100.

(11) Pimental, G.C.; McClellan, A.L. *The Hydrogen Bond;* Freeman: San Francisco, **1960**

(12) Schuster, P.; Zundel, B.; Sandorfy, C. *The Hydrogen Bond: Recent Developments in Theory and Experiments*; North Holland: New York, **1976.**

(13) Dore, J. C.; Teixeira, J. *Hydrogen-Bonded Liquids*; Kluwer Academic: Boston, **1991**

(14) Horng, M. L.; Gardecki, J. A.; Papazyan, A.; Maroncelli, M. *J. Phys. Chem.* **1995**, *99*, 17311-17317.

(15) Benigno, A. J.; Ahmed, E.; Berg, M. *J. Chem. Phys.* **1996**, *104*, 7382-7394.

(16) Yu, J. W.; Berg, M. *Chem. Phys. Lett.* **1993**, *208*, 315-320.

(17) Tanaka, H.; Kokai, F.; Brauman, J. I.; Fayer, M. D. *Chem. Phys. Lett.* **1987**, *142*, 371- 375.

(18) Schellenberg, P.; Friedrich, J. *J. Lumin.* **1993**, *56*, 143- 149.

(19) Cave, R. J.; Burke, K.; Castner, E. W. *J. Phys. Chem. A* **2002,** 106, (40), 9294-9305.

(20) Walker, G. C.; Jarzeba, W.; Kang, T. J.; Johnson, A. E.; Barbara, P. F. *J. Opt. Soc. Am. B-Opt. Phys.* **1990**, *7*, 1521.

(21) Suppan, P. *J. Chem. Soc.-Faraday Trans. I* **1987**, *83*, 495-509.

(22) Nad, S.; Pal, H. *J. Phys. Chem. A* **2001,** 105, (7), 1097-1106.

(23) Castner, Cave, *J. Phys. Chem. A*, **2000**, 104 (13), 2869–2885.

(24) Rechthaler, K.; Kohler, G. *Chem. Phys.* **1994,** 189, (1), 99-116.

(25) Satpati, A.; Senthilkumar, S.; Kumbhakar, M.; Nath, S.; Maity, D. K.; Pal, H. *Photochem. and Photobio.* **2005,** 81, (2), 270-278.

(26) Nad, S.; Kumbhakar, M.; Pal, H. *J. Phys. Chem. A* **2003**, 107, (24), 4808-4816.

(27) Bank, A.; Kumbhakar, M.; Nath, S.; Pal, H. *Chem. Phys.* **2005**, 315, (3), 277-285.

(28) Dahiya, P.; Kumbhakar, M.; Mukherjee, T.; Pal, H. *Chem. Phys. Lett.* **2005**, 414, (1-3), 148-154.

Chapter 7. Summary and Future Directions

Surfaces, unlike bulk solution, are intrinsically anisotropic and can induce changes in solute conformation and reactivity. However, a systematic understanding of interfacial solvation remains elusive**.** In this context, the present studies used steady state and time resolved techniques to compare the behavior of 7-aminocoumarin (7AC) dyes in bulk solution and adsorbed to polar hydrophilic silica substrates. 7AC dyes used in the present study are categorized as either primary amine coumarins (C151, C440) or secondary amine coumarins (C445, C450) or tertiary amine coumarins (C152, C461) based on the alkylation of the amine group. A second structural element differentiating these solutes from each other is the functional group in the 4- position: C151 and C152 both have electron withdrawing –CF_3 groups whereas the other solutes all have weakly electron donating –CH_3 groups.

Solute structure as well as solvent polarity and hydrogen bonding play key roles in determining the excited state conformation and relaxation pathways of solutes in solution and adsorbed to silica surfaces. To test the effect of solvents' identity on interfacial solvation; solvents used in this work were systematically chosen with varying polarity and hydrogen bonding characteristics. Solvents used were a methanol (polar and protic), decane (nonpolar and aprotic), and *n*-decanol (amphiphilic and protic). Additional solvents including acetonitrile (polar and aprotic) were sampled selectively and those results are tabulated in Appendix X. Our findings suggest that the strong hydrogen bond donating properties of the silica

surface can induce anisotropic ordering in the adjacent solvent molecules as well as the adsorbed solutes resulting in the alteration of interfacial polarity.

7.1. Steady State Characteristics

Solute-solvent interactions of the coumarins in bulk media were characterized by their respective absorption and emission spectra. Results show that the absorption and emission of all solutes studied depended considerably on solvent polarity and hydrogen bonding ability. All 7AC solutes tested in the present study have similar ground state dipole moments and undergo large changes in $\Delta\mu$ upon photoexciation.[1] Our result showed that larger Stokes shifts were observed in polar protic solvents (MeOH, DeOH) than nonpolar aprotic solvent (decane), implying that the excited states of the solutes are more stabilized due to H-bonding interactions. Next, adsorption experiments were performed to characterize the respective surface activities of these solutes. All solutes showed similar free energies of adsorption – ΔG_{ads} ~ -25 –-30 kJ/mole – regardless of solute structure. These results suggested that the structural differences between the molecules do not play as significant a role in adsorption to hydrophilic silica surfaces. However, the photophysical properties of the adsorbed solutes showed a much larger dependence on respective solute structure.

Structurally, 7ACs with tertiary amines (C152, C461) can only accept hydrogen bonds, whereas the coumarins with primary amines (C151, C440) can both donate and accept hydrogen bonds. Adsorption spectra of C152 and C461 showed a larger red shift in the adsorbate emission spectra with increasing surface coverage due to the formation of multilayers. The alkyl groups of tertiary 7ACs sterically hinder the

solute's ability to accept hydrogen bonds from the surface. Hence these solutes can readily interact with the adsorbed neighbors rather than the hydrophilic surface, making the surface appear more polar at high solute concentrations. Furthermore, the emission spectra of C152 (-CF_3 in the 4-position) of adsorbed solute molecules from high concentration methanol solutions (> 0. 4mM) displayed two distinct emission features whereas C461 (–CH_3 in the 4-position) was characterized with single emission feature even at higher concentration. We proposed that the electron-withdrawing -CF_3 causes a small change in dipole orientation ($\Delta\theta$) upon photoexcitation that allows the excitation to be delocalized over two (or more) monomers with emission occurring at much lower energies (or longer wavelengths). In contrast, the electron-donating -CH_3 group of C461 causes this solute to experience a larger change in dipole orientation ($\Delta\theta$) upon photoexcitation. It was inferred that the resulting condition could disrupt any extended structure in adsorbed multilayers and the excited C461 adsorbates would emit as monomers. The primary amine coumarins (C151 and C440) showed no evidence of multilayer formation and no evidence of aggregate formation at the silica surface. Evidently, the sterically unhindered primary 7ACs are more likely to be "attached" to the surface and are not as mobile as their tertiary analogs.

7.2. Time –Resolved Studies in Bulk

Steady state emission data were correlated with time resolved studies at the different silica/liquid interfaces. We initiated these studies by characterizing the solutes' excited state, time-resolved photophysical properties and relaxation dynamics

in bulk solution of different solvents. Except for C152, the coumarins studied here showed a single exponential decay in methanol with ~3-5 ns lifetimes. In polar solvents like methanol, photoexcitation leads to the amine adopting a planar (sp^2) geometry and the carbonyl oxygen assumes a formal negative charge. However, previous studies have shown that C152 forms a nonradiative TICT excited state in polar solvents. This new relaxation pathway shortened the observed emission lifetime to ~1.00 ns. The unique structure of C152 with the presence of an electronegative (-CF_3) at the 4-position and the electron donating groups $(–CH_3)_2$ attached to amine facilitates formation of TICT state.

In nonpolar solvents like decane, primary amine coumarins showed a biexponential decay, which was attributed to a rapid *flip-flop* motion around the nitrogen of the amine group. These two lifetimes were assigned to the planar (sp^2) and non-planar or pyramidal (sp^3) hybridized states of the solutes formed when the solute interconverts between the two equivalent minima on the excited state potential energy surface. Tertiary amine coumarins were characterized by a single exponential time constant at low concentration. Single exponential decay of tertiary coumarins could be attributed to the high inversion barrier of the amine group restricting the energy state to the pyramidal conformation. Interestingly, the fluorescence decay of tertiary coumarins at higher concentrations, unlike the primary analogs, showed evidence of distinctive rise time due to formation of dimers in solutions.

To further evaluate the effect of solvent's identity on the tendency of solutes to aggregate in the ground state and undergo conformational changes in the excited state we chose to study 7AC photophysical properties in 1-decanol. This solvent

offers both polar solvating opportunities with its terminal –OH group and non-polar solvating capability derived from its long chain alkyl group. Results showed that the functional group in the 4–position of the 7AC solutes' played a major role in determining the solvation properties of the solute. A biexponential decay was observed for primary and tertiary amine 7AC solutes when a -CF_3 group was at the 4-position. In the ground state, the solute molecule is attached to the solvent molecule through a hydrogen bond. Following excitation, the H-bond breaks and solvent molecules starts reorganize around the excited solute. However, the solvent reorganization time in bulk decanol is much longer than the other protic solvent namely methanol that we studied.[2] We argued that this longer timescale of solvent reorganization helps in detecting fluorescence from non H-bonded solutes at shorter emission wavelength with short lifetime. The longer lifetime was assigned to the fully solvated solute.

Probing 7ACs with -CH_3 at 4-position resulted a negative amplitude that we associated with the longer solvent reorganization process. The time measured for solvent reorganization appeared quite consistent with the earlier published literature. Since -CH_3 at 4-position is known to account for larger dipole orientation in comparison to -CF_3, a longer solvent reorganization time is expected in the C440 and C461 with respect to C151 and C152.

7.3. Time Resolved Studies at Silica/liquid Interfaces

The result of the bulk studies were then compared to data acquired from different silica/liquid interfaces. The TIR fluorescence decay data for the primary

coumarins at the silica/methanol interface showed that solutes interacting directly with the surface have much shorter lifetimes than solutes in bulk methanol. The lifetimes of the interfacial coumarin species matched closely to those observed in bulk nonpolar solvents like decane. These results were surprising because polar solvents stabilize charge a transfer (CT) state following excitation, but nonpolar solvents leave the excited coumarin solute in a less polar conformation having decidedly less CT character. We discussed the result in the context of hydrogen bonding donating properties of the silica surface that keeps the solute's stabilized into the less polar, non-CT state, despite the fact that both the silica surface and methanol are individually known to create very polar solvation environments. These results further motivated us to study tertiary coumarins at silica/methanol interface. For C461, the lifetime values at silica/methanol remained largely unchanged compared to bulk solution limits. However the TIR data for C152 again showed an emergence of a second lifetime in addition to the original lifetime observed in the bulk. The longer lifetime assigned to the surface species was again attributed to the hydrogen bond donating properties of the silica surface that inhibits the formation of a TICT state observed in bulk. The lifetime of the species directly interacting with the surface has a lifetime that was similar to that observed in bulk decane for C152. The interfacial results with both primary and tertiary 7ACs showed consistent behavior.

The interfacial studies were further extended to different interfacial environments with silica/decane and silica/decanol interface. Due to the polar nature of the silica surface the charge transfer state of the primary amine 7ACs became more dominant at the silica/decane interface *relative to* bulk decane limits. Tertiary

coumarins adsorbed to silica/decane interface showed that the silica surface inhibited aggregate formation at all concentrations, presumably due to the hydrogen bond donating properties of the hydrophilic surface silanol groups. At the silica/decanol interface results were virtually identical to bulk solution limits, implying that the bulk environment persists right up to the silica surface or that the decanol solvent interacts with the surface strongly enough to prevent the 7AC solutes from accepting hydrogen bonds from the surface silanol groups.

7.4. Future direction

Research described in this work employed steady-state and time-resolved optical spectroscopy to quantify the influence of surfaces on interfacial photochemistry. Our results have successfully addressed a number of questions that were posed at the start of this project regarding the role of polarity and hydrogen bonding in controlling interfacial isomerization rates and the relative stabilities of adsorbed, photoexcited solute conformer, however new questions were also raised. Some of these questions that point the way towards new, interesting lines of inquiry are given below:

1. The 7AC solutes used in these studies could all undergo inversion around the nitrogen. Based on prior reports in the literature and additional findings from our own work, we believe that this degree of freedom plays an important role in determining the ground and excited state behaviors of the 7AC solutes in solution and adsorbed to interfaces. In this context, it would be interesting to study the photophysical behavior of the coumarin molecules that are unable to undergo inversion motion around the

amine. C314 and C343 are examples of popular 7AC solutes[3-4] that can't undergo inversion motion due to the locked fused ring attached to the N-position (Figure 7.1). Our results in Chapters 3 and 4 showed that the polar silica surface inhibits the formation of a CT state forcing adsorbed solutes to retain their pyramidal structure at the 7-position. It will be particularly interesting to explore the behavior of C314 or C343 under similar conditions to understand the extent of surface's influence over the excited state's molecular confirmation as the ground state for these coumarins typically have restricted conformation than the coumarins we studied.

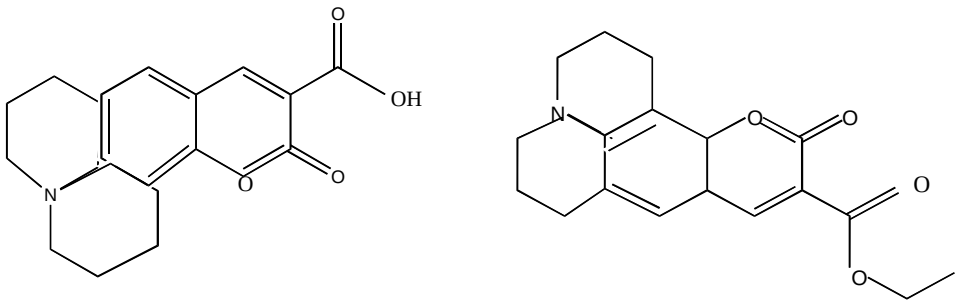

C343 **C314**

Figure 7.1. Structures of C343 and C314

2. The focus of the present thesis was to study solid/liquid interfaces. Results implied that substrate rigidity played an important role in controlling the time-dependent photophysical properties of solutes interacting directly with surface silanol groups. A logical extension of this work is to compare the findings from solid/liquid interface to data acquired for similar solutes adsorbed to liquid/liquid interfaces. Do

the aggregation and isomerization properties of solutes at solid/liquid interfaces also apply to the liquid/liquid interfaces where both phases are mobile? [5-6]

3. Our results suggested how polar hydrophyllic surface affects solute conformation. These results could be compared with surfaces having hydrophobic character. By changing the properties of the interface we can specifically identify and isolate the contributions of nonspecific and specific solvation forces arising from the surface itself. [7]

4. TIRF spectroscopy used in the present study sample response tens of nanometers into bulk solution due to the penetration depth of the evanescent field. To overcome this difficulty Time resolved SHG (TR-SHG) could be used an effective tool. TR- SHG signal is surface specific and generated by interfacial adsorbate. TR-SHG could also provide information about the changes in ground and excited state vibrational structure due to the conformational changes in photoexcited species at surfaces. In addition, TR-SHG could also be employed to characterize the solute reorientation rates and to search for evidence of dimer formation/dissociation at interfaces following photoexcitation.[8] These findings could then be correlated with our present findings. Time resolved fluorescence spectroscopy used in this project measured the fluorescence lifetimes of solutes adsorbed to silica/liquid interfaces to examine the excited state solute mobility at liquid surfaces. TR-SHG experiments can measure both in-plane and out-of-plane reorientation rates to determine how solute mobility depends upon interfacial solvation forces. These studies will build upon lessons learned about interfacial solvation specified above and advance systematically

our understanding of the photochemistry that occurs at weakly and strongly associating liquid interfaces.

Given the fundamental and applications-driven importance of solution phase photochemistry at surfaces, these predictive models account for changes in solvation that occur as a solute moves from an isotropic bulk solution to the asymmetric environments at interfaces.

References:

(1) Rechthaler, K.; Kohler, G. *Chem. Phys.* **1994**, 189, (1), 99-116.

(2) Horng, M. L.; Gardecki, J. A.; Papazyan, A.; Maroncelli, M. *J. Phys. Chem.* **1995**, 99, (48), 17311-17337.

(3) Zimdars, D.; Eisenthal, K.B. *J.Phys.Chem. A* **1999**, 103, (49), 10567-10560.

(4) Zimdars, D.; Eisenthal, K.B. *J.Phys.Chem. B* **2001**, 105, (18), 3993-4002.

(5) Benjamin, I.; *Chem. Rev*. **1996**, 96, (4), 1149-1476.

(6) Steel,W.H.; Walker, R.A. *Nature*. **2003**, 424, 296-299.

(7) Chandler, D. *Nature*. **2005,** 437, 64-647.

(8) Stienhurst, D.A.; Owrutsky, J.C. *J.Phys.Chem. B* **2001,**105,(15), 3062-3072.

Appendix A. IGOR Routine used to fit the Decay Curves

The Igor routines were developed and given to us by Dr. Ed Castner from Rutgers University. These Macros were written to load all the data files and then fit the data to the sum of the exponentials using the convolution routine.

1. To Load all files

```
#pragma rtGlobals=1		// Use modern global access method.
#pragma rtGlobals=1		// Use modern global access method.

//	LoadAllASCFilesInFolder(pathName)
//		Loads data from all of the ".igr" files in the folder associated with the specified symbolic path.
//		pathName is the name of an IGOR symbolic path which you can create with the New Path
//		dialog in the Misc menu.
//		I forced pathName to be "", so that it puts up a dialog from which you can choose the folder.
//
//		NOTE: This function assumes that ALL of the *.igr files in the specified folder are data
//			files and thus loads them all.

Macro LoadAllASCFilesInFolder()
	String pathName=""			// Name of an existing IGOR symbolic path or ""

	Silent 1
	PauseUpdate
	// If pathName is "", allow user to create a new symbolic path to the folder containing the runs of data.
	if (strlen(pathName) == 0)
		NewPath/O/Q/M="Choose folder containing data files" CurrentDataFilePath
		PathInfo CurrentDataFilePath		// Check to see if user created the path.
		if (V_flag == 0)
			return -1				// User cancelled.
		endif
		pathName = "CurrentDataFilePath"
	endif

	Variable i=0 , numFilesLoaded = 0
	String fileName,newname
//	numFilesLoaded = 0
//	i = 0
	do
		fileName = IndexedFile($pathName, i, "????")
		if (strlen(fileName) == 0)
			break
		endif
	if (strsearch(filename,".asc",0)>=0)
//	print "Pathname = ",pathname,"  Filename = ",filename
```

```
//		call a function to graph data, make semilog, apply cursors, etc.
		print "Loaded filename is: ", filename
		 LoadAndGraphTCSPC(filename,pathName)
			numFilesLoaded += 1
		endif
		i += 1
		while(1)
		silent 0
		ResumeUpdate
		Print "Loaded", numFilesLoaded,".asc TCSPC files"
End


function LoadAndGraphTCSPC(filename,pathname)
		string filename, pathname		// name of file, path to load, or "" to get a dialog
		string tempfilenam=filename[0,strlen(filename)-5]
		variable/g cursorA=150, cursorB=3850
		LoadWave /a=$tempfilenam /g/d/o/p=$pathname filename
		if (V_flag == 0)					// no waves loaded; perhaps user cancelled.
			return -1
		endif

		//display							// create a new graph

		//string TheWave
		//variable index=0

		//do							// append the waves to
the graph
		//		TheWave = stringfromlist (index, S_wavenames)	// next wave
		//		if (strlen(TheWave) == 0)				//
end of wavelist?
		//			break
		//		endif
		//		wave w = $TheWave
//		Later add SetScale commands here after obtaining TAC window and Gain settings from
//		B&H 'Ascii with Setup' file.
		//		appendtograph w
		//		index += 1
		//while (1)					// unconditionally loop back to 'do', w/ break
providing termination
		//ModifyGraph log(left)=1, rgb($TheWave)=(0,0,65000); showinfo
		//cursor A, $TheWave, cursorA
		//cursor B, $TheWave, cursorB
//		Insert request for user input (popup) for time window length; use SetScale x, ...
//		Or, better yet, obtain the window width from the ASCII with Setup or .SDT binary file.
		//textbox/A=RT/b=1/f=0 "Waves loaded from " + S_filename  // Annotate graph w/ filename
		//return 0					// success
end


Menu "Macros"
		"Load but don't graph all TCSPC *.asc files in folder", LoadAllASCFilesInFolder()
End
```

2. To make the decay curve in IGOR

```
#pragma rtGlobals=1                    // Use modern global access method.
function amy(srcwave, destwave)
wave srcwave, destwave
variable i = 0

duplicate /O /R=(0, 4096) srcwave destwave

Do
if (i>4096)
break
endif
destwave[i] = srcwave[4096-i]
i+=1

while(1)
display destwave
SetScale /P x 0, 0.012, destwave

end
```

3. To subtract the IRF:

```
#pragma rtGlobals=1                    // Use modern global access method.
String/g wv1,wv2,wv3,pwave,irfw



Window IRFEditor() : Panel
        PauseUpdate; Silent 1                  // building window...
        NewPanel /W=(717,280,900,555) as "IRF Editor"
        SetDrawLayer UserBack
        SetDrawEnv fsize= 18
        DrawText 49,24,"IRF Editor"
        Button zerobutton,pos={45,30},size={90,24},proc=zeroirf,title="Set Baseline to 0"
        Button subtractbutton,pos={45,60},size={90,24},proc=subtractirf,title="Subtract Baseline"
        Button rangebutton,pos={45,90},size={90,24},proc=rangeirf,title="Choose Range"
        Button rangebutton,help={"Set the cursor positions first."}
        SetVariable SetIRFbsln,pos={30,120},size={150,16},title="Baseline Cutoff:"
        SetVariable SetIRFbsln,frame=0,value= irfbsln
        PopupMenu popup0,pos={30,150},size={99,21},proc=SelectIRFProc,title="IRF Wave"
        PopupMenu popup0,mode=1,popvalue="irf",value= #"WaveList(\"*irf*\",\";\",\"\")"
        Button finalbutton,pos={45,180},size={90,24},proc=finalirf,title="Magic IRF"
        Button vmirfbut,pos={45,200},size={90,24},proc=vmirf,title="VM IRF"
        Button vhirfbut,pos={45,220},size={90,24},proc=vhirf,title="VH IRF"
        Button vvirfbut,pos={45,240},size={90,24},proc=vvirf,title="VV IRF"
EndMacro

Function vmirf(ctrlName) : ButtonControl
        String ctrlName
        wave irftemp
//      wave irfwave_vm
```

```
//                      if (WaveExists(irfwave_vm)==1)
 //                     irfwave_vm=irftemp
//          else

                        Duplicate/o irftemp irfwave_vm
                        variable vmsum=sum(irfwave_vm,-inf,inf)
                        irfwave_vm/=vmsum
//          endif
end

Function vhirf(ctrlName) : ButtonControl
          String ctrlName
          wave irftemp
          //wave irfwave_vh
          //          if (WaveExists(irfwave_vh)==1)
          //          irfwave_vh=irftemp
          //else
                        Duplicate/o irftemp irfwave_vh
                        variable vhsum=sum(irfwave_vh,-inf,inf)
                        irfwave_vh/=vhsum
          //endif
end

Function vvirf(ctrlName) : ButtonControl
          String ctrlName
          wave irftemp
          //wave irfwave_vv
//                      if (WaveExists(irfwave_vv)==1)
 //                     irfwave_vv=irftemp
//          else
                        Duplicate/o irftemp irfwave_vv
                        variable vvsum=sum(irfwave_vv,-inf,inf)
                        irfwave_vv/=vvsum
//          endif
end


Function finalirf(ctrlName) : ButtonControl
          String ctrlName
          wave irftemp
          //wave irf
//                      if (WaveExists(irf)==1)
 //                     irf=irftemp
//          else
                        Duplicate/o irftemp irf
                        variable irfsum=sum(irf,-inf,inf)
                        irf/=irfsum
//          endif
end

Function rangeirf(ctrlName) : ButtonControl
          String ctrlName
          wave irftemp

          variable startpt=pcsr(A)
          variable endpt=pcsr(B)
```

```
        variable irfnumpts = numpnts(irftemp)

variable x
for (x=0;x<startpt;x+=1)
  irftemp[x]=0

endfor

for (x=startpt;x<endpt;x+=1)
   irftemp[x]=irftemp[x]

 endfor


 for (x=endpt;x<irfnumpts;x+=1)

  irftemp[x]=0

 endfor

End

Function subtractirf(ctrlName) : ButtonControl
        String ctrlName
        wave irftemp
        nvar irfbsln
        irftemp=irftemp-irfbsln
End


Function zeroirf(ctrlName) : ButtonControl
        String ctrlName
        wave irftemp
        nvar irfbsln

variable z=numpnts(irftemp)

variable x

for (x=0;x<z;x+=1)

if (irftemp[x]<=irfbsln)
 irftemp[x]=0
 else
 irftemp[x]=irftemp[x]
 endif
 endfor

end


End
Function SelectIRFProc(ctrlName,popNum,popStr) : PopupMenuControl
        String ctrlName
        Variable popNum
        String popStr
```

```
	string/g irfstring
	wave irftemp

	irfstring = popStr
	//if (WaveExists(irftemp)==1)
	//		duplicate $irfstring irftempw
	//		irftemp=irftempw
	//		killwaves irftempw
	//else
			Duplicate/o $irfstring irftemp
			Display irftemp
			ModifyGraph log(left)=1

//		endif

End
```

4. Convolution routine

```
#pragma rtGlobals=1		// Use modern global access method.

Function ReducedChiSquared()

end

Function FitConvIRFMultExp(pw, yw, xw) : FitFunc
	Wave/Z pw, yw, xw
	variable dx=deltax(yw)
	Variable npnts = numpnts(yw)
	Duplicate/O yw, IM
	Wave IRF
	// external instrument response wave must be named IRF.
	Variable shift = pw[0]
	IM = IRF(x+shift)                                                    //
interpolates appropriate values from instrument response wave
	Variable IMsum = sum(IM, -inf, inf)
	IM /= IMsum                                                          //
normalize instrument response to 1.0
	yw = 0
	// initialize model values to zero so we can accumulate exponential terms
	Variable ii=2
	do
		yw += pw[ii]*exp(-pw[ii+1]*(p*dx))		// add up exp. plus  terms
		ii+=2
	While (ii < numpnts(pw) )
	Convolve IM,yw                                                       //
this operation lengthens yw to contain M+N points, where M is length of instrument response, and N is
length of yw
	yw+=pw[1]
	redimension/N = (npnts) yw                                           // this removes the
extra points
end


Function FitConvIRFMultExp_scatter(pw, yw, xw) : FitFunc
```

```
	Wave/Z pw, yw, xw
	variable dx=deltax(yw)
	Variable npnts = numpnts(yw)
	Duplicate/O yw, IM
	Wave IRF
	Variable shift = pw[0]
	IM = IRF(x+shift)                                                    //
interpolates appropriate values from instrument response wave
	Variable IMsum = sum(IM, -inf, inf)
	IM /= IMsum                                                          //
normalize instrument response to 1.0
	yw = 0
	// initialize model values to zero so we can accumulate exponential terms
	Variable numCoefs = numpnts(pw)                    // calculate number of
exponential terms desired
	Variable ii=2
	do
		yw += pw[ii]*exp(-pw[ii+1]*(p*dx))          // add up exp. plus  terms
		ii+=2
	While (ii < numCoefs)
	yw[0]+=pw[numCoefs - 1]
	Convolve IM,yw                                                       //
this operation lengthens yw to contain M+N points, where M is length of instrument response, and N is
length of yw
	yw+=pw[1]
	redimension/N=(npnts) yw                                    // this
removes the extra points
	return 0                                                             //
Igor doesn't use this return value in an all-at-once function
end


Function FitConvIRFMultStretchedExp(pw, yw, xw) : FitFunc
	Wave/Z pw, yw, xw
	variable dx=deltax(yw)
	Variable npnts = numpnts(yw)
	Duplicate/O yw, IM
	Wave IRF
	Variable shift = pw[0]
	IM = IRF(x+shift)                                                    //
interpolates appropriate values from instrument response wave
	Variable IMsum = sum(IM, -inf, inf)
	IM /= IMsum                                                          //
normalize instrument response to 1.0
	yw = 0
	// initialize model values to zero so we can accumulate exponential terms
	Variable numCoefs = numpnts(pw)                    // calculate number of
exponential terms desired
	Variable ii=2
	do
		yw += pw[ii]*exp(-(pw[ii+1]*(p*dx))^pw[ii+2])       // add up exp. plus  terms
		ii+=3
	While (ii<numCoefs)
	Convolve IM,yw                                                       //
this operation lengthens yw to contain M+N points,
```

```
	yw+=pw[1]                                                                    //
where M is length of instrument response, and N is length of yw
	redimension/N=(npnts) yw                                                     // this
removes the extra points

	end


Function FitGausConvMultExp(pw, xx) : FitFunc
	Wave/Z pw
	variable xx
// pw[0] = time shift
// pw[1] = baseline
// pw[2*m] = amp m
// pw[2*m+1] = exp rate m
// pw[n-1] = last point is gaussian width of instrument function
	Variable numCoefs = numpnts(pw)                                  // calculate number of
exponential terms desired
	Variable shift = pw[0],wid=pw[numCoefs-1]/sqrt(2)
	Variable yw = 0
	// initialize model values to zero so we can accumulate exponential terms
	Variable ii=2
	do
		yw+=pw[ii]/pw[ii+1]*ExGauss(xx-shift,pw[ii+1],wid)
		ii+=2
	While (ii<numCoefs)
	yw+=pw[1]
	return yw
	// Igor doesn't use this return value in an all-at-once function
end


Function/D ncdf(t)                                                               //
cumulative gaussian prob dist with unit sigma
	Variable/D t
	Variable/D r= GammP(0.5,0.5*t^2)
	if( t<0 )
		return (1-r)/2
	else
		return (1+r)/2
	endif
end


Function/D ExGauss(t,r,s)                                                // Convolution of
exponential and Gaussian probability distribution
	Variable/D t,r,s                                                             //functions r
is the exponential decay constant and s is the Gaussian sigma
	return r*exp( -r*t + s^2*r^2/2 )*ncdf( t/s - s*r )
end
```

5. Magic angle decay fitting

```
gma rtGlobals=1		// Use modern global access method.
```

```
Window MagicSuperPanel() : Panel
	variable/g numberofexps,pertv,startrate,ratefactor,ampfactor
	ratefactor=3
	ampfactor=.1
	startrate=.2
	PauseUpdate; Silent 1		// building window...
	NewPanel /W=(717,410,950,620) as "Magic Fitter"
	SetDrawLayer UserBack
	SetDrawEnv fsize= 18
	DrawText 49,24,"Magic Fitter"

	Button gofitbutton,pos={45,30},size={90,24},proc=fitallmagic,title="Fit Magic"
	Button gofitbutton,help={"Set the cursor positions first."}

	PopupMenu popup1,pos={10,60}, title="Magic
Wave",value=WaveList("*vm*",";",""),proc=SelectMagProc
	SetVariable setfitmodel,pos={45,85},size={150,14},title="Number of Exponentials"
	SetVariable setfitmodel,frame=0,limits={1,5,1},value= numberofexps
	SetVariable setper,pos={45,105},size={150,14},title="Perturbation Value (%)"
	SetVariable setper,frame=0,limits={-Inf,Inf,1},value= pertv
	SetVariable setsr,pos={45,125},size={150,14},title="Initial Rate Constant"
	SetVariable setsr,frame=0,limits={0,Inf,.1},value= startrate
	SetVariable setrf,pos={45,145},size={150,14},title="Additional Rate Factor"
	SetVariable setrf,frame=0,limits={0,Inf,.25},value= ratefactor
	SetVariable setaf,pos={45,165},size={150,14},title="Amplitude Factor"
	SetVariable setaf,frame=0,limits={0,Inf,.05},value= ampfactor
End

Function fitallmagic(ctrlName) : ButtonControl
	String ctrlName

	Execute "SuperFitMagic()"
end


Function SelectMagProc(ctrlName,popNum1,popStr1) : PopupMenuControl
	String ctrlName
	Variable popNum1
	String popStr1
	string/g magstring
	wave magicwave,magicweight

	magstring = popStr1
	if (WaveExists(magicwave1)==1)
	//	duplicate $magstring magicwave1pw
	//	magicwave11=magicwave1pw
	//	magicweight=magicwave1pw^.5
	//	killwaves magicwave1pw
	Print "New wave has been created from "+ magstring
	else

Make/o/N=4/D pw_1//,pw_SingleExp
Make/o/N=6/D pw_2//,pw_DoubleExp
Make/o/N=8/D pw_3//,pw_TripleExp
Make/o/N=10/D pw_4//,pw_QuadExp
```

```
Make/o/N=12/D pw_5//,pw_PentExp
Make/o/N=6/D chi_squared
Make/o/N=6/D chi_squared_delta
Edit pw_1,pw_2,pw_3,pw_4,pw_5,chi_squared,chi_squared_delta
  endif

                Duplicate/o $magstring magicwave1, magicweight
                magicweight=(magicweight+1)^.5
                Display magicwave1
                ModifyGraph log(left)=1
                ModifyGraph rgb=(0,0,0)

        //endif

end

Macro SuperFitMagic ()
//wavename magicwave1

Wavestats magicwave1
variable/g MagicMax=V_max
variable/g MagicRange=ABS(pcsr(B)-pcsr(A))

variable pvval=pertv/100
//variable startrate
//variable ratefactor


pw_1[0]=0
pw_1[1]=magicwave1[pcsr(A)]
pw_1[2]=MagicMax
pw_1[3]=startrate
//FuncFit/L=(MagicRange) /H="0111"  FitConvIRFMultExp pw_1 magicwave1[pcsr(A),pcsr(B)]
/W=magicweight /I=1 /D /R
//FuncFit/L=(MagicRange) /H="0011"  FitConvIRFMultExp pw_1 magicwave1[pcsr(A),pcsr(B)]
/W=magicweight /I=1 /D /R
FuncFit/L=(MagicRange)  FitConvIRFMultExp pw_1 magicwave1[pcsr(A),pcsr(B)] /W=magicweight
/I=1 /D /R
perturbwave(pw_1,pvval)
FuncFit/L=(MagicRange)  FitConvIRFMultExp pw_1 magicwave1[pcsr(A),pcsr(B)] /W=magicweight
/I=1 /D /R
//res_magicwave1=res_magicwave1/magicweight
//duplicate/o res_magicwave1,res_1
//AppendToGraph/L=Res_Left res_1
//ModifyGraph rgb(res_1)=(65280,0,0)
//perturbwave(pw_1,.02)
//FuncFit/L=(MagicRange)  FitConvIRFMultExp pw_1 magicwave1[pcsr(A),pcsr(B)]
/W=magicweight /I=1 /D /R

chi_squared[1]=V_chisq/(MagicRange-4)

if (numberofexps>1)
pw_2=pw_1*.5
pw_2[2]=pw_1[2]*(1-ampfactor)
pw_2[3]=pw_1[3]
pw_2[4]=pw_1[2]*ampfactor
```

```
pw_2[5]=pw_1[3]/ratefactor
FuncFit/L=(MagicRange)  FitConvIRFMultExp pw_2 magicwave1[pcsr(A),pcsr(B)] /W=magicweight
/I=1 /D /R
perturbwave(pw_2,pvval)
FuncFit/L=(MagicRange)  FitConvIRFMultExp pw_2 magicwave1[pcsr(A),pcsr(B)] /W=magicweight
/I=1 /D /R
//res_magicwave1=res_magicwave1/magicweight
//duplicate/o res_magicwave1,res_2
//AppendToGraph/L=Res_Left res_2
//ModifyGraph rgb(res_2)=(0,0,65280)
//perturbwave(pw_2,.01)
//FuncFit/L=(MagicRange)  FitConvIRFMultExp pw_2 magicwave1[pcsr(A),pcsr(B)]
/W=magicweight /I=1 /D /R

chi_squared[2]=V_chisq/(MagicRange-6)
ra2(pw_2)
variable change=ABS(chi_squared[2]-chi_squared[1])//chi_squared[2]
chi_squared_delta[2]=change
endif
//if (change>.01)

if (numberofexps>2)
pw_3=pw_2
pw_3[6]=pw_2[4]/ampfactor
pw_3[7]=pw_2[5]*ratefactor

//pw_3[7]=.5*(pw_2[3]+pw_2[5])*MagicMax/(pw_2[2]+pw_2[4])
FuncFit/L=(MagicRange)  FitConvIRFMultExp pw_3 magicwave1[pcsr(A),pcsr(B)] /W=magicweight
/I=1 /D /R
perturbwave(pw_3,pvval)
FuncFit/L=(MagicRange)  FitConvIRFMultExp pw_3 magicwave1[pcsr(A),pcsr(B)] /W=magicweight
/I=1 /D /R
//res_magicwave1=res_magicwave1/magicweight
//duplicate/o res_magicwave1,res_3
//AppendToGraph/L=Res_Left res_3
//ModifyGraph rgb(res_3)=(0,0,0)
//perturbwave(pw_3,.01)
//FuncFit/L=(MagicRange)  FitConvIRFMultExp pw_3 magicwave1[pcsr(A),pcsr(B)]
/W=magicweight /I=1 /D /R
chi_squared[3]=V_chisq/(MagicRange-8)
ra2(pw_3)
change=ABS(chi_squared[3]-chi_squared[2])//chi_squared[3]
chi_squared_delta[3]=change
endif

//if (change>.01)
if (numberofexps>3)
pw_4=pw_3
pw_4[8]=pw_3[6]/ampfactor
pw_4[9]=pw_3[7]*ratefactor
FuncFit/L=(MagicRange)  FitConvIRFMultExp pw_4 magicwave1[pcsr(A),pcsr(B)] /W=magicweight
/I=1 /D /R
perturbwave(pw_4,pvval)
FuncFit/L=(MagicRange)  FitConvIRFMultExp pw_4 magicwave1[pcsr(A),pcsr(B)] /W=magicweight
/I=1 /D /R
//res_magicwave1=res_magicwave1/magicweight
```

```
///duplicate/o res_magicwave1,res_4
//AppendToGraph/L=Res_Left res_4
//ModifyGraph rgb(res_4)=(0,65280,0)
//perturbwave(pw_4,.01)
//FuncFit/L=(MagicRange)  FitConvIRFMultExp pw_4 magicwave1[pcsr(A),pcsr(B)]
/W=magicweight /I=1 /D /R
chi_squared[4]=V_chisq/(MagicRange-10)
ra2(pw_4)
change=ABS(chi_squared[4]-chi_squared[3])//chi_squared[4]
chi_squared_delta[4]=change
//pw_QuadExp=pw_4
endif

//if (change>.01)
if (numberofexps>4)
pw_5=pw_4
pw_5[10]=pw_4[8]/ampfactor
pw_5[11]=pw_4[9]*ratefactor
FuncFit/L=(MagicRange)  FitConvIRFMultExp pw_5 magicwave1[pcsr(A),pcsr(B)] /W=magicweight
/I=1 /D /R
perturbwave(pw_5,pvval)
FuncFit/L=(MagicRange)  FitConvIRFMultExp pw_5 magicwave1[pcsr(A),pcsr(B)] /W=magicweight
/I=1 /D /R
//res_magicwave1=res_magicwave1/magicweight
//duplicate/o res_magicwave1,res_5
//AppendToGraph/L=Res_Left res_5
//ModifyGraph rgb(res_5)=(65280,65280,0)
//perturbwave(pw_5,.01)
//FuncFit/L=(MagicRange)  FitConvIRFMultExp pw_5 magicwave1[pcsr(A),pcsr(B)]
/W=magicweight /I=1 /D /R
chi_squared[5]=V_chisq/(MagicRange-12)
ra2(pw_5)
change=ABS(chi_squared[5]-chi_squared[4])//chi_squared[5]
chi_squared_delta[5]=change
//endif
chi_squared_delta=Round(chi_squared_delta*1000)/1000
endif
res_magicwave1=res_magicwave1/magicweight
//wavestats res_magicwave1
//•SetAxis Res_Left (V_min-1,V_max+1)
//RemoveFromGraph Res_magicwave1
//print pvval
//res_magicwave1=res_magicwave1/magicweight
//pw_SingleExp=pw_1
//pw_DoubleExp=pw_2
//pw_TripleExp=pw_3
//pw_QuadExp=pw_4
//pw_PentExp=pw_5
//variable x=0
//Print "Reduced Chi Squared Values"
//Do
//x=x+1
//Print x+" Exponential Fit = " + chi_squared[x]
//While(x<5)

End
```

```
Macro Killem()
KillWaves  pw_1,pw_2,pw_3,pw_4,pw_5,chi_squared,changewave
End

Function perturbwave(alterwave,variance)
wave alterwave
variable variance

variable alterwavepts=numpnts(alterwave)
variable x
variable y
Do
	y = gnoise(10)
	if (ABS(y)>10)
		alterwave[x]=alterwave[x]
	//	print "zero"
	else
		if (ABS(y)<5)
			alterwave[x]=alterwave[x]*(1-variance)
					//	print "less"
		else
			alterwave[x]=alterwave[x]*(1+variance)
		//	print "more"
		endif
	endif
x=x+1
While(x<alterwavepts)

end
```

Appendix B. Drawing of Home-built Cell and TIRF Setup

The figure below represents the cell used for the TIRF experiments. The specific detail and the geometric of the cell have been discussed in Chapter 2.

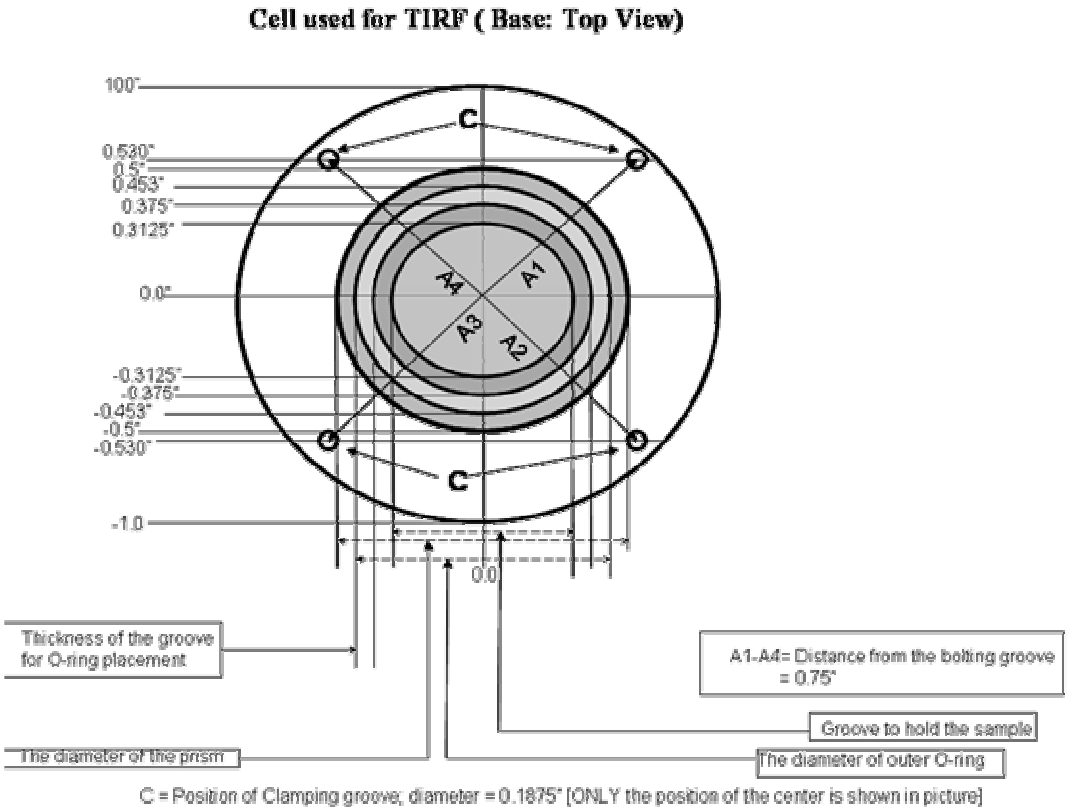

Cell used for TIRF Base: Side view

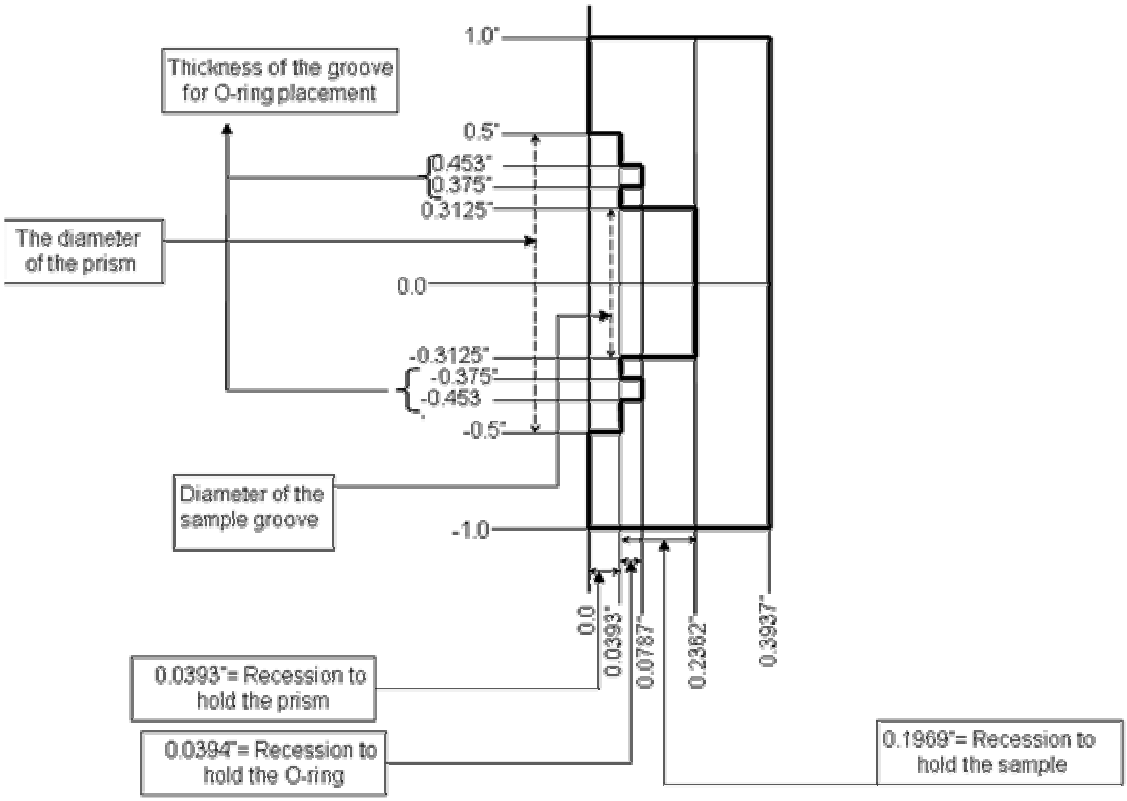

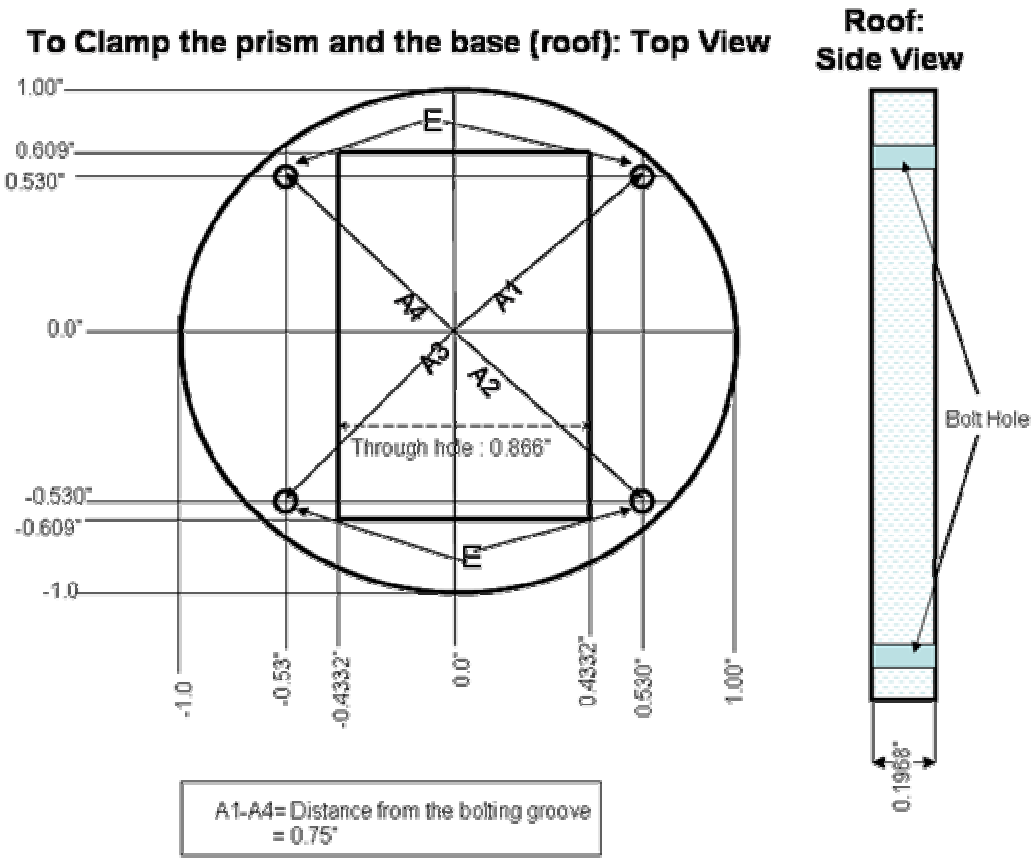

E= Position of Bolting groove; diameter = 0.1875" [ONLY the position of the center is shown in picture]

Drawing of the base used to align the optics for TIRF measurements

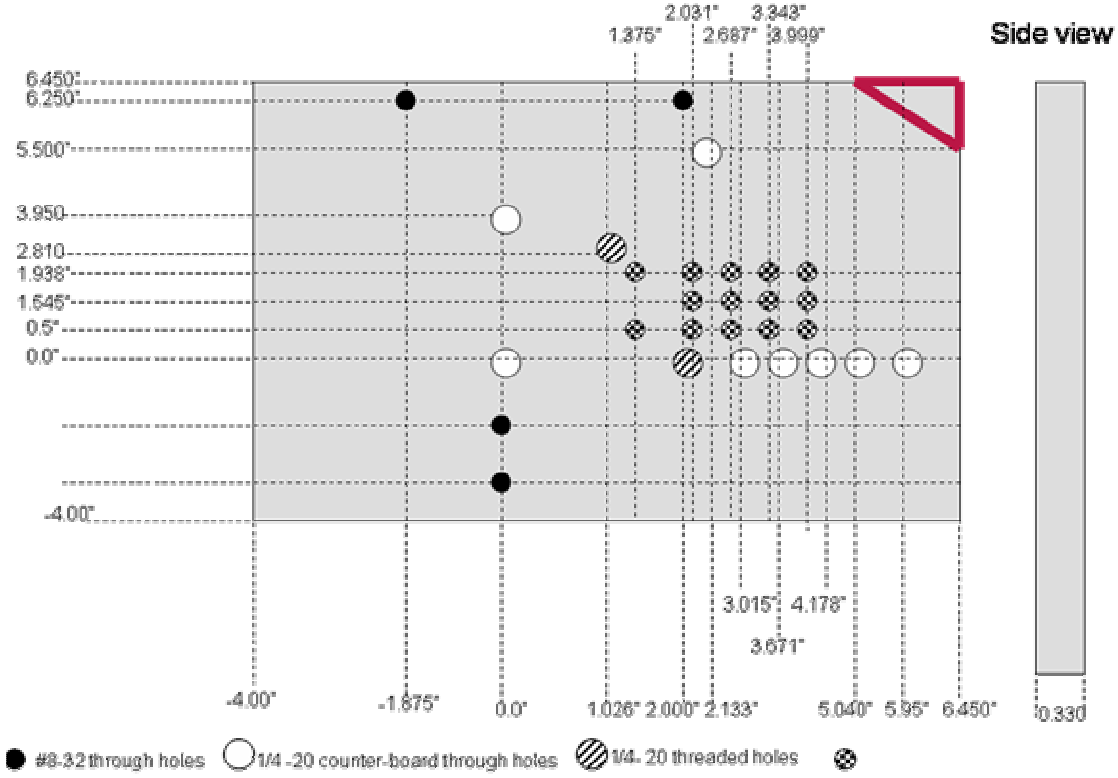

Picture of the TCSPC-TIRF setup

Picture of the cell used for solid/liquid interface study. The cell is made of Kel-F:

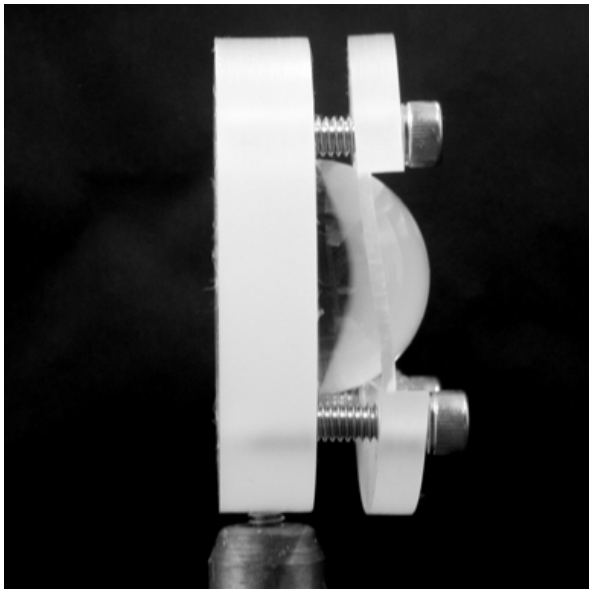

Appendix C. Supporting Information for Chapter 3

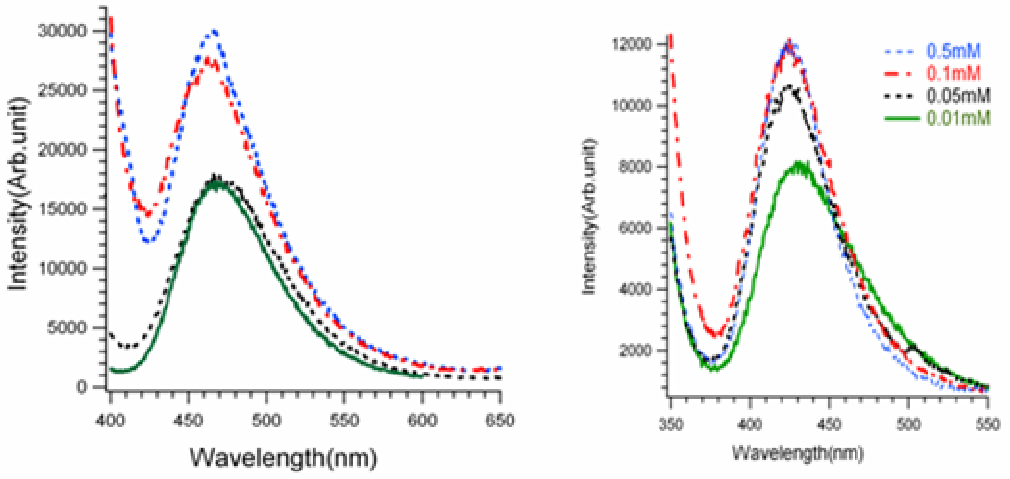

C151 C440

Figure A.3.1. Representative emission spectra for C151(Left) and C440 (Right) adsorbed to the hydrophilic silica surface from methanol solutions having different concentrations. As described in the text, these samples were prepared by allowing silica slides to equilibrate in the methanol solution and then removing the slides slowly from the solutions allowing the excess solvent to accumulate at the bottom of the (1" x 1") slide. Emission spectra were then acquired using a Spex Fluorolog having crossed polarizers set for the excitation (90˚) and emission (0˚) light. Spectra were acquired from the top, front surfaces of the slides and are assumed to reflect those solutes that remain strongly adsorbed to the silica surface. Acquisition parameters were 1 nm/s with slit widths set for 5 nm resolution both for excitation and emission

Appendix D. Supporting Information for Chapter 4

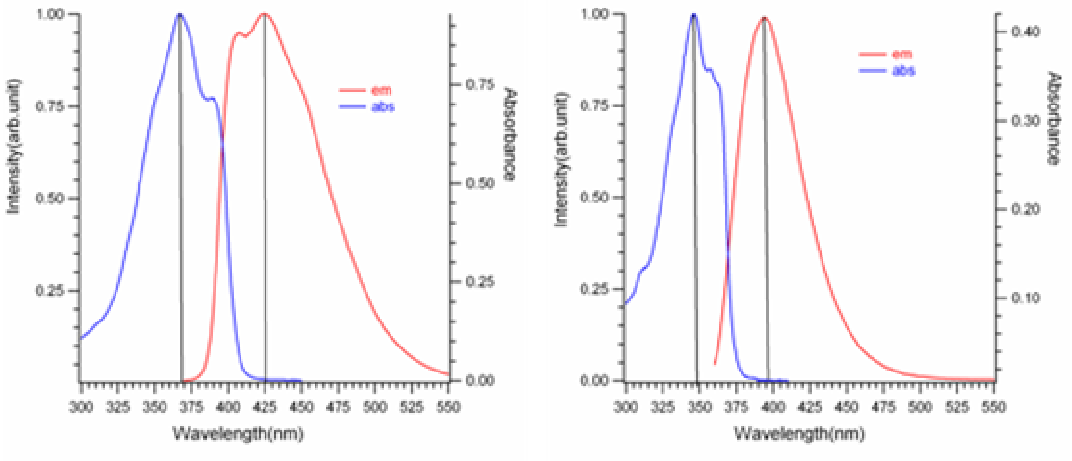

Figure A. 4.1: Steady state absorption and emission spectra of (Left) C152 in bulk decane, absorption peak at 368nm and emission peak at 426nm (Right) C461 in bulk decane, absorption peak at 348nm and emission peak at 396nm.

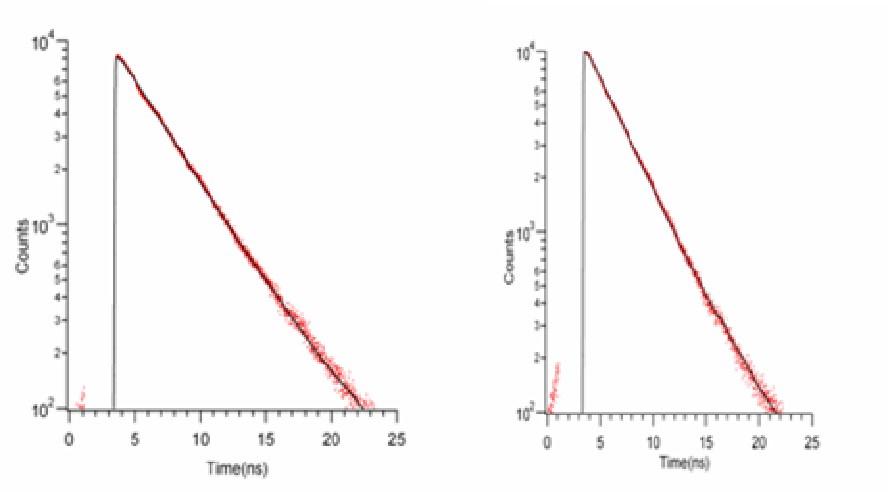

Figure A.4.2. Fluorescence decay curve of (A) C152 in bulk decane, τ ~ 4.00 ns (B) C461 in bulk decane, τ ~ 3.45 ns.

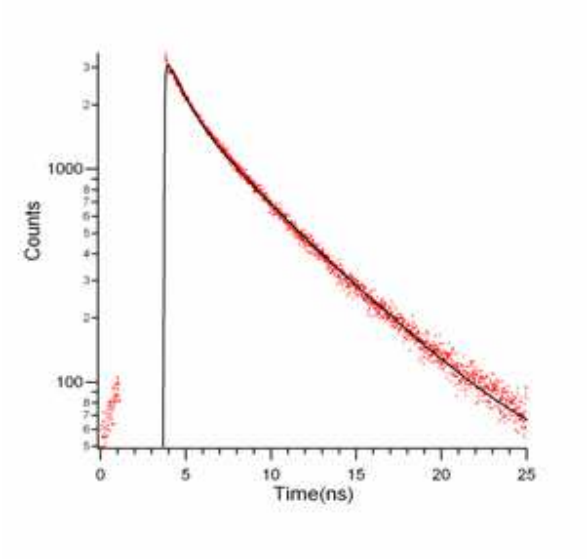

Figure A.4.3 Fluorescence decay curve of C152 at silica/vapor interface

Table A. D.1. Fluorescence lifetime values of C152 at silica/vapor interface

Filters	A_1	τ_1 (ns)	A_2	τ_2 (ns)	χ^2
420 LPF	0.42	0.98	0.68	5.26	1.5

Appendix E. Supporting Information for Chapter 6

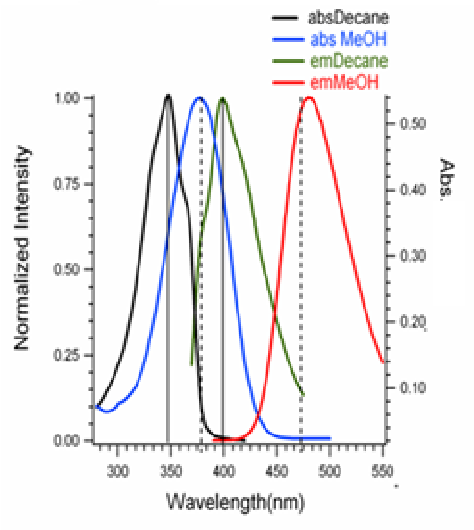

C151

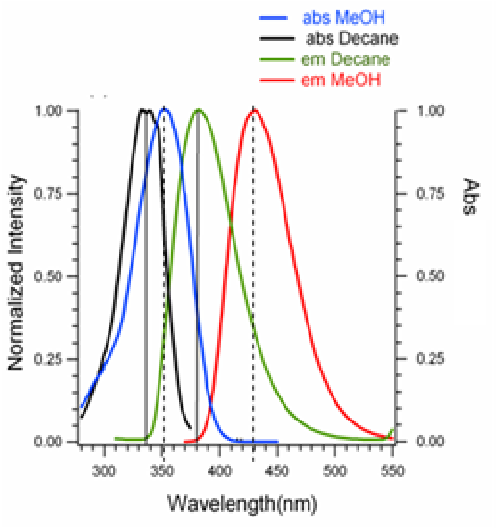

C440

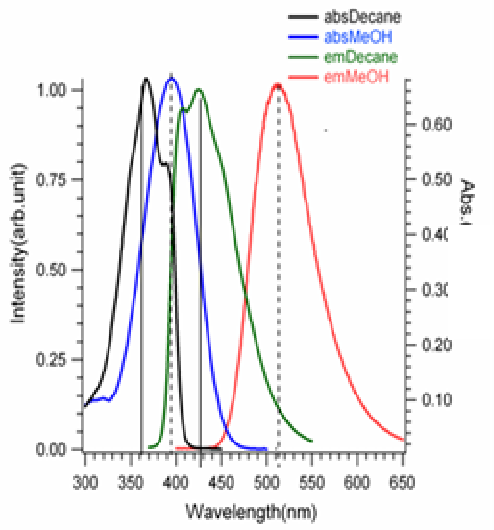

C152

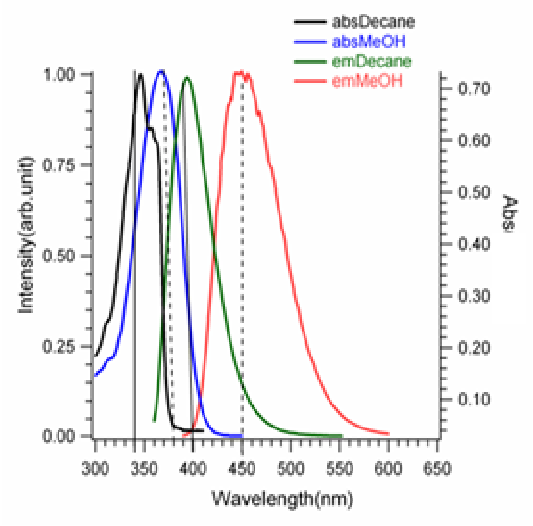

C461

Figure A.6.1 Spectra of 7-aminocoumarins in bulk MeOH and in bulk decane

Table. A.E.1. Spectral data of 7-aminocoumarins in bulk MeOH and decane

Solutes	Solvent	Peak difference in Abs and Em (nm)
C151	MeOH	102
C440		80
C152		125
C461		90
C151	Decane	52
C440		45
C152		70
C461		52

Appendix F. Additional Steady State and Time Resolved Data in Acetonitrile

Table A.F.1. Spectral data of 7-aminocoumarins in bulk acetonitrile. Some of the values reported here are from literature [1,2] and also taken by Milton Liu an undergraduate student in our group.

Solute	Absorption Peak (nm)	Emission Peak (nm)
C151	367	460
C440	343	412
C152	393	504
C461	364	431

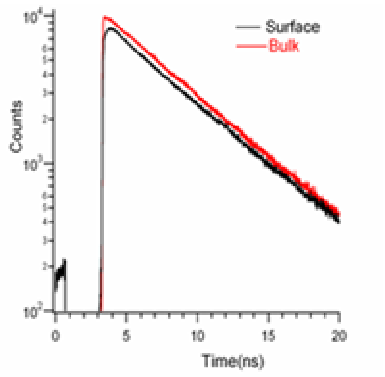

C151

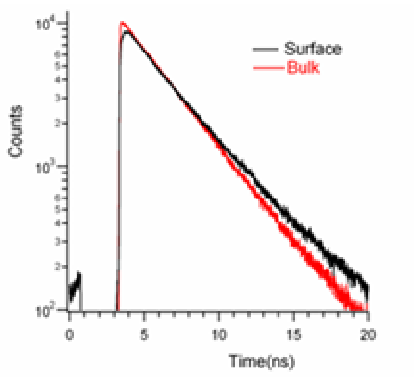

C440

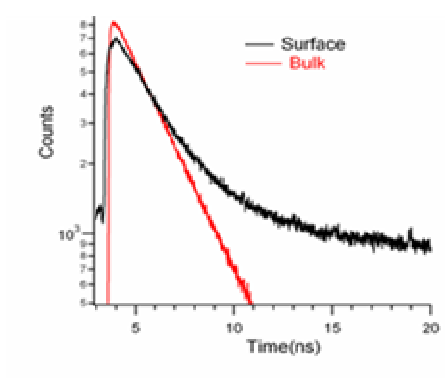

C152

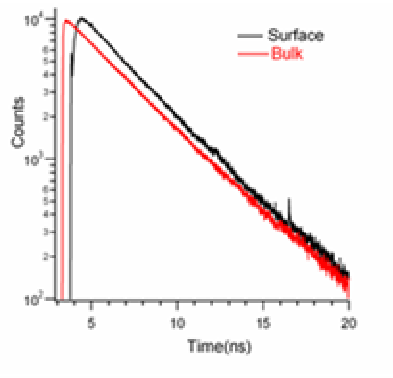

C461

Table A.F.2. Fluorescence lifetime values in bulk acetonitrile and at silica/acetonitrile interface

Solute	Solvent/Surface	A_1	τ_1 (ns)	A_2	τ_2 (ns)
C151	Bulk ACN	1.00	5.26	-	-
C440		1.00	3.12	-	-
C152		1.00	2.00	-	-
C461		1.00	2.78	-	-
C151	Silica/ACN	1.00	5.00	-0.35	0.12
C440		1.00	3.44	-0.30	0.15
C152		1.00	2.38	-0.40	0.13
C461		1.00	3.33	-0.70	0.18

(1) Nad, S.; Pal, H. *J. Phys. Chem. A* **2001,** 105, (7), 1097-1106.

(2) Nad, S.; Kumbhakar, M.; Pal, H. *J. Phys. Chem. A* **2003**, 107, (24), 4808-4816.

References

(1) Hagfeldt, A.; Gratzel, M. *Chem. Rev.* **1995**, *95*, 49-68.

(2) Corn, R. M..; Higgins, D. A. *Chem. Rev.* **1994**, *94*, 107-125.

(3) Hoppe, H.; Sariciftci, N.S. Organic solar cells: An overview. *J. Mat. Res.* **2004**, 19, 1924-1945.

(4) Kamat, P.V. *Chem. Rev.* **1993,** 93, 267-300.

(5) Gust, D.; Moore, T.; A.L. *Acc. Chem.Res.* **2001,** 34**,** 40-48.

(6) Kurashige, Y.; Nakajima, T.; Kurashige, S.; Hirao, K.; Nishikitani, Y. *J. Phys. Chem. A* **2007,** 111, 5544- 5548.

(7) Weaver, M.J. *J.Phys.Chem***. 1996,** 100, 13079-13089

(8) Du, Q.; Freysz, E.; Shen, Y.R.; *Phys.Rev.Lett.* **1994**, 72, 238-241

(9) Wirth, M. J.; Burbage, J.D. *Anal. Chem.* **1991,** 63, 1311-1317.

(10) Liu G.; Li, Y.; Jonas, J. *J. Chem. Phys.* **1991,** 95, 6892-6901.

(11) Suppan, P.J.; *Chem. Soc. Faraday Trans.1* **1987**,83,495- 509.

(12) Richert R.; Wagener, A. *J. Phys. Chem.* **1991**, 95 (24), 10115–10123.

(13) Gardecki, J.; Maroncelli, M.; *Chem Phys Lett*., **1999**, 301, 571- 578.

(14) Jarzeba,W.; Walker, G.W.; Johnson, A.E.; Barbara, P.F. *Chem Phys.* **1991**,152, 57- 68

(15) Jimenez, R.; Fleming, G. R.; Kumar, P. V.; Maroncelli, M. *Nature* **1994**, *369*, 471-473.

(16) Jarzeba, W.; Walker, G. C.; Johnson, A. E.; Kahlow, M. A.; Barbara, P. F. *J. Phys. Chem.* **1988,** *92*, 7039-7041.

(17) Horng, M. L.; Gardecki, J. A.; Papazyan, A.; Maroncelli, M. *J. Phys. Chem.* **1995,** *99*, 17311-17337.

(18) Ware, W. R. Baldwin, B. A. *J..Chem. Phys.* **1964**, *40*, 1703-7.

(19) Strickler, S. J.; Berg, R. A. *J. Chem. Phys.* **1962**, *37*, 814.

(20) Elbayoum, M. A.; Halim, F. M. A. *J. Chem. Phys.* **1968**, *48*, 2536-7.

(21) Ware, W. R.; Chow, P.; Lee, S. K. C*hem. Phys. Lett.* **1968**, *2*, 356-358.

(22) Higgins, D.A.; Abrams,M.B.; Byerly, S.K.; Corn, R. M. Langmuir **1992,** 8, 1992-2000

(23) Lagugne-Labarthet, F.; Yu, T.; Barger,W.R.; Shenoy, D.K.; Dalcanale, E.; Shen,Y.R. Chem Phys Lett**. 2003**, 381, 322-328.

(24) Perrenoud-Rinuy, J.; Brevet, P.F.; Girault, H.H; *Phys Chem Chem Phys.* **2002**,4, 4774-4781.

(25) Choudhury, S. D.; Kumbhakar, M.; Nath, S.; Pal, H. *J. Chem. Phys.* **2007,** 127, (19), 194901(1)-194901(11).

(26) Nag, A.; Bhattacharyya, K. *Chem. Phys. Lett.* **2007**, 169, 12-16.

(27) Nad, S.; Pal, H., *J. Phys. Chem. A* **2001,** 105, (7), 1097-1106.

(28) Belostoskii, A.M.; Aped. P.; Hasner, A. *J.Mol. Struct. (Theochem)* **1997,** 398-399, 427-434.

(29) Benjamin, I. *Chem Rev*. **1996**, 96, (4) , 1449-1476.

(30) Senapati, S.; Chandra, A. *Chem. Phys*. **1998,** 231, (1) 65-80.

(31) Senapati,S.; Chandra, A. *J. Chem. Phys.* **1999**,111,1223-1230.

(32) Hamai, S.; Tamai, N.; Yanagimachi, M.; Masuhara, H. *Chem. Phys. Lett.* **1994,** *229,* 389-393.

(33) Hamai, S.; Tamai, N.; Masuhara, H. *J.Phys. Chem.* **1995**, *99*, 4980-4985.

(34) Pant, D.; Girault, H. H. *Phys.Chem. Chem.Phys.* **2005**, 7, 3457-3463.

(35) Ishizaka, S.; Satoshi, H.; Kim, H.; Kitamura, N.; *Anal.Chem*. **1999**, 71, 3382-3389.

(36) Ishizaka, S.; Ueda, Y.; Kitamura, N. *Anal. Chem.* **2004** 76, 5075-5079.

(37) Zimdars, D.; Dadap, J. I.; Eisenthal, K. B.; Heinz, T. F. *J. Phys. Chem. B* **1999,** 103, (17), 3425-3433.

(38) Yanagimachi, M., Tamai, N. and Masuhara, H.*Chem. Phys. Letts* **1992**, *200,* 469-474.

(39) Zhong, D. P.; Pal, S. K.; Zhang, D. Q.; Chan, S. I.; Zewail, A. H. *Proc. Nat. Acad. Sci. USA*, **2002**, *99*, 13-18.

(40) Wang, H.; Harris, J.M. J.Phys.Chem. **1995**,99, 16999-17004.

(41) Wirth, M. J.; Swinton, D.J.; Ludes, M.D. *J.Phys. Chem. B* **2003**, 107, 6258-6268.

(42) Iler, R.K. *The chemistry of silica*; Wiley: New York, **1979.**

(43) Righetti, P.G.; GElfi, C.; Sebastiano, R.; Citterio, A. *J. Chrom.* A, **2004,** 1053**,** (1-2), 15-26.

(44) Revesz, A.G.; Hughes, H.L. *A Review : J. Non-Cryst. Solids* 2003,328, (1-3), 48- 63.

(45) Rechthaler, K.; Kohler, G. *Chem. Phys.* **1994,** 189, (1), 99-116.

(46) Jones, G.; Jackson, W. R.; Kanoktanaporn, S.; Halpern, A. M. *Opt. Comm.*, **1980**, *33*, 315-320.

(47) Sarkar, N.; Das, K.; Datta, A.; Das, S.; Bhattacharyya, K. *J. Phys. Chem.* **1996**, 100, 10523-10527.

(48) Pal, H.; Shirota, H.; Tominaga, K.; Yoshihara, K.; *J. Chem. Phys.* **1999**, *110*, 11454-11465.

(49) Chu, G.; Yangbo, F. *J. Chem. Soc. Fard. Trans* **1987**, *83*, 2533-2539.

(50) Jones, G., Jackson, W. R., Choi, C.; Bergmark, W. R. *J. Phys. Chem.* **1985**, *89*, 294-300.

(51) Brindza, M.R.; Walker, R.A. *J. Am.Chem. Soc* **2009,**131(17) 6207-6214.

(52) Lakowicz, J. R.; *Topics in Fluorescence Spectroscopy*; Kluwer Academic / Plenum: New York, **1999**.

(53) Ingle, J.D.; Crouch, S.R. *Spectrochemical Analysis;* Prentice Hall: NJ, **1988.**

(54) Deak, J.C; Rhea, S.T.; Iwaki, L. K.; Dlott,D.D. *J. Phys. Chem. A*, **2000**, 104, 4866-4875

(55) Rosen, M.J., Surfactant and Interfacial Phenomena; *John-Wiley & Sons, Inc.: NJ,* **2004**

(56) Stock, K.;Sailer, R.; Straus, W. S. L.; Lyttek, M.; Steiner, R. Schneckenburger, H. *J. Microscopy-Oxford,* **2003**, 211, 19.

(57) O'Connor, D.V.; Phillips, D. *Time correlated single Photon Counting; Acad. Press:* London, 1984.

(58) Fleming, G.R.; *Chemical applications of ultrafast spectroscopy*, International series of Monongraphs on Chemistry 13; Oxford University Press: 91-95.

(59) Becker, W. Advanced time-correlated single photon counting techniques; *Springe*r: Berlin, Heidelberg, NY, **2005**.

(60) *What is TCSPC*? Technical Note by Edinburgh Instrument

(61) Why TCSPC for Fluorescence Lifetime Measurements? Technical Note by Edinburgh Instruments.

(62) Hamai, S.; Tamai, N.; Yanagimachi, M.; Masuhara, H. *Chem. Phys. Lett.* **1994,** *229*, 389-393.

(63) Mirabelle, F.M. Jr. *Internal Reflection Spectroscopy Theory and applications;* Marcel Dekker, Inc.: New York, 1993.

(64) Horng, M. L.; Gardecki, J. A.; Maroncelli, M. *J. Phys. Chem. A* **1997,** 101, 1030-1047.

(65) Sharma, V. K.; Saharo, P. D.; Sharma, N.; Rastogi, R. C.; Ghoshal, S. K.; Mohan, D. *Spectrochim Acta Part a-Mol. and Biomol. Spect.* **2003,** 59, (6), 1161-1170.

(66) Nemkovich, N. A.; Reis, H; Baumann,W. *J. Lumin.* **1997**, 71, 255-263

(67) Satpati, A.; Senthilkumar, S.; Kumbhakar, M.; Nath, S.; Maity, D. K.; Pal, H. *Photochem. Photobio.* **2005,** 81, 270-278.

(68) Nad, S.; Kumbhakar, M.; Pal, H. *J. Phys. Chem. A* **2003,** 107, (24), 4808-4816.

(69) Barik, A.; Nath, S.; Pal, H. *J. Chem. Phys.* **2003,** 119, (19), 10202-10208.

(70) Daisuke, K.; Arora, P.; Nakayama, A.; Noro, T.; Gordon, M.S.; Taketsugu,T. *International. J. Quant. Chem.* **2009,** 109, 2308-2318.

.

(71) Oki, M. *Application of Dynamic NMR spectroscopy to Organic Chemistry; VCH: Deerfield Beach*, **1985**.

(72) Cave, R. J.; Burke, K.; Castner, E. W. *J. Phys. Chem. A* **2002**, 106, 9294-9305.

(73) Arbeloa, T. L.; Arbeloa, F. L.; Arbeloa, I. L. *J. Lumin.* **1996,** 68, 149-155.

(74) Lindrum,M.; Glismann, A.; Moll, J.; Daehne, S. *Chem. Phys*. **1993**, 178,423-432.

(75) Moll, J.; Daehne, S.; Durrant, J. R.; Wiersma, D. A. *J Chem Phys.* **1995,** 102, (16), 6362-6370.

(76) Ichino, Y.; Minami, N.; Yatabe, T. *J. Lumin.* **2000,** 87-9, 727-729.

(77) Suratwala, T.; Gardlund, Z.; Davidson, K.; Uhlmann, D. R.; Watson, J.; Peyghambarian, N. *Chem Mater.* **1998,** 10, (1), 190-198.

(78) Hair, M. L.; Hertl, W. *J. Phys. Chem.* **1969,** 73, (12), 4269-4276.

(79) Carlson, H. A.; Nguyen, T. B.; Orozco, M.; Jorgensen, W. L. *J. Comp. Chem.* **1993,** 14, 1240- 1249.

(80) Grimes, A. F.; Call, S. E.; Vicente, D. A.; English, D. S.; Harbron, E. J. *J. Phys. Chem. B* **2006** , 110, 19183-19190.

(81) Avnir, D.; Levy, D.; Reisfeld, R. *J. Phys. Chem.* **1984,** 88, (24), 5956-5959.

(82) Avnir, D.; Kaufman, V. R.; Reisfeld, R. *J. Non-Crys. Solids* **1985,** 74, (2-3), 395- 406.

(83) Knobbe, E. T.; Dunn, B.; Fuqua, P. D.; Nishida, F. *App. Optics* **1990,** 29, (18), 2729-2733.

(84) Turro, N. J. *Modern Molecular Photochemist;*University Science Books: **1991.**

(85) Lee, M.; Kim, J.; Tang, J.; Hochstrasser, R. M. *Chem. Phys. Lett.* **2002**, 359, 412-419.

(86) Ambrose, P. W.; Goodwin, P. M.; Martin, J. C.; Keller, R. A. *Science* **1994** 265, 361-364.

(87) Gu, G.; Ong, P.P.; Li, Q. *J. Phys. D.: Appl. Phys.* **1999,** 32, 2287-2289.

(88) Cook, W.G.; Ross, R. *A Canadian Journal of Chemistry* **1972**, 50, 1666 - 1674.

(89) Arbeloa, T. L.; Arbeloa, F. L.; Tapia, M. J.; Arbeloa, I. L. *J. Phys. Chem.* **1993**, 97, (18), 4704-4707.

(90) Atkins, R. L.; Bliss, D. E. *J. Org. Chem.* **1978**, 43, (10), 1975-1980.

(91) Jones, G.; Jackson, W. R.; Halpern, A. M. *Chem. Phys. Lett.* **1980**, 72, (2), 391-395.

(92) Jones, G.; Jackson, W. R.; Choi, C.; Bergmark, W. R. *J. Phys. Chem.* **1985**, 89, (2), 294-300.

(93) Bank, A.; Kumbhakar, M.; Nath, S.; Pal, H. *Chem. Phys.* **2005**, 315, (3), 277-285.

(94) Atkins, R. L.; Bliss, D. E. *J. Org. Chem.* **1978,** 43, (10), 1975-1980.

(95) Kahlow, M. A.; Jarzeba, W.; Kang, T. J.; Barbara, P. F. *J. Chem. Phys.* **1989**, 90, (1), 151-158.

(96) Senthilikumar, S.; Nath, S.; Pal, H. *Photochem. and Photobio.* **2004**, 80, (1), 104-111.

(97) Kim, T. G.; Topp, M. R. *J. Phys. Chem. A* **2004**, 108, (38), 7653-7659.

(98) Jin, H.; Baker, G. A.; Arzhantsev, S.; Dong, J.; Maroncelli, M. *J. Phys. Chem. B* **2007**, 111, (25), 7291-7302.

(99) Cave, R. J.; Burke, K.; Castner, E. W. *J. Phys. Chem. A* **2002**, 106, (40), 9294-9305

(100) Riter, R. E.; Willard, D. M.; Levinger, N. E. *J. Phys. Chem. B* **1998**, *102, (15*), 2705-2714.

(101) Yamashita, T.; Amino, Y.; Yamaguchi, A.; Teramae, N. *Chem. Lett.* **2005**, 34, (7), 988-989.

(102) Shi, X.; Borguet, E.; Tarnovsky, A. N.; Eisenthal, K. B. *Chem. Phys.* **1996**, *205, (1-2), 167-178.*

(103) Kovaleski, J. M.; Wirth, M. J. *J. Phys. Chem. B* **1997**, 101, (28), 5545-5548.

(104) Wirth, M. J.; Legg, M. A. *Ann. Rev. Phys. Chem.* **2007**, 58, 489-510.

(105) Wong, A. L.; Harris, J. M. *J. Phys. Chem.* **1991**, 95, (15), 5895-5901.

(106) Al-Abadleh, H. A.; Voges, A. B.; Bertin, P. A.; Nguyen, S. B. T.; Geiger, F. M. *J. Am. Chem. Soc.* **2004**, 126, (36), 11126-11127.

(107) Dahiya, P.; Kumbhakar, M.; Mukherjee, T.; Pal, H. *Chem. Phys. Lett.* **2005**, 414, (1-3), 148-154.

(108) Choudhury, S. D.; Kumbhakar, M.; Nath, S.; Pal, H. *J. Chem. Phys.* **2007**, 127, (19), 194901(1)-194901(11).

(109) Ohline, S. M.; Lee, S.; Williams, S.; Chang, C. *Chem. Phys. Lett.* **2001,** 346, (1-2), 9-15.

(110) Heinz, T. F.; Chen,C. R.; Ricard, D.; Shen Y. K. *Phys. Rev. Lett.* **1982**, 48 , (7), 478 – 481.

(111) Higgins, D.A.; Byerly, S.K.; Abrams, M. B.; Corn, R. M. *J. Phys. Chem.* **1991**, 95 (18),6984–6990.

(112) Halstead, J. A.; Reeves, R. R. Optics Communications **1978,** 27, (2), 273-276.

(113) Fletcher, A. N. *Appl. Phys*. **1977**, 14, 295- 302.

(114) Nemkovich, N. A.; Reis, H; Baumann,W. *J. Lumin.* **1997**, 71, 255-263

(115) Parkanyi, C. ; Antonious, M. S;Aaron, J. J.; Buna, M.;Tine, A.;Cisse, L. *Spectrosc.Lett.* **1994**, 27, 439-449

(116) Samanta, A.; Fessenden, R. W. *J. Phys. Chem. A* **2000,** 104, 37, 8577-8582.

(117) Tominaga, K.; Walker, G.C. *J. Photochem. Photobio. A: Chem*, **1995**, 87,127-133

(118) Demelo, J. S. S.; Becker, R. S.; Macanita, A. L. *J. Phys. Chem.* **1994,** 98, (24), 6054-6058.

(119) Song, P.S.; Gordon (III), W.H. *J. Phys. Chem.*, **1970**, 74 (24), 4234–4240

(120) Yamazaki, I.; Tamai, N.; Yamazaki, T., *J. Phys. Chem.* **1987,** 91, 3572-3577

(121) March, N.H.; Toshi, M.P. *Introduction to Liquid State Physic;*, World Scientific: NJ, **2002**.

(122) Wurthner, F.; Yao, S.; Debaerdemaeker, T.; Wortmann, R. *J. Am. Chem.l Soc.* **2002,** 124, (32), 9431-9447.

(123) Forster, T. *Laboratorium fur physicalische Chemie, Technische Hochshule;* Stuttgart, Deutschland

(124) Martinez, V. M.; Arbeloa, F. U.; Prieto, J. B.; Lopez, T. A.; Arbeloa, I. L. *J. Phys. Chem. B* **2004,** 108, 20030- 20037.

(125) Zhang, X.; Steel, W.H.; Walker, R.A. *J. Phys. Chem. B* **2003**, 107, 3829-3836.

(126) Negrerie, M.; Gai, F.; Bellefeuille, S. M.; Petrich, J. W. *J. Phys. Chem*. **1991,** 95, 8663-8670.

(127) Moog, R.S.; Maroncelli, M. *J. Phys. Chem*. **1991**, 95, 10359-10369.

(128) Schwartz, B.J.; Peteanu, L.A.; Harris, C.B. *J. Phys. Chem*. **1992,** 96, 3591-3598.

(129) Barbara, P.F.; Walsh, P.K.; Brus, L. E. *J. Phys. Chem*. **1989,** 93, 29-34.

(130) Marcus,Y. *J. Sol.Chem.* **1991 ,**20, 929- 944.

(131) Reid, P.J.; Alex, S.; Jarzeba,W.; Schlief, R.E.; Johnson, A.E.; Barbara, P.F. *Chem. Phys. Lett.* **1994**, 22, 93 – 100.

(132) Pimental, G.C.; McClellan, A.L. *The Hydrogen Bond;* Freeman: San Francisco, **1960**

(133) Schuster, P.; Zundel, B.; Sandorfy, C. *The Hydrogen Bond: Recent Developments in Theory and Experiments*; North Holland: New York, **1976.**

(134) Dore, J. C.; Teixeira, J. *Hydrogen-Bonded Liquids*; Kluwer Academic: Boston, **1991**

(135) Benigno, A. J.; Ahmed, E.; Berg, M. *J. Chem. Phys.* **1996**, *104*, 7382-7394.

(136) Yu, J. W.; Berg, M. *Chem. Phys. Lett.* **1993**, *208*, 315-320.

(137) Tanaka, H.; Kokai, F.; Brauman, J. I.; Fayer, M. D. *Chem. Phys. Lett.* **1987**, *142*, 371- 375.

(138) Schellenberg, P.; Friedrich, J. *J. Lumin.* **1993**, *56*, 143- 149.

(139) Walker, G. C.; Jarzeba, W.; Kang, T. J.; Johnson, A. E.; Barbara, P. F. *J. Opt. Soc. Am. B-Opt. Phys.* **1990**, *7*, 1521.

(140) Suppan, P. *J. Chem. Soc.-Faraday Trans. I* **1987**, *83*, 495-509.

(141) Benjamin, I.; *Chem. Rev*. **1996**, 96, (4), 1149-1476.

(142) Steel,W.H.; Walker, R.A. *Nature*. **2003**, 424, 296-299.

(143) Chandler, D. *Nature*. **2005,** 437, 64-647.

(144) Stienhurst, D.A.; Owrutsky, J.C. *J.Phys.Chem. B* **2001,**105,(15), 3062-3072.